This is to certify that the
dissertation entitled

FUNCTIONAL ANALYSIS OF THE POLYKETIDE SYNTHASE GENES IN THE FILAMENTOUS FUNGUS *Gibberella zeae* (ANAMORPH *Fusarium graminearum*)

presented by

Shidad I. Gaffoor

has been accepted towards fulfillment
of the requirements for the

Ph.D. degree in Plant Biology

Frances Trail
Major Professor's Signature

8/19/05
Date

FUNCTIONAL ANALYSIS OF THE POLYKETIDE SYNTHASE GENES IN THE FILAMENTOUS FUNGUS *Gibberella zeae* (ANAMORPH *Fusarium graminearum)*

By

Shidad I. Gaffoor

A DISSERTATION

Submitted to
Michigan State University
in partial fulfillment of the requirements
for the degree of

DOCTOR OF PHILOSOPHY

Department of Plant Biology

2005

ABSTRACT

FUNCTIONAL ANALYSIS OF THE POLYKETIDE SYNTHASE GENES IN THE FILAMENTOUS FUNGUS *Gibberella zeae* (ANAMORPH *Fusarium graminearum*)

By

Shidad I. Gaffoor

The fungus *Gibberella zeae* Schw. [Schwein.] Petch (anamorph *Fusarium graminearum* Schwabe) is a major causal agent of the disease Fusarium Head Blight when it infects cereals such as wheat, oats, barley and corn. The fungus produces several mycotoxins both during infection of the grain and storage of that infected grain. The myxotoxins characterized to date include zearalenone, fusarin C and aurofusarin which are of polyketide origin and deoxynivalenol which is a trichothecene.

Polyketides are a class of secondary metabolites that exhibit a vast diversity of form and function. In fungi, these compounds are produced by large, multi-domain enzymes classified as Type I polyketide synthases (PKS). In the past, most PKS genes were identified because they produced a compound of interest. However, with the recent advent of the genomic era, it is possible to clone and characterize the entire suite of PKS genes within a genome, contributing to the overall analysis of the total polyketide potential of an organism. Although PKSs are composed of several highly conserved domains, the extensive diversity of the PK products arise from the number and kind of domains present on the enzyme and the type of starter and extender units selected by the enzyme. In this study we identified all fifteen PKS genes within the genome of the

filamentous fungus *G. zeae*. We succeeded in identifying five genes responsible for producing the previously identified compounds zearalenone, aurofusarin, fusarin C and the black perithecial pigment by analysis of disrupted mutants of all fifteen genes. A comprehensive expression study revealed several interesting expression patterns. However we were unable to detect expression of one of the PKS genes under any of seventeen conditions tested. This is the first study to genetically characterize a complete set of PKS genes from a single organism.

Zearalenone is a mycotoxin of worldwide economic and health importance. It is most commonly found as a contaminant in stored corn and wheat grain and has chronic estrogenic effects on mammals. Zearalenone has been known to be a polyketide, derived from the sequential addition of multiple acetate units by a polyketide synthase (PKS). However, the genetics of zearalenone biosynthesis and the identification of associated modifying enzymes have not been elucidated. Herein, we describe the cloning of two genes, designated *ZEA1* and *ZEA2*, that encode the polyketide synthases responsible for zearalenone production in *G. zeae*. Disruption of either of these genes results in the loss of zearalenone production by the resulting mutant. *ZEA1* and *ZEA2* are transcribed divergently from a common promoter region. Analysis of this region gives clues to the regulation of these genes. Examination of the region of the chromosome involved in zearalenone biosynthesis shows the presence of two possible regulatory proteins. A putative mechanism for the synthesis of zearalenone by the two PKSs is proposed.

TABLE OF CONTENTS

LIST OF TABLES

LIST OF FIGURES

INTRODUCTION

The class of compounds known as Polyketides (PKs) are myriad in form, function and distribution but have a common biosynthetic origin. PKs have been traditionally classified as a group of secondary metabolites. The secondary metabolites are defined as a "heterogeneous group of compounds, usually of low relative molecular mass, and made mostly but not exclusively by organisms without a nervous system (i.e. bacteria, fungi and plants) (14). The PKs themselves have been identified in organisms ranging from bacteria and fungi to members of the plant and animal kingdoms. Although the term "Polyketide", to indicate compounds composed of multiple ketomethylene groups was coined in 1907 (14), PK compounds have been know and utilized for centuries. Their uses are as diverse as their nature. These compounds have mainly been exploited for their pharmacological properties ranging from immunosuppressant agents (e.g. mycophenolic acid, rapamycin, tacrolimus), antibacterial agents (e.g. erythromycin, tetracycline, tylosin), antifungal agents (e.g. amphotericin, griseofulvin), anticancer agents (e.g. daunomycin), cholesterol-lowering agents (e.g. lovastatin, squalestatin, compactin), veterinary products (e.g. avermectin, monesin), antiparasitic agents (e.g. avermictin), antitumor agents (e.g. Doxorubicin), to murder weapons, a historic example of this last is the use of coniine-containing hemlock to execute Socrates (14, 30, 100, 127).

Although numerous PKs have been widely exploited by humans, their purpose in the producing organism remains a mystery. Large quantities of resources are employed by an organism to produce a bank of these compounds. These resources include the carbon, nitrogen and energy resources needed to synthesize the compound as well as the

resources required to store and maintain the genetic information coding for the enzymes and the transcription factors needed to regulate the production of the necessary enzymatic machinery. Therefore it seems highly unlikely that an organism would continue to produce these compounds if they serve no ecological or evolutionary advantage. Numerous studies over the past decades have resulted in the assignment of functions to a relatively few compounds. While pathogenicity and virulence factors dominate the list of roles for PKs, they also play a role in eliminating competitors, resisting environmental stress, as signaling molecules and as avirulence factors as described below.

A pathogenicity factor is defined as a metabolite produced by a pathogen that is essential for that pathogen to infect and cause disease on its host (2). When possible, the role of a compound as a pathogenicity factor is verified by using mutant strains of the wild type pathogen that are unable to produce the compound in pathogenicity assays to show that these strains are unable to cause disease. In *Magnaporthe grisea,* the dihydroxynaphthalene (DHN) melanin which is a black pigment formed by the polymerization of a monomer of PK origin (49) is produced in the appresoria. This compound has been shown to be necessary for the build-up of appressorial turgor pressure required for direct penetration of the host (9). Disruption of the PKS gene involved in producing this compound resulted in the inability of the fungus to penetrate the host and cause disease (62). T-toxin produced by *Cochliobolus heterostrophus* (138) and PM toxin produced by *Mycosphaerella zeae-maydis* (141) are host-specific toxins of PK origin. These toxins are able to bind to specific proteins in the mitochondria of T-cytoplasm maize and have been shown to be essential for pathogenicity. These fungi are

una

rec

the

by

cor

cor

pro

cer

cor

Sp

cor

spe

(63

sh

rad

the

rea

hy

fac

rec

eith

unable to cause disease in cultivars of maize that do not produce the specific proteins recognized by the toxins.

There are also several instances where PK compounds play a role in virulence on their plant or animal host. A virulence factor has been defined as a metabolite produced by a pathogen that are helpful but not essential for disease induction (2). The phytotoxin coronatine produced by *Pseudomonas syringae* which contains a PK component, coronafacic acid; causes diffused chlorosis on the host (10). Disruption of coronatine production resulted in a reduction of virulence (21). Similarly, null mutants of the cercosporin PKS gene of *Cercospora nicotianae* produced significantly fewer lesions compared to the wild type (33). DHN melanins produced by several fungi including *Sporothrix schenckii* (108), *Exophiala dermatitidis* (112) and *Aspergillus fumigatus* (126) confer an increased virulence compared to the corresponding albino mutants of these species that are unable to produced this pigment. In other fungi like *Alternaria alternata* (63), *Verticillium dahliae* (55) and *Monilinia fructicola* (107) the melanization has been shown to increase resistance to harsh environmental conditions, specially exposure to UV radiation and thereby increase the ability to cause disease. It has been hypothesized that the increased virulence in these fungi is due to the melanin's being able to quench the reactive oxygen species produced by the host in response to infection (60). Recently, a hybrid PK-non-ribosomal peptide compound has been shown to act as an avirulence factor in *M. grisea*. Disruption of the gene coding for this compound abolished the recognition of the fungus by the resistant rice cultivars (19).

PKs may permit the producing organism to better colonize a particular niche by either eliminating competition or by helping the organism to resist environmental

str
sec
flu
and
fur
acc
ph
Wi
mu
to r
ider
may
sign
mol
assi
give
may
suit
Cha
seve
strep
strep

stresses. Several organisms eliminate competition from surrounding organisms by secreting antibiotic compounds. Mupirocin (pseudomonic acid A) produced by *P. fluorescens* exhibits strong antibacterial activity against the gram-positive staphylococci and streptococci (11). Soraphen A, a PK produced by *Sorangium cellulosum* is a potent fungicide. This compound is able to bind and thereby inhibit the activity of the eukaryotic acetyl-CoA carboxylase (131), a key enzyme in fatty acid biosynthesis. Dimycocerosyl phthiocerol, a compound of PK origin is a major cell wall lipid of *Mycobacterium avium.* When the *pks12* gene required for the biosynthesis of this compound is disrupted, the mutant colonies became drug susceptible (97) thereby making these organisms less able to resist adverse environmental conditions. Although the above compounds have been identified in culture and their role *in vivo* has not been investigated as yet, further studies may reveal a competitive edge for the producing organism. PKs may also play a role as signaling molecules. For instance DIF-1 which is a chlorinated PK acts as a signaling molecule to coordinate development in *Dictyostelium* (121). Although roles have been assigned to several PKs, a large number of them remain unaccounted for.

There are several hypotheses for the role of PKs in the producing organism. Any given organism may produce numerous compounds which when considered individually may not contribute significantly to the fitness of the organism, but when considered as a suite of compounds acting synergistically may give the organism a competitive edge (31). Challis and Hopwood (31) describe the role played by the streptogamins produced by several *Streptomyces spp.* A single organism produces two types of compounds, type A streptogamins which have a mixed polyketide/nonribosomal peptide origin and type B streptogamins which have a nonribosomal peptide origin. When exposed to individually,

both type A and B streptogamins are bacteriostatic by binding to two different sites on the bacterial ribosome. However the binding of streptogamin A to the ribosome increases the affinity of streptogamin B to its binding site by up to 40-fold. The binding of both compounds simultaneously is irreversible. Thus compounds that are bacteriostatic individually become bactericidal when acting synergistically. Additional roles may include a shunt for eliminating unbalanced metabolic intermediates (48) and a mechanism to engage cellular machinery when resources are scarce (25).

PKs are produced by polyketide synthases (PKS), multi-domain enzymes that iteratively catalyze the condensation of several rounds of CoA thioesterified carboxylic acids. Unlike fatty acid synthases which are limited to condensation of acetate and malonate thioesters, PKSs are able to utilize larger carboxylic acids that may even be branched or cyclic, in addition to using acetate and malonate moieties. This is one source of the immense diversity of PK compounds. The basic PKS consists of β-ketoacyl synthase (KS); β-ketoacyl transferase (AT) and acyl carrier protein (AC) domains required condense the carboxylic moieties. In addition to these, a PKS may also contain β-ketoacyl reductase (KR), dehydratase (DH), enoyl reductase (ER), methyl transferase (MT) and cyclase (CY) domains that further tailor the PK backbone. This variability in domain architecture and the ability of the PKS to selectively utilize these domains during each round of catalysis is another source of PK diversity. PKSs are classified based on the coding of the genes. All the domains of a type I PKSs are coded by a single gene and are the most prevalent type of PKS in the fungi. The domains of type II PKSs are coded by separate genes and are generally found among prokaryotes. Type III PKSs are found

in both prokaryotes and plants. Of the three requisite domains, this type of PKSs contain only a KS domain, and therefore does not fit the classical definition of the PKS (37).

The type I PKSs are further classified as being modular or iterative. The modular enzymes are composed of several modules, each module containing the numerous domains required to add on and modify a single carboxylic acid. Thus it is possible to predict the number and type of carboxylic acids that are condensed by these enzymes and the expected structure of the final compound by examination of the predicted amino acid sequence of a modular enzyme.

The iterative enzymes are composed of a single suite of domains that act iteratively. The KS, AT and AC domains involved in chain elongation are active during each round of condensation while the other domains (e.g. KR and MT domains) that catalyze modification reactions are active during selective rounds of condensation. Although numerous PKSs belonging to this class have been identified recently due to the sequencing of several fungal genomes, the products of a majority of these genes have not yet been identified. Unlike the modular PKSs, not enough is known about the iterative PKSs to be able to predict the nature of the compound that is produced. However enough is known that it is possible to identify the catalytic domains coded by the enzyme and thereby predicts the broad class of compound that is produced. The kind of domains present and the extent of their activity during each condensation cycle determine the state of reduction of the final compound. If the enzyme contains the reducing domains KR, DH and ER, the resulting compound is classed as a reduced compound. The KR domain will reduce the ketone group to an alcohol, the DH domain will further reduce this alcohol to an alkene by the removal of a molecule of H_2O and the ER domain fully reduces the

alkene to an alkane. PKSs that have all three reducing domains that are active during most of the condensation cycles result in highly reduced compounds that are linear such as T-toxin (109) and fumonisin (103). The PKS that produces the backbone of fusarin C has only KR and DH domains (115). The product of this PKS is not as extensively reduced. The absence of these reducing domains results in the production of a compound that is unreduced. Since the unreduced compounds have their ketone groups intact it makes the PK backbone highly reactive and the resulting molecules tend to be cyclic (76, 133). This cyclization may occur via a Claisen type condensation or a Knoevenagel (aldol-like) type condensation. With the characterization of an increasing number of entire fungal PKS sequencess, it is possible to identify a PKS as being reducing, by simply determining the conserved domains present in the amino acid sequence. Previously, the sequence of the KS domain was the information most readily available for a larger proportion of the PKS genes. Bingle *et al* analyzed the sequences of KS domains from several characterized and putative fungal PKSs and identified a dichotomy in the sequences. Closer examination of the characterized PKSs revealed that the sequence of the KS domains predicted if the gene would be classified as being reducing or non-reducing. They referred to these two groups the MSAS type and wA type PKSs (16).

A major portion of the PKs studied to date are of bacterial origin, the Actinomycetes being the major contributors (31). Mining the numerous genomes that have been recently sequenced indicates that the filamentous fungi rival prokaryotes in the number of putative PKS genes identified in each organism. While *Neurospora crassa* is predicted to have only seven PKS genes (20), *C. heterostrophus* is predicted to have 25 with several other Ascomycetes ranging inbetween (73). Evidence suggests that the

lichens may prove to have the largest number of PKS genes within a single organism (86). PKs of bacterial origin have been extensively studied and their vast diversity exploited for numerous uses. Though this resource is not yet exhausted, the vast array of potential PKS genes along with genes for numerous other "natural products" that are emerging with the each new genome that is sequenced, represent an untapped goldmine of novel compounds that can be investigated for various activities from antibiotics and anti-cholesterol agents to numerous other industrial uses.

In the past the study of PKSs involved the identification of a bioactive compound and the subsequent elucidation of the biosynthetic pathway. Identification and cloning of the pathway genes came last. The most productive method of isolating the PKS genes was to use degenerate primers to amplify the highly conserved KS domain (16, 103). Other options were to screen mutant libraries generated by either random insertional mutagenesis (80) or by exposure to either chemical mutagens or ionizing radiation. Since the mutants generated by random insertional mutagenesis are "tagged" because the mutation is caused by the insertion of a plasmid containing a selectable marker, it is possible to identify the locus where the plasmid is inserted with a relative degree of ease once a mutant of interest has been identified. However, the generation of such a library is labor and resource intensive. On the other hand using either chemical mutagens or ionizing radiation is both easier and cheaper, although it is laborious to identify the mutated gene in the mutant of interest. With the availability of whole genome sequences this tedious and time consuming venture has been greatly simplified. It is still not simple to visualize a compound based on the sequence of the synthetic gene(s), however we are able to identify these genes and manipulate them with much more ease. Upregulation of

genes in the native system or expression in a heterologous system should facilitate the identification and characterization of the compound produced. This pool of novel compounds can be further expanded by modification of the biosynthetic genes or by the combination of parts of different genes. The ultimate goal would be to tailor the biosynthetic gene(s) to produce the required compound. This would enable the production of compounds with very specific activity, an invaluable attribute especially for the pharmaceutical and agrochemical industries. PKS genes are a prime for this purpose since they are multidomain enzymes. The synthetic product can be modified by manipulating the domains or swapping domains from other PKS genes thereby modifying the extent of reduction of the ketide and the kind of carboxylic acid incorporated during the condensation cycle. An exhaustive study of PKS genes in fungi should provide the necessary database to formulate these modifications. Since the advent of the Golden Age of antibiotic discovery in the 1950's, a large number of secondary metabolites of pharmaceutical interest were identified (31). Although a number of compounds have been discovered in recent years, the rate of discovery has declined drastically while the need for novel compounds has grown. Several factors have contributed to this demand including the emergence of resistant strains and novel strains of pathogens and the growing prominence of previously obscure diseases like aspergillosis or candidiasis due to compromised immune systems as a result of HIV/AIDS infections or patients using antirejection drugs. The need to identify novel compounds has never been greater.

The fungus *Gibberella zeae* Schw. [Schwein.] Petch (anamorph *Fusarium graminearum* Schwabe) is a major causal agent of the disease Fusarium Head Blight when it infects cereals such as wheat, oats and barley and corn. Characteristic symptoms of the disease include the initial water soaked brownish spots on the developing head that spread throughout the head progressing to premature bleaching of the spikelets (94). As the season progresses, the normally vertical awns become deformed and horizontal on the infected spikelets. The saprophytic mycelia of the fungus are able to over winter in the debris left over in the field after the previous year's harvest. In springtime, when as conditions become warmer and in the presence of adequate moisture perithecia begin to develop on the exposed parts of these debris. Perithecia are the sexual fruiting bodies produced by asocomycetous fungi including *G. zeae*. The fungus undergoes sexual reproduction to produce meiotic spores known as ascospores within the asci, which are sac like structures. The perithecium develops around these structures and may offer a degree of protection both from physical forces and UV radiation since it is composed of heavily pigmented cells. In *G. zeae* this appears to be a melanin-like black pigment. Under optimal conditions the mature ascospores are forcibly ejected from the perithecia. Although the exact signals that trigger ascospore discharge are not known as yet; light, temperature and moisture have been shown to play a role (110, 125). Ascospore discharge in *G. zeae* occurs around the time of anthesis in the wheat heads. The airborne ascospores are deposited on the extruded anthers where they initiate a primary infection (96). Wheat heads are most susceptible to infection during this period (46). Macroconidia (asexual spores) also develop on the debris and are able to infect the anthers (99). The germinating spores grow saprophytically as they proceed to colonize the dead anthers.

The hyphae subsequently penetrate the ovary and eventually infect the floral bracts including the inner and outer glumes, lemma and palea initiating an infection. As the fungal hyphae ramify throughout the spikelet, it also spreads to other spikelets on the wheat head as the disease progresses and eventually spreads through the culm to colonize the vegetative tissue. While infection results in sterile florets if the fungus reaches the ovary prior to fertilization, infections that occur during the later stages [from fertilization to the soft dough stage (99)] of grain development result in low weight, deformed grain that is extensively colonized by the mycelium. The macroconidia persist in the atmosphere may cause secondary infections in the tillers that mature later on (46) and it is possible that they infect and colonize the vegetative parts. This infected vegetative matter that is left over in the field at harvest acts as a source of inoculum during the following season.

A consequence of Fusarium Head Blight infections is the contamination of the grain with the numerous mycotoxins produced by the fungus. To date the characterized mycotoxins produced by this fungus include deoxynivalenol (DON), zearalenone (zen), fusarin C and aurofusarin. Although infection can be rampant under conducive conditions such as high moisture and low temperature, the extent of infection is not always a reliable indicator of the extent of mycotoxin contamination since mycotoxin production continues post harvest. The pathogen's interactions with stressful environmental conditions including fungicides (79) and competing micro-organisms (89) may also result in unexpected levels of mycotoxins. Studies show that DON is produced throughout seed development in the infected plant (4) and levels of the toxins may increase during storage

(17). Zen is generally detected during storage of grain under sub-optimal conditions (57). Aurofusarin and fusarin C have not been investigated in depth as yet

DON, also known as vomitoxin; is a type B trichothecene compound. Although the type B compounds are much less potent than the type A compounds, the effects of exposure to the type B compounds are likely to be of greater importance in practical situations due to their prevalence, their wide spread effect on numerous species and synergistic effects with the co-occurring mycotoxins fusaric acid and fumonisins (38). Symptoms of exposure to DON in humans and animals include a decrease in food intake or feed refusal, vomiting and digestive disorders. This results in losses in weight gain (35), an undesirable feature in animals reared for meat production. Swine are the most susceptible to DON, whereas poultry and ruminants are affected to a lesser extent (35). It is believed that the microflora in the rumen of the ruminants are able to break down the trichothecene compounds and thereby reduce their toxicity (38). Extensive studies have revealed that all trichothecenes are able to bind to a single site on the eukaryotic 60S ribosomal subunit and thereby inhibit peptidyl transferase activity which is required for polypeptide elongation and termination. In addition to the effects on animals, DON also affects the host plant during pathogenesis. Disruption of the Tri5 gene coding for the enzyme that catalyzes the first committed step in trichothecene biosynthesis has shown that DON acts as a virulence factor since the strains unable to produce it are reduced in virulence (105).

Fusarin C, a mycotoxin of PK origin, is produced by a number of Fusaria including *G. zeae* (115). Toxicological studies of this compound have demonstrated that the mutagenic activity of this compound is comparable to that of aflatoxin B1 (27). It has

also

nap

as a

effe

Stu

acc

this

dev

sym

whi

by (

gra

ever

als

stuc

Chr

hyp

of th

by U

of z

PK

wh

also been implicated in esophageal cancer. Aurofusarin is a homodimeric naphthoquinone with a deep carmine hue (114). Aurofusarin has recently been classified as a mycotoxin because studies have shown that changes in egg yolk color and a negative effect on meat quality in chicken were associated with exposure to this compound. Studies revealed that exposure to aurofusarin affected carotenoid and vitamins A and E accumulation in the egg yolk, thereby affecting the antioxidant status (42). In chicken, this would not only reduce the consumer value of the eggs but also affect the development of the chicken embryo. Descriptions of Fusarium Head Blight disease symptoms are linked to the pink or red hue aurofusarin lends to the infected tissue (54) which has been detected in concentrations as high as 4.2 mg/kg in stored grain (71).

During the 1950s and 1960s there were severe epidemics of maize ear rot caused by *G.* zeae in Minnesota and the surrounding states. Farmers who used this contaminated grain to feed swine initially reported symptoms of vomiting and feed refusal which was eventually attributed to trichothecene contamination. In addition to these symptoms they also noticed symptoms of hyperestrogenism in the swine (129). This outbreak led to the study of zen as a mycotoxin. The initial studies were pioneered by Stob (118) and Christensen (34) who identified it as the compound responsible for causing the hyperestrogenic syndrome in swine. This was followed by identification of the structure of the compound as a 6-(10-hydroxy-6-oxo-*trans*-1-undecenyl)-β resorcylic acid lactone by Urry (130). Much work has also been done to elucidate the biosynthetic mechanisms of zen. Steele (116) used a two pronged approach to show that zen was synthesized via a PK pathway. They were able to show that only labeled acetate and malonate moieties which are precursors for the PK pathway, were incorporated into zen while precursors of

other pathways involved in secondary metabolism (shikimate, senecioate and mevalonic acid) were not incorporated in any significant amount. They confirmed their findings using degradation studies. Despite this, no efforts had been made to identify the genes involved in the biosynthesis of zen to date even though the biosynthetic mechanism of several other PK mycotoxins such as fumonisin (101) and aflatoxins (23) to name a few have been studied in great detail. Therefore the quest for the genes involved in zen biosynthesis is pertinent and timely.

As a mycotoxin, zen has been shown to have estrogenic activity on consumption by mammals. Therefore ingestion of zen can have a range of effects similar to exposure to high levels of estrogen. However, poultry appear to be resistant to the adverse effects of this compound. Acute tests indicate that zen has a very low toxicity (LD_{50}=2-10 g/kg body weight), while chronic investigations reveal that it has adverse effects on mammals at levels as low as 1.5-3 mg/kg body weight) (98). Swine, specially pre-pubertal gilts, have been found to be the most sensitive to zen exposure, affecting the reproductive system and reproductive health of these animals (78). Low doses (1 ppm) of exposure to zen result in fertility disorders in swine and cattle while higher doses (50–100 ppm) adversely affect reproductive processes such as ovulation, conception, implantation, fetus development and the newborn's viability. Some of the more common symptoms of hyperestrogenism include enlargement of mammary glands, vulvovaginitis, atrophy of ovaries and spontaneous abortions in females and enlargement of mammary glands and atrophy of testes in males [reviewed by (35)]. These adverse effects of zen have lead to a much more comprehensive investigation of the effects of exposure to this compound.

In addition to cereals, zen has also been shown to contaminate a range of other foodstuffs including sorghum, sesame seed meal, pecans and bananas (75). Processing of some foods has led to increased levels of the toxin. It may also be transmitted to humans from contaminated feed via milk products (75) and via meat products from cattle treated with zearanol, a derivative commercially used as a growth promoter (66). Although zen has fairly low toxicity and carcinogenicity levels with an LD_{50} of 2-10 g/kg (75), chronic exposure and synergistic effects of other environmental estrogens of both plant and anthropogenic origin establish effects on mammals as low as 1.5-3 mg/kg body weight. These levels have been detected in world wide food supplies (38, 98). More susceptible sub-populations such as the unborn and very young would be affected by much lower levels of the toxin (113). It is thought that zen is able to elicit these effects by its ability to bind the human nuclear estrogen receptor (69, 83). Although zen does not have a typical steroidal structure, studies have shown that it is able to bind to the estrogen receptor, albeit with a 10-100 fold lesser efficiency than the native 17β-estradiol (75).

The effects of the several mycotoxins presented here are observed by feeding the sensitive test subjects relatively pure forms of the compounds. However in nature, especially under agricultural conditions the feedstuffs will be contaminated with several species of *Fusarium, Aspergillus* and numerous other fungi notorious for producing mycotoxins including fumonisins, aflatoxins. Even though the animals or humans may not usually encounter lethal doses of any one toxin, they will be exposed to varying levels of several toxins, each exerting its characteristic impact. Over time these effects will be cumulative and cause greater damage. In addition, some of the toxins may have synergistic effects which are much more deleterious (38).

In summary PKs are a family of compounds produced by a wide range of organisms, but most extensively studied in bacteria and fungi. These compounds have a wide range of activities that have long been exploited by man. In recent years they have yielded a number of useful compounds and revolutionized several fields including medicine and agriculture. Several PKs have also been found to play important roles in the producing organisms as pathogenicity and virulence factors and less commonly as signaling molecules and avirulence factors. In fungi, PKs are produced by the iterative condensation of a variety of carboxylic acids by multidomain enzymes. The specific carboxylic acid incorporated into the compound, the kinds of domains present in the enzyme and specific domains that are active during a particular round of condensation all contribute to the immense diversity of PKs.

G. zeae, the fungus that infects cereals to cause the devastating disease Fusarium Head Blight, produces three characterized PK mycotoxins, namely zearalenone, aurofusarin and fusarin C. The toxigenic effects of zearalenone have been studied extensively since the 1960's. Both aurofusarin and fusarin C had been identified previously; however their importance of mycotoxins was recognized only recently. The PKS genes involved in the biosynthesis of these compounds have been identified, but much of the biochemistry remains to be understood. Further study of the biochemistry of these and other PK compounds is pertinent with the present demand for novel compounds for a variety of purposes, most importantly for use as antibiotics and agrochemicals.

In this study we have identified and characterized all fifteen of the PKS genes encoded in the genome of *G. zeae* and were able to assign function to five of the genes. Characterization of these genes will enable us to identify the corresponding PK

compounds themselves and also demarcate the gene cluster encoding the enzymes needed to tailor the PK backbone. This study would not only yield novel compounds to be assayed for bioactivity but also the information needed to modify the genes to modify the compound as needed. We were also able to specifically identify two PKS genes involved in the biosynthesis of zen. This is the first reported instance where two PKS genes may be involved in producing the backbone of a PK compound.

FUNCTIONAL ANALYSIS OF THE POLYKETIDE SYNTHASE GENES IN THE FILAMENTOUS FUNGUS *Gibberella zeae* (ANAMORPH *Fusarium graminearum*)

Iffa Gaffoor, Daren W. Brown, Ron Plattner, Robert Proctor, Weihong Qi, and Frances Trail

Abstract

Polyketides are a class of secondary metabolites that exhibit a vast diversity of form and function. In fungi, these compounds are produced by large, multi-domain enzymes classified as Type I polyketide synthases (PKS). In this study we identified and functionally disrupted 15 PKS genes from the genome of the filamentous fungus *Gibberella zeae*. We found that five of them are responsible for producing the mycotoxins zearalenone, aurofusarin, fusarin C and the black perithecial pigment. A comprehensive expression analysis of these genes revealed diverse expression patterns. during grain colonization, plant colonization, sexual development, and mycelial growth. We were unable to detect expression of one of the PKS genes under any of 18 conditions tested. This is the first study to genetically characterize a complete set of PKS genes from a single organism. The role of PKs in the fungal life cycle and in evolution is discussed.

Introduction

Secondary metabolites are a remarkably diverse class of cellular products that often exhibit taxonomic specificity. In microbes, these unique biochemicals are usually produced after a period of active growth has depleted the substrate (13, 18) and biosynthesis often coincides with differentiation, especially sporulation (12). Polyketides (PKs; derived from poly-ketone) are a class of secondary metabolites produced by most organisms, but they have been most extensively examined in bacteria and fungi. In fungi, PKs include a range of compounds such as the mycotoxins aurofusarin (114) aflatoxin (15), and zearalenone [zen, (130)] and the green spore pigment of *A. nidulans* (84, 133).

Secondary metabolites are generally considered "nonessential" for organismal growth under culture conditions (12). However, their role in life cycles in the natural environment is not well understood. Many functions have been proposed for PKs, including: 1) a shunt for eliminating unbalanced metabolic intermediates (48): 2) a mechanism to engage cellular machinery when resources are scarce (24); and 3) a means to control differentiation (135). However, the most plausible explanation for the diversity of secondary metabolites is that the ability to produce a wide variety of compounds is ecologically and evolutionarily advantageous as a resource for bioactive compounds (31, 47). For example, several actinomycetes synthesize two chemically unrelated metabolites that act against the same target organism (31). Thus unrelated compounds may be selected for the same activity when important to organism survival.

The study of fungal PKs has been limited by the difficulty of detecting and characterizing the PK itself. Complete analysis of the genetic potential of fungi to produce PKs became possible only recently when the genomic sequences of several

fungal species became available. Now, the selective cloning of genes encoding polyketide synthases (PKSs) can precede identification of a product and contribute to the overall analysis of the total PK potential of an organism.

PKs are synthesized by adding successive acetate groups to form a chain of C_2 units with alternating ketones and the resulting chain is modified to form a unique compound which could be either linear or aromatic. The minimal PKS consists of three domains; a ketosynthase (KS) domain, an acyltransferase (AT) domain and an acyl carrier protein (ACP) domain. Such an enzyme is said to be non-reducing and the resulting PK is aromatic with unmodified ketone groups. In addition to the three requisite domains, some PKSs may also have a β-keto reductase (KR) and a dehydratase (DH) domain and occasionally enoyl reductase (ER) domain which are able to reduce the ketone groups to varying extents (51, 93). The resulting enzymes are said to be reducing and produce linear PK compounds. Reducing PKSs often also have a methyl transferase (ME) domain. Variability in the type, number and activity of these domains after each condensation cycle contributes to further diversity of metabolites generated by fungal PKSs.

Sequence comparisons of the fungal KS domains support the existence of two major groups of PKSs: the reducing PKSs and the non-reducing PKSs (16, 92). Recently, Kroken *et al.* (73) conducted a thorough phylogenetic analysis of putative PKS genes from the fungal genomes of *Neurospora crassa, Cochliobolus heterostrophus, Gibberella moniliformis, Botryotinia fuckeliana, Saccharomyces cerevisiae, Eremothecium gossypii, Schizosaccharomyces pombe, G. zeae* and previously characterized fungal and bacterial

PKS genes. This analysis also suggests that the filamentous fungi rival the actinomycetes in PK numbers and diversity.

In fungi, many PKS genes so far characterized have been found within a gene cluster, which also includes genes for further modification of the PK. The aflatoxin biosynthetic gene cluster is one example consisting of the PKS gene, two genes that encode for a fatty acid synthase, seven monooxygenase genes and seven dehydrogenase genes that are required for aflatoxin biosynthesis (139, 140).

The filamentous fungus *Gibberella zeae* [Schwein.] Petch (anamorph *Fusarium graminearum* Schwabe) is a major causal agent of Fusarium head blight of wheat and barley worldwide and produces the trichothecene mycotoxin deoxynivalenol, which is a significant contaminant of human food and animal feed (36). The fungus also produces three PK derived mycotoxins zen (130), aurofusarin (114) and fusarin C (115). Zen is an important source of environmental estrogens when contaminated grain is consumed by humans (74) and may also have effects on sexual development in fungi (91, 137). The toxicological effects of aurofusarin and fusarin C have not been studied extensively. Aurofusarin is known to have adverse effects on avian species; it affects the antioxidant composition and the fatty acid profile of the eggs (42). Fusarin C has been shown to have mutagenic properties in the Ames test. It has also been shown to cause chromosomal aberrations in mammalian cell cultures (53).

We initiated the work described here to identify the genes responsible for production of zen in *G. zeae* (52). During the investigation, the genomic sequence of *G. zeae* was completed, allowing us to identify all 15 PKS genes. To determine the functions

of the products of these PKS genes in the life cycle of *G. zeae,* we have genetically disrupted each of the 15 PKS genes and characterized the mutated transformants. A complete analysis of the phenotypes of the individual mutants indicates a variety of roles, some obvious and others more subtle, for these PKs in the growth and development of the organism. We also analyzed the expression of each of the genes under a range of developmental, nutritional and pathogenic conditions. This is the first study to genetically characterize a complete set of PKS genes from a single organism.

Materials and Methods

Fungal strains and growth conditions.

The strain of *G. zeae* used for this study was a Michigan field isolate, PH-1 (FGSC 9075, NRRL 31084). All strains were maintained as mycelia in 30 % glycerol at -80 ^{o}C and subcultured on V8 juice medium (128) as needed. PH-1 was also maintained on sterile soil at -20 ^{o}C for use as inoculum.

Identification of PKS genes.

To identify the set of putative PKS genes from the *G. zeae* genome, we analyzed the first released version of the sequence, before automated gene calling had been done. The genomic sequence of *G. zeae* was obtained from the Broad Institute at MIT (http://www.broad.mit.edu/). *Ab initio* gene identification was accomplished using FGENESH (http://www.softberry.com) with organism-specific parameters for *Neurospora crassa* (26). The local *F. graminearum* genome database, predicted ORF

database, predicted protein database and EST database were set up using FORMATDB in the NCBI stand-alone BLAST tool (ftp://ftp.ncbi.nih.gov/blast/executables/). Sequence similarity searches were applied to the local *F. graminearum* database using BLASTN, BLASTP, and TBLASTN in the NCBI stand-alone BLAST tool. Default parameters were used but the cut off E-value was set at 1 instead of 10. The initial queries for the searches used the nucleotide sequences for *F. graminearum* PKS clones to perform the BLASTN search against the *F. graminearum* genome database. For each PKS gene identified, the predicted protein sequence was used to perform the TBLASTN search against the *F. graminearum* genome database to identify additional related sequences. Similarly, the twelve known fungal PKSs obtained from NCBI were used to perform TBLASTN and BLASTP, searching against the *F. graminearum* genome database and predicted protein database. The twelve known fungal PKS sequences were aligned using the CLUSTAL W (122) default parameters in slow/accurate mode. The multiple alignment was used as input for the HMMBUILD module of HMMER 2.2g (41) to build the profile Hidden Markov Model (HMM). The profile HMM was used to search the *F. graminearum* predicted protein database using HMMSEARCH. The default cutoff values were used to filter the query results. Twelve previously characterized fungal PKS sequences (*Aspergillus nidulans* wAp, GenBank Q03149; *A. fumigatus* ALB1p, GenBank AAC39471; *A. terreus* LOVBp, GenBank AAD39830; *A. terreus* MSASp, GenBank AAC49814; *A. parasiticus* PKSL2p, GenBank AAC23536; *Cochliobolus heterostrophus* PKS1p, GenBank AAB08104; *Colletotrichum lagenarium* PKS1p, GenBank BAA18956; *Emericella nidulans* PKSSTp GenBank Q12397; *G. moniliformis* FUM1p, GenBank AAD43562; *G. fujikuroi* PKS4p, GenBank CAD19100; *Nodulisporium* sp.

ATCC74245 PKS1p, GenBank AAD38786; and *Penicillium patulum* MSASp, GenBank P22367) were used as input for the motif discovery tool Multiple Expectation-maximization for Motif Elicitation (MEME) to build PKS motif profiles (6). The log-odds matrix of the motif(s) was used to search the *F. graminearum* predicted protein database by using the Motif Alignment Search Tool (MAST) (7) with default parameters. The search results were also curated manually as described above. For each putative gene identified, and for known fungal PKS genes used in this study, BLASTP, CDART and RPS_BLAST searches were applied to the GenBank nr database and the conserved domain database, respectively, using NCBI web services (http://www.ncbi.nlm.nih.gov/BLAST/) to obtain and compare domain structures of these genes. Each putative PKS gene was also used to perform a TBLASTN search against the F. *graminearum* EST database to investigate the transcription of the predicted genes. Amino acid (aa) sequences were analyzed by the PILEUP and PRETTY programs of the Wisconsin Package version 10.3-UNIX (40).

Fungal transformation and gene disruption.

To determine functions of each of the 15 PKS genes, we genetically disrupted them individually and subsequently analyzed the disrupted transformants for changes in phenotype under a variety of conditions. Disruption vectors were generated by PCR amplification of a 500 bp-1750 bp fragment located downstream of the start codon of each predicted gene (Table 1, Appendix A). The amplified fragment was then ligated into the *SmaI* site of pHYG4, a vector carrying the selectable marker hygromycin B phosphotransferase (*hph*) (29). These vectors were used to transform the wild type PH-1

as described below. Genes were disrupted by single crossover integration of the disruption vector into the homologous portion of the genome.

Transformations were performed on germinated conidia using a previously published protocol (104) with the following modifications. Approximately 0.3 g soil stock was used to inoculate carboxymethylcellulose (CMC, Sigma Chemical Co., St. Louis, MO) medium which was then incubated for 72 hr at 25 ^{o}C at 250 rpm (28). Conidia were harvested by centrifugation and germinated in YEPD (0.3% yeast extract, 1% bactopeptone, and 2% D-glucose) broth for 12-14 h at room temperature at 175 rpm. Isolation of protoplasts occurred in 25 mg/ml driselase (InterSpex Products, Inc. San Mateo, CA.), 0.05 mg/ml chitinase (Sigma Chemical Co., St. Louis, MO), and 5 mg/ml lysing enzyme (Sigma Chemical Co., St. Louis, MO) in a 1.2 M KCl buffer. Protoplasts were collected by filtration through a 30 μm Nitex nylon membrane (Tetko Inc., Kansas City, MO) and washed three times in STC buffer (1.2 M sorbitol; 10 mM Tris-HCl, 50 mM CaCl2, pH 8.0). Transformation was performed in a 500 μl volume with 10^{6}-10^{8} protoplasts, 25 μg of the disruption vector, and was mediated by 30% polyethylene glycol solution (30% PEG 8 000, 10 mM Tris-HCl, 50 mM $CaCl_2$, pH 8.0) in STC buffer). Protoplasts were transferred to 250 ml Regeneration Medium (RM; 0.1% yeast extract, 0.1% casein enzyme hydrosylate, 0.8 M sucrose and 0.75% agarose) and distributed to Petri plates (15 ml each). Cultures were incubated for 15 hr and then overlaid with 10 ml RM amended with 150 μg/ml hygromycin B (HygB; Calbiochem-Novabiochem Corp., San Diego, CA) to recover transformants. Putative transformants were selected within 4-7 days and hygromycin resistance was confirmed by growth on V8 juice medium amended with 450 μg/ml HygB. Hygromycin resistant (HygR) colonies were transferred

to a 2% water agar medium and genetically pure single spore isolates were obtained for further analysis.

Single spore isolates of putative transformants were screened for gene disruption using Southern blot analysis. Genomic DNA was isolated from putative transformants as previously described (61, 68) and cut independently with two different restriction enzymes. The restriction enzymes chosen for each analysis were paired such that one recognized a unique site within the disruption vector and one recognized sites only outside the vector. Restriction cut DNA was separated by electrophoresis and Southern analysis was performed for each of the digested samples. Probes were based on the specific amplicon used for gene disruption and a portion of hph (588 bp). Based on Southern data, we selected, for further analysis, two independent disruption mutants for each PKS gene and one transformant that resulted from ectopic integration of each vector. All nucleic acid manipulations and molecular procedures were carried out according to standard methods (111).

Characterization of growth and pathogenicity of PKS mutants.

Transformants were characterized for their ability to produce perithecia and to discharge normal ascospores and their mycelial growth compared to the parent PH-1. Both PKS mutants and the ectopic transformant for each target PKS were center inoculated onto carrot agar (70) in 100 mm Petri dishes, and two diameters were measured per plate after 3.5 days of growth (days after inoculation - dai) to determine the area of the growing colony. The experiment was performed in triplicate for each isolate. A mixed model ANOVA (SAS PROC UNIVARIATE) was used to compare the growth

rates between the mutants and the wild-type. Differences in growth rate were compared using a Tukey's comparison (72). Once the mycelia grew to the edge of the plate, mature perithecia were generated as previously described (70). On 10 dai, the gross morphology of the perithecia were observed and ascospore discharge was characterized as previously described (123).

Transformants were screened for changes in pathogenicity on wheat. Five greenhouse virulence tests were conducted on the wheat cultivar Wheaton essentially as described (39). Inocula were generated by growth on mung bean liquid medium for 4 d at 28 ^{o}C with shaking at 200 rpm (5). The macroconidia were filtered, concentrated by centrifugation, rinsed and suspended in water. Wheat heads were inoculated by injecting a drop of water containing approximately 10^{3} macroconidia into one floret of a spikelet located in the lower third of each head. Ten heads were injected for each treatment and control heads were injected with water. Injected heads were enclosed in plastic bags for three days. Visual disease assessments were recorded at 2- to 3- day intervals 18 to 21 days after inoculation and overall disease severity was calculated as a percentage of blighted spikelets in each head. The wheat heads were allowed to mature, then were harvested and individually threshed to collect seeds.

Chemical analysis of PKS mutants.

Transformants were tested to detect the loss of ability to produce zen, fusarin C, aurofusarin. To test whether zen was accumulating in the disrupted transformants, we used thin layer chromatography (TLC). Transformants were grown on Uncle Ben's®

Original Converted Rice (MasterFoodServices, San Antonio, TX), a vitamin-supplemented parboiled rice, found to stimulate zen production (95, 117). Rice (25 g) was aliquoted into Erlenmeyer flasks and soaked in 20 ml of distilled water for 2 h. After autoclaving for 1 h, the clumps of rice were broken up and allowed to stand over night. The following day the rice was re-autoclaved for 1 h and inoculated with 10^6-10^8 conidiospores in 2 ml of distilled water. The culture was transferred to Petri dishes (100 mm X 25 mm), taped with Tenderskin hypoallergenic paper tape (The Kendall Company, Mansfield, MA) and incubated at room temperature for one week. During this period, cultures were monitored to confirm uniform colonization of rice across all samples. After one week, the cultures were transferred to an incubator at 11 ^{o}C for two more weeks (120). At harvest, the cultures were dried in an oven at 55 ^{o}C for 3–4 days and ground to a fine powder using a domestic coffee grinder. For TLC analysis, 200 mg of each powdered sample was extracted in 100% methanol for two hours and TLC was performed as previously described (120). The area on the TLC plate with a similar RF to authentic zen was collected, resuspended in methanol, and a spectrum analysis performed according to Mirocha *et al.* (88).

Although the trichothecene mycotoxins deoxynivalenol (DON) and 3-acetyl DON are not derived from a PK, their critical importance in the wheat disease process prompted us to examine if any of the PKS mutants were affected in DON production. Quantitative combined measurements on both mycotoxins were made on transformants grown in liquid culture under DON-inducing conditions (85) and the results were

compared to those of the wild type, PH-1. DON quantification data were generated using the commercial competitive ELISA-based Veratox 5/5 kit (Neogen Corp., Lansing, Michigan) and using a standard curve for DON ranging from 0.25 to 3.00 ppm. OD_{650} values were measured after the addition of the stop solution to the multiwells. To ensure accuracy, each sample was quantified twice. DON analysis of transformants grown *in planta* were performed differently. Following virulence assays, seed samples for all transformants and for wild type PH-1 were tested for DON. Harvested seeds were ground to a fine powder and extracted with 4 ml of acetonitrile-water (86:14) per gram with shaking for 2 h. The solvent extract was filtered through Whatman filter paper and stored at 4 ^{o}C until analyzed. The concentration of DON was determined by liquid chromatography-mass spectrometry as described in Baker and Roberts (8).

For fusarin C analysis, transformants and the wild type, PH-1, were grown in liquid YES medium (yeast extract 2%, sucrose 6%, pH 5.5). An equal volume of acetonitrile was added to 16-day-old cultures. The resulting solution was mixed briefly and filtered through 0.2 μm nitrocellulose filters. The filtrate was examined for the presence of fusarins by HPLC-UV absorbance-mass spectrometry (MS). The HPLC system employed an Intersil ODS3 column (10 cm, 5 μm), a flow rate of 0.3 ml/min, and a gradient solvent system beginning with water:methanol 65:35 (v/v) and changed to water:methanol 30:70 (v/v) over the course of 5 min. The latter solvent composition was held isocratic for 25 minutes. The HPLC column was coupled to a UV detector and the API source of a Finnigan LCQ Deca MS system (ThermoQuest, San Jose, CA) operated in the electrospray (ESI) mode. The presence of fusarins was determined by their retention time and ultra-violet and mass spectra in comparison with authentic Fusarin C.

For example, the UV spectrum of a peak with a retention time of 19.2 min showed a single broad peak with an absorption maximum of 365 nm that was identical to the spectrum of fusarin C. The mass spectrum of this component was also identical to that of fusarin C and included signals with masses of 432, 454, and 885, which correspond to the MH+, MNa+, and 2MNa+ ions, respectively.

For aurofusarin analysis, transformants and wild type, PH-1 were grown on potato dextrose agar (PDA; Difco Laboratories, Detroit, MI) medium for 10 days. A single 10 cm agar plate per transformant was extracted by first cutting the agar into small pieces and soaking with 30 ml of a 95:5 chloroform/methanol solution overnight. The extract was then filtered through Whatman #1 paper. The filtrate was examined by HPLC-UV absorbance-mass spectrometry (MS) and found to contain a broad peak at 17.0 min with an associated molecular ion of 571 mu. This mass is consistent with that of aurofusarin, which has been characterized (8).

Expression analysis of PKS genes.

To determine when the PKS genes were expressed in wild type PH-1, we employed reverse transcriptase PCR (RT-PCR) of mRNA harvested under a variety of growth and developmental conditions. Efforts were made to choose some conditions that resembled those the fungus would encounter in nature during its normal life cycle. Growth on nutrient rich grains was examined using rice agar (91) and moist cracked corn. Gene expression during sexual development was examined using developing perithecia harvested from carrot agar 4, 5 and 6 days after induction, representing very young, near-mature and mature perithecia, respectively (123). Gene expression during plant infection

and colonization was observed using wheat tissue harvested from infected heads 1, 4 and 5 dai. Expression during growth on a variety of standard laboratory growth conditions was also examined. These conditions included an undefined medium rich in reduced nitrogen (YES) to simulate saprophytic growth under ideal conditions, a natural plant-based medium (Potato Dextrose broth; Difco Laboratories, Detroit, MI), a synthetic, defined minimal medium with nitrate as the sole nitrogen source [Czapek-Dox broth (0.6 g $NaNO_3$, 0.6 g K_2HPO_4, 0.2 g $MgSO_4$, 0.2 g KCl, 0.01 g $FeSO_4.7H_2O$, 30 g sucrose per liter)] and starvation conditions (Czapek-Dox broth lacking either a carbon or a nitrogen source). The last three conditions were selected to simulate the conditions encountered as the fungus survives winter in the plant debris. Mycelia grown in YES and PDB were harvested at 48 h and 60 h dai, when mycelia are actively growing, and nutrients are not yet depleted. The mycelia grown in minimal medium were harvested after 4 days due to slower growth in these media. Mycelia grown in starvation conditions were initiated in standard Czapek-Dox broth for 4 days before being transferred to starvation media where they were harvested after 24 h incubation. Mycotoxin-inducing conditions were generated on rice agar (91) and DON-inducing medium (85). In addition, we examined conditions for conidiation (CMC medium); conidia and mycelia were harvested 5 days after inoculation.

All samples were harvested from 2-8 independent replicate cultures, pooled, frozen at -80 ^{o}C and lyophilized overnight. RNA was extracted using TRIzol Reagent (Invitrogen Life Technology, Carlsbad, CA) and treated with RNase-Free DNase I (Roche Diagnostics Corporation, Indianapolis, IN) as per manufacturer's instructions.

First strand cDNA synthesis was carried out with SuperScript II Rnase H- Reverse transcriptase (Invitrogen life technologies, Carlsbad, CA) using random hexamers. Gene-specific primers (Table 2, Appendix A) were used to amplify regions of each PKS gene to identify the conditions under which they were expressed. The primers used to generate the disruption vector were used to amplify the genes *AUR1, GzFUS1, PGL1, PKS2, PKS11, PKS14,* and *PKS17.* For genes *KSA1, PLSP1, ZEA1, PKS1, PKS5, PKS6, PKS7,* and *PKS9,* alternate primers were designed. In all cases, except for *PKS11* and *PLSP1,* primers were designed either to amplify a product that included an intron so as to distinguish between amplicons generated from contaminating DNA and mRNA or to span an exon-exon junction to ensure that no residual DNA was amplified. Although the primers used to amplify the mRNA of *PKS11* and *PLSP1* could not distinguish between a DNA and mRNA template, they were not redesigned because these two genes had very specific expression patterns, indicating genomic DNA was not being amplified. In all analyses, amplification was repeated 3 to 6 times to confirm results. To thoroughly test expression of all 15 PKS genes under conditions representing those encountered during the life cycle, 16 different treatments were designed. Due to this large number of conditions, quantitative PCR was prohibitively expensive.

Results

Identification of PKS genes.

We have identified fifteen putative PKS genes by analyzing the raw genomic sequence. PKS genes were designated using the previously assigned designations (73)

except where function has been determined during this analysis. Examination of the sequence using HMMER yielded eight putative PKS genes: *GzFUS1, AUR1, PGL1, ZEA2, PKS6 PKS9, PKS11* and *PKS17*. MEME/MAST applications recognized these eight genes and an additional seven genes: *ZEA1, PKS1, PKS2, PKS5, PKS7, GRS1* and *PLSP1*. All fifteen predicted genes had expect values of $E \leq 10^{-90}$ when compared to the conserved motifs. The expect value is the probability of this match being found merely by chance (www.ncbi.nih.gov). In addition to the 15 predicted genes, a sixteenth gene, designated *KSA1* (KetoSynthase-ACP), was predicted and had the next lowest E-value of those genes predicted, $E= 10^{-3}$. We included KSA1 in our expression analysis for comparison. Based on the high similarity of KSA1 to ß-ketoacyl- acyl carrier protein synthases ($E = 3 \times 10^{-125}$, RPS-BLAST 2.2.9) it is unlikely that this enzyme belongs to the PKS family. ß-ketoacyl- acyl carrier protein synthases are generally involved in the elongation step of fatty acid biosynthesis.

The complete set of domains comprising each PKS gene was identified by BLASTX, PILEUP and PRETTY analysis (Table 1, Appendix A). These domains were verified by aligning the predicted protein sequences with domains identified in previously characterized PKSs (76, 102) using CLUSTAL W (122). According to the domain analysis there are five non-reducing PKSs (*AUR1, GRS1, PGL1, PLSP1* and *ZEA1*) and 10 reducing PKSs (*GzFUS1, ZEA2, PKS1, PKS2, PKS5, PKS6, PKS7, PKS 9, PKS11* and *PKS17*). Using the chromosomal map of *G. zeae* provided by the Broad Institute (www.broad.mit.edu), we found that 13 of the PKS genes are scattered across the four

chromosomes. *ZEA1* and *ZEA2* appear to be divergently transcribed from a shared 1 kb promoter while *AUR1* is located 15 kb upsteam from *ZEA1*. The next closest PKSs are *PKS1* and *PKS9* which are 247 kb apart.

Functional analysis of PKS genes.

To identify the function of the PKS genes, all 15 genes were disrupted individually using the single-crossover integration approach (Table 2, Appendix A) to cause insertional mutagenesis of the gene. Up to 16 transformed hygromycin-resistant transformants were examined for each gene to identify two confirmed disrupted transformants and one ectopic transformant for further analysis. Southern analysis was performed on genomic DNA isolated from each transformant and from the PH-1 parent to confirm the location of the inserted plasmid in the disrupted strains (see appendix).

Growth, development, pathogenicity and mycotoxin production were analyzed for the set of disrupted transformants of each gene to determine how the functional disruption affected normal fungal growth and development. Mycelial growth, as measured by colony area relative to wild type, was similar to the wild type for transformants disrupted in *AUR1, ZEA1, ZEA2, PKS17, PLSP1*, and *GzFUS1*. For transformants disrupted in *ZEA2, PKS6, PKS7, PGL1, PKS9, PKS1*, and *PKS11*, significant increases in growth (113%–117%) were observed. Significant decreases in growth (86% and 68%, respectively) were noted for the *GRS1* mutants and the *PKS2* mutants. Disruption of the PKS genes did not affect either perithecium production or function *in vitro* and perithecia developed and discharged ascospores normally. Disruption of the PKS genes did not significantly affect pathogenicity on wheat.

Several of the PKS disruptants revealed function based on the loss of a known PK. The effects of disruption of *ZEA1* and *ZEA2* on zen production have been described elsewhere (52). Based on the similarity between *GzFUS1* and PKSs from related *Fusarium* spp. shown to synthesize fusarin C (115), we predicted that *GzFUS1* mutants would also be unable to synthesis fusarin C. We found this to be the case as both *GzFUS1* mutants failed to synthesize fusarin C while the ectopic transformant synthesized fusarin C at levels similar to those of the wild type. Similarly, both *AUR1* mutants failed to produce aurofusarin, the characteristic red mycelial pigment and mycotoxin, in contrast to ectopic control strains.

Examination of the *PGL1* mutants indicated that they did not produce the black perithecial pigment characteristic of the perithecia of both the wild-type PH-1 and the ectopic mutant (Figure 1, Appendix B). The structure of this pigment has not been characterized at this time.

In summary, we disrupted 15 genes and were able to determine the function of five of them: mutants of *ZEA1* and *ZEA2* revealed two genes responsible for zen production; mutants of *AUR1* revealed a gene responsible for aurofusarin biosynthesis; mutants of *GzFUS1* revealed a gene responsible for fusarin C biosynthesis and the mutants of *PGL1* revealed a gene involved in the biosyntheis of the black perithecial pigment.

Expression analysis of PKS genes.

The wild type PH-1 was grown under 11 different conditions and harvested at 1-3 time points for each condition. We then harvested total RNA from lyophilized mycelia

and used reverse-transcriptase PCR to determine the expression patterns of the 15 PKS genes and *KSA1*. Results of the expression analysis revealed seven groups of genes with similar expression patterns (Figure 2, Appendix B). We designated these groups as follows: constitutively expressed (*PKS6, KSA1* also follows this pattern); plant specific (*PLSP1*); grain specific (*GRS1, ZEA1, ZEA2*); sexual development related (*PKS7, PGL1, PKS9, PKS11*); mycelial growth related (*GzFUS1, PKS1, PKS2, PKS17*); not expressed *in planta* (*AUR1*) and expression not detected (*PKS5*). The sexual development group is also expressed during grain colonization. Interestingly, *PKS2*, which we relegated to the mycelial growth related group was expressed only in YES48, a condition of active mycelial growth.

Discussion

Here we present the first comprehensive functional analysis of all predicted PKS genes from a single filamentous fungus. The complete set of PKS genes in *G. zeae*, includes 15 distinct genes and we have identified the functions for five of them. Our work shows that PKs affect many aspects of fungal biology and are associated with diverse life cycle stages. Although the patterns of expression appear to be distinct among the different genes, it is worthwhile, however, to broadly group the genes by expression patterns (Figure 2, Appendix B), as this will provide a means for pursuing further functional analysis. In the future we will use groups of PKS genes that are similarly expressed to determine overlapping functions for the PK products. For example, the group expressed only during grain colonization includes *ZEA1, ZEA2* and *GRS1*. The product of *GRS1* is not known, but it is intriguing to think that zen and the *GRS1* product

might function similarly (the function of zen, however, is not yet clear). Similarly, the two pigment-producing PKSs have overlapping expression. We can speculate that they both provide UV and/or desiccation protection for the sexual fruiting body. Both are expressed in the perithecial wall, contributing to the blue-black color characteristic of *G. zeae* perithecia. We are currently exploring the relationship of the groups of PKS genes by stacking disruption of genes through mating to determine if the effects of disruption are correspondingly enhanced by the disruption of an entire expression group.

To determine function of individual genes, each of the genes was disrupted and the mutants examined for changes in development and pathogenicity. Interestingly, the only PKS (*PLSP1*) expressed exclusively during plant infection had no pronounced effect on pathogenicity when disrupted. This gene appears to have a disrupted ACP domain and therefore may not produce an active compound in the wild type. A detailed analysis of the expression of this gene over the course of plant infection and colonization would be necessary to clarify any role it may have during plant colonization. Disruption of two PKS genes, *GRS1* and *PKS2*, resulted in mycelial growth inhibition during a period of active mycelial growth. Expression of *PKS2* was detected only during the early stages of active mycelial growth in YES (Figure 2, Appendix B). A closer analysis of the disrupted mutants of these two genes, including microarray analysis, might reveal a possible function as a regulator in controlling mycelial proliferation. An example of a PKS that acts as a signaling molecule is DIF-1; it acts as a signal molecule in regulation of differentiation in *Dictyostelium* and is believed to be produced by a Type I PKS (64, 121). A similar phenomenon was observed in *A. parasiticus* in which disruption of the PKS *FLUP* eliminated asexual sporulation, inhibited mycelial growth and significantly

reduced aflatoxin production (142). A different type of signaling was observed to involve a PKS from *Magnaporthe grisea* in the initial host-pathogen interface. *ACE1*, a homologue to GzFUS1, was shown to be an avirulence factor recognized specifically by resistant rice (19). Such an interaction has not been observed for *GzFUS1*. These three examples from other fungal species illustrate the very important life cycle roles that PKs play.

Based on the striking phenotype of the disrupted mutants, we identified *AUR1* as the PKS responsible for the biosynthesis of the carmine pigment aurofusarin in *G. zeae* (114). A number of the genes flanking *AUR1* encode for enzymes consistent with the conversion of the initial PK monomer to the final dimeric structure. A recent report is consistent with our findings (81). In contrast to the *GRS1* and *PKS2* disrupted mutants, *AUR1* disrupted transformants were able to grow faster than the wild type on PDA, suggesting that aurofusarin production taxes the fungus thereby limiting growth or the compound itself is inhibitory to growth. Interestingly, on carrot agar, this growth differential was not observed for *AUR1* mutants.

We were unable to detect expression of *PKS5*, under any of the conditions tested and disruption of this gene did not yield a distinctive phenotype. It is possible that *PKS5* is either expressed under highly specialized conditions hitherto untested or at very low levels. It is also possible that *PKS5* may not produce a functional PKS in *G. zeae*, a hypothesis that is supported by the lack of a functional KS domain.

The domain analysis of the predicted PKSs of the reducing group revealed the presence of all of the expected domains as well as a few domains not previously described in PKSs. The presence of an acyl-CoA reductase (AR) domain in *PGL1* and a

carnitine O-acyltransferase (CA) domain in *PLSP1* has not previously been described for Type I PKSs. The predicted function of the TE, AR and CA domains is the same: release of the PK from the enzyme. The TE (or cyclase) domain is thought to play a role in cyclizing the nascent carbon chain (51). The AR domain may function to release the enzyme and generate a terminal aldehyde (59); while the CA domain may function to transfer the polyketide to carnitine or a related molecule. We also found a PKS with a domain duplication; PGL1 contains two ACP motifs. The presence of a second ACP has been observed previously in the fungal PKS wAp (51) but the function of this apparent redundancy in unknown. The subset of reducing PKSs that contain a non-functional ME domain (*PKS1*, *ZEA2* and *PKS7*) supports previous work that suggested that the ancestral domain structure of this type of PKS was KS-AT-DH-ME-ER-KR-ACP (73). The pattern of amino acid insertions and deletions scattered throughout the non-functional, remnant ME domains is perfectly conserved in the three PKSs and suggest that they share a common ancestor.

Kroken *et al.* (73) described 16 putative PKS genes in *G. zeae* in their analysis of several fungal genome sequences, which was based on an analysis of a preliminary 2X coverage of the genomic sequence. Reexamination of their data indicated that the Kroken *PKS14* and *PKS16* both correspond to the *GRS1* described here. In addition, *PKS1* and *PKS8* as described by Kroken *et al.* encode a single PKS, designated *PKS1*. Therefore, Kroken *et al.* (73) describe fourteen PKS genes in *G. zeae*, but they did not describe *PKS17*. However, the genome analyzed by Kroken *et al.* (73) and the sequence generated by the Broad Institute each were based on different isolates of *G. zeae*, and although there

is no reason to assume the sequences might vary significantly, it is possible these differences are due to altered genomes

There has been speculation regarding the physiological costs of producing extra metabolites that do not contribute directly to the health of the organism (31), but that may serve as auxiliary pools for novel compounds. The results presented here suggest that individual mutations in 7 of 15 PKS genes results in transformants with increased growth on a rich medium (carrot agar). This certainly implies a cost to colonization; however, these costs were determined in a nutrient-rich, sterile environment. The present data do not preclude the possibility that accumulation of other metabolites, resulting from disruption of a pathway in these mutants, affects growth. In the field, *G. zeae* is most often associated with plant tissue that it has initially parasitized and must subsequently defend itself after harvest. It would not naturally encounter conditions similar to those in culture. In nature, these fungi must balance resource acquisition with resource protection, a prospect that may shift the value of these novel compounds. In the analysis of PKSs by Kroken *et al* (73), the only fungi that did not have PKS genes in the genome were the yeasts *Saccharomyces cerevisiae* and *Schizosaccharomyces pombe*, primitive ascomycetes. These are also unicellular yeasts found in sugary environments, where they colonize when the resource appears, and then seek dormancy as the sugars become scarce. The complexity of the niche which an organism fills may well result in increased selection for a pool of active compounds. This hypothesis is certainly supported by studies of the actinomycetes. Members of the polyketide-rich actinomycetes (31) and the filamentous fungi presented by Kroken are soil inhabitants. The soil provides a diverse and competitive environment where availability of resources is in constant flux. Fungi,

such as *G. zeae*, that function in a number of capacities, including that of plant pathogen and soil saprophyte, might need a pool of secondary metabolites from which to develop protective mechanisms. As for functions for these secondary metabolites, we can see biological activity in the products of 6 of the 15 PKSs described here. As genomic sequences of fungi from a broad group of lifestyles is accomplished, we will be able to come closer to understanding the functions of this diverse group of compounds.

Acknowledgements

The authors wish to thank the following collaborators on the *G. zeae* sequencing project: Bruce Birren and Li-Jun Ma of the Broad Institute, H. Corby Kistler of the USDA in Minnesota and Jin-Rong Xu (Purdue University). They also wish to thank Lan Xiao of The CANR Biometry Group, Statistical Consulting Center, Michigan State University for statistical analysis of growth data. Assistance with the DON analyses was provided by Benjamin Munn and L. Patrick Hart. This project was funded by USDA-NRI grant 2001-352-1-10062 to F.T. and the Michigan Agricultural Experiment Station.

CHARACTERIZATION OF TWO DISTINCT POLYKETIDE SYNTHASE GENES INVOLVED IN ZEARALENONE BIOSYNTHESIS IN *Gibberella zeae*

Iffa Gaffoor and Frances Trail

Abstract

Zearalenone is a mycotoxin of worldwide economic and health importance. It is most commonly found as a contaminant in stored grain and has chronic estrogenic effects on mammals. Zearalenone is synthesized by several species of the filamentous fungus, *Fusarium.* Since the 1970's, the compound zearalenone has been known to be a polyketide, derived from the sequential addition of multiple acetate units by a polyketide synthase (PKS). However, the genetics of zearalenone biosynthesis has not been elucidated. Herein, we describe the cloning of two genes, designated *ZEA1* and *ZEA2* that encode the polyketide synthases responsible for zearalenone production in *Gibberella zeae* (anamorph *Fusarium graminearum*). Disruption of either of these genes results in the loss of zearalenone production by the resulting mutant. *ZEA1* and *ZEA2* are transcribed divergently from a common promoter region. Identifying the genes flanking *ZEA1* and *ZEA2* and their putative functions gives clues to the regulation of these genes. Examination of the region of the chromosome involved in zearalenone biosynthesis shows the presence of two possible regulatory proteins. Strikingly, no other genes

typically associated with polyketide modification flank the two PKS genes. An oxidoreductase that is regulated similarly may be involved in modifications of zearalenone to form natural derivatives. A putative mechanism for the synthesis of zearalenone by the two PKSs is proposed.

Introduction

The filamentous fungus *Gibberella zeae* Schw. [Schwein.] Petch (anamorph *Fusarium graminearum* Schwabe) is a worldwide pathogen of corn and small grain cereals such as wheat, barley, and oats. In infected grain, *G. zeae* produces several mycotoxins, including the trichothecene deoxynivalenol, and the polyketides (PKs) zearalenone (zen) and fusarin C, thereby causing losses of both yield and quality. The genetics and biosynthesis of both deoxynivalenol and fusarin C have been the subject of intensive study in recent years (22, 115). In contrast, the genetics and biosynthesis of zen have received little attention (113), despite its deleterious effect on human health.

Zen is produced by several other species of *Fusaria*, including *F. culmorum, F. sporotrichioides, F. equiseti*, and *F. semitectum* (75). However, in North America it is most commonly associated with *G. zeae* infections of corn (113). The toxin may be transmitted to humans from cattle, via milk products from cows consuming contaminated food (75) and via meat products from cattle treated with zearanol, a zen derivative commercially used as a bovine growth promoter (66). Although zen has fairly low toxicity and carcinogenicity levels (LD_{50} of 2-10 g/kg), chronic exposure and synergistic effects of other environmental estrogens can elicit effects on mammals at levels as low as 1.5-3 mg/kg body weight (75). Surveys carried out in several countries indicate that these levels are present in food supplies world wide (38). More susceptible sub-populations, such as the unborn and the very young, would be affected by much lower levels of the toxin (113).

The incorporation of [1-^{13}C]-acetate and [2-^{13}C]-acetate into the structure of zen illustrates that it is a PK (87). In fungi, PKs are produced by Type I iterative polyketide synthases (PKSs). These are large, multidomain enzymes that iteratively catalyze several rounds of condensation of CoA thioesterified carboxylic acids, usually acetate and malonate. A minimal PKS consists of β-ketoacyl synthase (KS), β-ketoacyl transferase (AT), and acyl carrier protein (ACP) domains. A PKS also may have one or more other domains, such as β-ketoacyl reductase (KR), dehydratase (DH), enoyl reductase (ER), methyl transferase (MT), and cyclase (CY) (50). The number of reducing domains present determines the extent of reduction of the keto group after each successive condensation event, and in extreme cases reduction can produce a linear PK such as fumonisin (103) and t-toxin (138). However, in the absence of reducing domains, the keto group remains intact and yields unreduced and often cyclic PKs: including bikaverin, the red mycelial pigment formed by *Gibberella fujikuroi* (76), and the green spore pigment of *Aspergillus nidulans* (132, 133). The type of PK (reducing or nonreducing) has been predicted based on analysis of the highly conserved KS domains (16, 73). Recently, a phylogenetic analysis of the PKS genes identified in several filamentous fungi, including *G. zeae* was done (73).

In fungi, genes involved in secondary metabolism are generally located within a cluster, which may include a regulatory gene(s) (32, 101). Most clusters involved in PK biosynthesis consist of a single PKS and several genes, such as P450 monooxygenases, that are involved in modifying the PK backbone (65). However, clusters that include two PKS genes exist, such as those involved in the biosynthesis of lovastatin (56) and compactin (1). Lovastatin and compactin are very similar in structure, as are the genes of

their biosynthetic clusters (1). Existing evidence suggests that the two PKs composing lovastatin are produced independently and that the shorter product (a diketide) is subsequently added onto the longer product [a nonaketide; (56, 58)]. The diketide is not considered to contribute to the PK backbone because of its delayed attachment to the main molecule. In contrast, the biosynthesis of the polyketide aflatoxin, a mycotoxin produced by *Aspergillus spp.*, involves two fatty acid synthases, which produce a fully reduced hexanoyl chain that acts as a primer for the PKS to complete the backbone (134).

We initiated a study to identify the PKS gene(s) involved in zen biosynthesis using degenerative primers designed to amplify the KS region of the PKS genes. Since initiating the study, the complete genome sequence was released by the Broad Institute (www.broad.mit.edu) and we used sequence analysis to identify all of the PKS genes in the *G. zeae* genome and to genetically disrupt each of them (Gaffoor *et al.*, in preparation. As part of that study), we identified two PKS genes, subsequently designated *ZEA1* and *ZEA2* and described here, which when genetically disrupted, caused *G. zeae* to lose its ability to accumulate zen. These genes were contiguous in the genomic sequence and transcribed divergently. ZEA1 was a reducing PKS, and ZEA2 was a non-reducing PKS and the products of both form the backbone of the zen molecule. Analysis of the flanking region of *ZEA1* and *ZEA2* did not reveal any other genes that are likely to be part of the biosynthetic machinery; thus, we propose that these two PKs are solely responsible for the synthesis of zen.

Methods

Fungal strains and growth conditions.

The strain of *G. zeae* used for this study was a Michigan field isolate, designated PH-1 (FGSC 9075, NRRL 31084). All strains were maintained on sterile soil at –20 ^{o}C for rapid sporulation.

Fungal transformation.

Transformations were performed on germinated conidia using a previously published protocol (104) with the following modifications. Approximately 0.3 g soil stock was used to inoculate carboxymethylcellulose (CMC, Sigma Chemical Co., St. Louis, MO) medium, which was then incubated for 72 hr at 25 ^{o}C at 250 rpm (28). Conidia were harvested by centrifugation and germinated in YEPD (0.3% yeast extract, 1% bactopeptone, and 2% D-glucose) broth for 12–14 hr at room temperature at 175 rpm. Isolation of protoplasts occurred in 25 mg/ml driselase (InterSpex Products, Inc. San Mateo, CA.), 0.05 mg/ml chitinase (Sigma Chemical Co., St. Louis, MO), and 5 mg/ml lysing enzyme (Sigma Chemical Co., St. Louis, MO) in a 1.2 M KCl buffer. Protoplasts were collected by filtration through a 30 μm Nitex nylon membrane (Tetko Inc., Kansas City, MO) and washed three times in STC buffer (1.2 M sorbitol, 10 mM Tris-HCl, 50 mM $CaCl_2$, pH 8.0). Transformation was performed in a 500 μl volume with 10^{6}–10^{8} protoplasts and was mediated by 30% polyethylene glycol solution (30% PEG 8,000, 10

mM Tris-HCl, 50 mM $CaCl_2$, pH 8.0), STC buffer, and 25 μg of the disruption vector. Protoplasts were transferred to 250 ml molten regeneration medium (RM: 0.1% yeast extract, 0.1% casein enzyme hydrosylate, 0.8 M sucrose, 1% agarose) and distributed to 100 mm diameter Petri plates and incubated for 15 hr before being overlaid with 10 ml of RM amended with 150 μg/ml hygromycin B (HygB) (Calbiochem-Novabiochem Corp., San Diego, CA) to recover transformants. Putative transformants were selected within 4–7 days and hygromycin resistance was confirmed by growth on V8 juice medium amended with 450 μg/ml HygB. Resistant (Hyg^R) colonies were transferred to a 2% water agar (WA) medium, and genetically pure single spore isolates were obtained for further analysis.

Gene structure and analysis.

The genes *ZEA1* and *ZEA2* were designated *PKS8 and PKS7,* respectively by Kroken *et al.* (2003), in their phylogenetic analysis. Since they are now functionally described, we have renamed them to reflect this information. The predicted PKS protein sequences for *ZEA1* and *ZEA2* were analyzed by both CDART and RPSBLAST (www.ncbi.nih.gov) to determine domains. Subsequently, amino acid sequences of both genes were aligned with the conserved domains from previously characterized fungal PKS genes using ClustalW (http://www.ebi.ac.uk) (76, 103) to assist in the manual annotation.

Gene disruption

To determine the function of the two PKS genes, we generated disruption vectors by ligation of a PCR-amplified fragment from each predicted gene into the *SmaI* site of pHYG4, a vector carrying the selectable marker hygromycin B phosphotransferase (*hph*) (29). The location of the amplified fragments on contig 119 were: *ZEA1* = 2628–3760 (1133 bp) and *ZEA2* = 6149–7355 (1207 bp) based on the Broad sequence. The disruption vectors were used to transform the wild type PH-1 as described above. Putative transformants were purified by single spore isolation and screened for gene disruption using Southern blot analysis. Genomic DNA was isolated (61, 67) from putative transformants and cut independently with two different restriction enzymes. Two restriction enzymes were chosen for each analysis; one recognized a site within the disruption vector and one recognized sites outside the vector. Restriction- cut DNA was separated by electorphoresis and Southern analysis was performed for each of the digested samples. Probes were based on the specific amplicon used for gene disruption and a portion of *hph* (588 bp long). Based on Southern data, we selected two independent disruption mutants for each PKS gene and one transformant that resulted from ectopic integration of each vector for further analysis. The disrupted mutants from *ZEA1* were designated zea1m1 and zea2m2 and the ectopic transformant , zea1E. The disrupted mutants from *ZEA2* were similarly designated zea2m1 andzea2m2 and ectopic zea2E. All other nucleic acid manipulations and molecular procedures were carried out according to standard methods (111).

Identification of the Intercontig Region of *ZEA1*

Since the sequence of *ZEA1* was incomplete, due to the lack of sequence for the region connection contigs 118 and 119 (www.broad.mit.edu), we generated the following primers to amplify the region spanning these two contigs. Primer 5'TACAAGCATGGCGCAACAATAGAC3' located on contig 119 (465–488) was used with either 5'GTGGCTGATCCCGCTCTTTGACG3' (2,989–3,011, contig 118) or 5'GACGGCCTCAACCTTTTCAGTG3' (2437–2458, contig 118). The amplicons were cloned into a pCR2.1-TOPO vector using the TOPO TA Cloning kit (Invitrogen Life Technologies, Carlsbad, CA) and sequenced at the Genomic Technology Support Facility at Michigan State University. The BLAST Tool (www.ncbi.nih.gov) was used to align the resulting sequences. Initially, the amplicon sequences were aligned to determine a consensus sequence, and this sequence was in turn aligned with those of contigs 118 and 119 to confirm that these two contigs were physically linked and to identify the novel sequence. The new sequence was used to link contigs 118 and 119 to form a single contig. This new sequence was used to identify the complete gene for *ZEA1* and the putative transcription start sites for both *ZEA1* and *ZEA2* using FGENESH (http://www.softberry.com) with organism-specific parameters for *Fusarium graminearum*.

Expression Analysis

To determine whether *ZEA1* and *ZEA2* were expressed in the disrupted transformants, Reverse Transcriptase PCR was used. To induce zen production, cultures were inoculated onto rice agar (91) at room temperature for five days and subsequently

transferred to an incubator at 11 ^{o}C for five more days. Surface and subsurface mycelia were harvested with a scalpel. For control conditions (noninducing), cultures were grown in Czapek-DoxBroth (Becton Dickinson, Sparks, MD) medium for seven days. RNA was extracted from lyophilized hyphae harvested from both conditions, using TRIzol Reagent (Invitrogen Life Technologies, Carlsbad, CA) as per manufacturer's instructions. First strand cDNA synthesis was carried out with SuperScript II RNase H^{-} Reverse Transcriptase (Invitrogen Life Technologies, City, State) using random hexamers. Gene-specific primers were used to amplify regions of each PKS gene to identify the conditions under which they were expressed. Primers were designed such that the annealing region of one primer of each pair spanned the exon junction in the mRNA, thereby ensuring amplification of only the spliced mRNA. The following primers were used: *ZEA1*, forward 5'GAAGAGGCCCCGGTAGCGATAAC3', reverse 5'TGAAGCCACTCCAGCAGCAGATT3'; ZEA2 forward 5'GTCTCACTGACTTTGTTCGCAT3', reverse 5'TCAAAGGATGTTCCTGGTTGCT3' As a control, the PKS gene FG02324.1, known to be expressed under zen inducing conditions (Gaffoor *et al.*, in preparation) was used (forward 5'GGATTCACCGTGCCCGACAT3' and reverse 5'TTCAACGCAGAGCTCCATTACGC3').

To identify genes in the region of *ZEA1* and *ZEA2* that were coregulated, rice samples described above were used, and for noninducing conditions, mycelia was grown in liquid YES medium (2% yeast extract, 6% sucrose) for 48 hours before harvest. In this case, YES was used as a control because it is a rich medium, and we felt would be more likely to upregulate genes. Extraction of RNA was performed as described above. Since

these genes were much smaller than the PKS genes, it was not possible to design primers around predicted introns (several did not have introns). However, results showed differential amplification of genes, indicating the lack of presence of DNA. The following primers were used: FG2393.1, forward 5'-CAGTGTCTGTCCAAAGACATT-3', Reverse 5'-CTTGTCAACACACCAACGTA-3'; FG2394.1, forward 5'-CCGCTTGGGCTGTCCTTATGG-3', reverse 5'-TTCCTCTCGGTCCTTTATGGCCAG-3'; fgd117-550, forward 5'-TCTACATGGCAGTTCAGCAGTC- 3', reverse 5'-ACTGCTCTCTATGACTC-3'; Fg12015, forward 5'AACTACGGTTTATCGCGGAAGC-3', reverse 5'-ATGATCTCGTCGGTCAACTTGG-3'; Fg12056 forward 5'-ATTTACCCGTTCTTCTGGGAAC-3', reverse 5'ACTTGTGGAAAGTGCAGAATGG-3', FG02398.1, forward 5'-TCGTTCCATGCGTTACCCACTC-3', reverse 5'CCGACTTCGACTCTGCCTTTGG-3'; For comparison, *ZEA1* and *ZEA2* were amplified as inducible controls. A note about gene designations: two websites have been set up to document the functional assignments of genes in the *G. zeae* genome. The Broad Institute at Massachusetts Institute of Technology website (www.broad.mit.edu) and the Munich Information Center for Protein Sequences (MIPS) website (www.mips.gsf.de) both record gene calls using the same gene designations with one exception: Genes with designations above fg12000 are recorded only on the MIPS website. In addition, fgd117-550 was only recognized by the MIPS website. The designation ".1" after a gene indicates the annotation version of this gene. We will include this designation only in the methods section.

Chemical analysis of zen accumulation

To test whether zen was accumulating in the disrupted transformants, we used two methods of analysis: thin layer chromatography (TLC) and competitive ELISA. To analyze for zen production, transformants were grown on Uncle Ben's converted rice (Master Food Services, San Antonio, TX), a vitamin-supplemented parboiled rice, known to stimulate zen production (95, 116). Uncle Ben's converted rice (25 g) was aliquoted into Erlenmeyer flasks and soaked in 20 ml of distilled water for 2 h. After autoclaving for 1 h the clumps of rice were broken up and allowed to stand over night. The following day the rice was re-autoclaved for 1 h and inoculated with 10^6-10^8 conidiospores suspended in 2 ml of distilled water. This inoculated rice was transferred to Petri dishes (100 mm X 25 mm), taped with Tenderskin hypoallergenic paper tape (The Kendall Company, Mansfield, MA) and incubated at room temperature for one week. During this period, cultures were observed to detect any contamination and to confirm uniform colonization of rice across all samples. At the end of one week, when the rice was fully colonized, the cultures were transferred to an incubator at 11^{o}C for two more weeks (116) Samples were harvested by placing the open Petri dishes in an oven at 55^{o}C for 3–4 days. Samples were ground to a fine powder using a domestic coffee grinder and used for further analysis.

For TLC analysis, 200 mg of each rice sample was extracted in 100 % methanol for two hr and TLC was performed as previously described (120). PKS mutants that did not produce zen were rescreened using the commercial competitive ELISA-based

Veratox kit for zen (Neogen Corp., Lansing, MI). Samples were prepared and assayed following manufacturer's directions. Extracts were initially diluted 50X prior to adding assay reagents to ensure zen levels were within the detection limits of the kit (50–600 ppb). Uninoculated Uncle Ben's rice was used as a control in the assay. Additionally, the extracts were separated by TLC as previously described by Swanson *et al.* (120). Following separation, the area in the zen region was collected, resuspended in methanol, and a spectrum analysis performed according to Mirocha *et al.* (116).

Results

Analysis of zearalenone biosynthesis in *ZEA1* and *ZEA2* mutants

Disruption of two PKS genes, designated *ZEA1* or *ZEA2,* by insertional mutagenesis resulted in isolates that lacked detectable quantities of zen under inducing conditions. Direct competitive ELISA analysis revealed high zen levels in cultures of the parent PH-1 (31.2 +/- 4.7 ppm) compared to the transformed deletion mutants (0.9 +/- 0.2), which had levels below those of the rice control extracts (1.7 ppm). Ectopic transformed isolates produced wild type levels. TLC analysis supported these findings (Figure 5, Appendix B). The absorbance spectrum of the band that co-migrated with zen in wild type and ectopic controls was indistinguishable from the spectrum for zen. This band was absent in disrupted transformants.

Identification and analysis of *ZEA1* and *ZEA2*

ZEA1 and *ZEA2* were transcribed divergently, with 1040 bp between their start codons. Based on comparative sequence analysis, *ZEA1* spanned contigs 118 and 119,

with the 5' end, including the KS and AT domains located on contig 119, and the ACP domain at the 3' end of contig 118. In the genomic sequence, there is a gap in the sequence between these two contigs, leaving *ZEA1* incomplete. We used PCR to clone a fragment of the *G. zeae* genome spanning contigs 118 and 119 and sequenced the region (Figure 3, Appendix B). The complete mRNA of *ZEA1* was then predicted to be 5988 bp. *ZEA2* is located in its entirety on contig 119 and consists of the following domain sequence: KS-AT-DH-ER-KR-ACP. Conserved domain sequences are presented in Table 3 (Appendix A).

ZEA1 and *ZEA2* were examined for unique sites with which to generate insertional mutants. Single crossover integration of a unique internal fragment was chosen because of the difficulty in disrupting these large genes and because of the possibility of similarities among PKS genes in the genome. Southern analysis of the transformants revealed the integration of the entire disruption plasmid at the appropriate site and a single integration in each of three transformants examined (data not shown). Reverse transcriptase PCR was used to confirm loss of expression of both genes in the deletion mutants (Figure 4, Appendix B).

Identification of Cluster

Expression analysis of genes flanking *ZEA1* and *ZEA2* was done by reverse transcriptase PCR to identify genes in the region of *ZEA1* and *ZEA2* that were coregulated (Figure 4, Appendix B). Of the genes assayed, only fg12056 mips (www.mips.gsf.deP) and FG02393 was expressed in a similar pattern to *ZEA1* and *ZEA2*.

Analysis of the promoter region

Sequence analysis revealed that the *ZEA1*, *ZEA2* intergenic region (3444–5335, contig 119) encompasses the promoter region, and was examined for transcription elements that would give clues to the regulation of the two PKS genes. The results of the promoter analysis are presented in Figure 6 (Appendix B). Two TATA boxes were identified, between the two proposed Transcription Start Sites (TSSs). In addition, nine GATA sites and two AbaA sites were in the region.

Discussion

We have identified and disrupted two PKS genes from *G. zeae* that are responsible for the biosynthesis of zen. Disruption of either of the genes results in the loss of the isolate's ability to accumulate zen under normally inductive conditions, as indicated by both ELISA assay and TLC analysis of extracts of induced cultures. Interestingly, it appears that zen in *G. zeae* is synthesized entirely by these two PKSs from one acetyl CoA and eight malonyl CoA molecules, a unique model for PK biosynthesis.

Expression studies of the genes flanking *ZEA1* and *ZEA2* indicate only FG02397 and FG02393 are expressed in a manner similar to the zen PKSs. FG02397 has an FAD binding domain and may be an oxygen oxidoreductase. Several natural derivatives of ZEN have been documented (88) and this enzyme could reduce the ketone groups at either C4 or C6 to yield natural variants. FG02393 is expressed similarly to the zen PKS genes and has ankyrin repeat motifs and a conserved region of approximately 150 residues long that is found within various heterokaryon incompatibility proteins that

appear to be restricted to the ascomycetes. Ankyrin repeats are commonly involved in protein-protein interactions and are found in transcriptional initiators. Further testing will be needed to determine a possible role in regulating the zen PKSs. The other genes flanking *ZEA1* and *ZEA2* are, FG02394 (a putative AM toxin synthetase), FG02398 (a GAL4 –type transcriptional regulator), FG03299 (a protein kinase gene) and two partial genes, fgd117-550 (monocarboxylate transporter) and fg12015 (K+ channel, beta subunit). FG02398 encodes a conserved GAL4-like Zn2Cys6 binuclear cluster DNA-binding transcription factor and is expressed in both noninduced and induced conditions. Since the promoter region shared by *ZEA1* and *ZEA2* contains Gal4 binding sites, this protein should be considered a possible regulator of zen production. FG02398 is expressed in both inducing and at least one noninducing condition (Figure 3, Appendix B). Thus, expression is not limited to conditions where the zen biosynthetic genes are expressed. Disruption of this gene is in progress and will be used to determine its role in regulation of the zen biosynthetic genes.

Because both *ZEA1* and *ZEA2* are required for zen biosynthesis, a single bi-directional promoter would ensure that both genes are expressed simultaneously, as has been shown in other systems (43, 77, 82, 119). We plan to verify the bi-directionality of the promoter, and the function of promoter elements by using a plasmid construct consisting of the putative promoter region flanked by two divergently transcribed reporter genes (106). We analyzed the 1040 bp region between *ZEA1* and *ZEA2* for the presence of fungal promoter elements. The *ZEA1–ZEA2* intergenic region has three regions containing GAL4-binding motifs and nine copies of the consensus sequence for binding of the GATA factor (Figure 6, Appendix B). The GAL4 family of Zn2Cys6 binuclear

cluster protein transcription factors recognize a palindromic sequence in which the 5'CGG3' motif is separated by up to eleven non-conserved bases. The pathway-specific transcription factor for aflatoxin biosynthesis, AflR, which belongs to this family, recognizes the sequence 5'TCGN$_5$CGA3' (45). Fungal GATA factors generally have a single Zn-finger motif that is responsible for DNA binding and may be involved chromatin remodeling (90, 136). An interaction between a GATA factor and a Zn2Cys6 binuclear cluster protein to regulate gene expression has been demonstrated in *Neurospora crassa* and *A. nidulans* (12, 27). Thus it is possible that the zen PKS genes are regulated in a similar manner. The annotated genome sequence indicates for *F. graminearum* contains six genes with putative GATA-binding Zn-finger domains.

Two motifs recognized by the AbaA-type transcription factor were identified in the bidirectional promoter. AbaA, along with two other transcription factors, is involved in regulating the genes expressed during asexual reproduction (3) and has been identified in the promoters of aflatoxin biosynthesis genes in *Aspergilli* (43). The role of zen in development and the possible role of an AbaA like protein needs to be further investigated. A single consensus sequence for the PacC transcription factor was also present in the region, however, multiple copies of the motif are usually present when this factor is involved in regulating a gene (82), making it an unlikely candidate for regulating gene expression in this instance.

A proposed mechanism for synthesis of zen by the two PKSs is presented in Figure 7 (Appendix B). The first 10 carbon additions are catalyzed by ZEA2p, which has reductive domains KR, DH, and ER, and is thereby able to variably reduce the keto groups on the PK chain. The keto group can be partially reduced to yield an alkene or

fully reduced to an alkane depending on the length of the carbon chain growing on the ACP domain (1) as can be seen in Figure 7 (Appendix B). The remaining three rounds of C2 additions are generated by ZEA1p, which is a non-reducing PKS, lacking KR, ER, and DH domains. The unreduced ketones added on by ZEA1p are highly reactive and form a ring which is rapidly aromatized due to enolization of the ketone groups. This is most likely a nonenzymatic process. A viable alternative model would have C11 and C12 added by *ZEA1p*, not *ZEA2p*, a possibility that will have to be determined experimentally. Interestingly, the ACP domain of *ZEA2* appears to be divided in the resulting protein (Table 3, Appendix A). If this ACP is nonfunctional, one possibility is that the ACP from the *ZEA1* would function for both, similarly to the Type 2 PKSs. Such a mechanism would require close association of both PKSs. The two ZEA proteins may be dimerized or act independently. Dimerization would facilitate the transfer of the product of ZEA2 to ZEA1 (Figure 7, Appendix B). In *in vitro* studies, PKSs have been shown to be promiscuous in terms of the starter unit specificity (44). Therefore, another advantage of ZEA1p and ZEA2p being associated is that it would ensure that ZEA1p use the correct primer to maximize the efficiency of zen biosynthesis. The interactions between these two enzymes will have to be determined experimentally.

Since 1962, at the first characterization of the potent mycotoxin, ZEN, the mechanism of biosynthesis and regulation of expression has remained elusive. With the identification of the two polyketide synthase genes involved in ZEN biosynthesis, and a putative regulatory protein, our understanding of the process of ZEN production in stored grain will be greatly facilitated. Hopefully, such information will lead to more improved designs for control of this toxin, worldwide.

Acknowledgements

This work was funded by USDA-NRI-CGP grant no. 2001-35201-10062 and the Michigan State University Agricultural Experiment Station.

The authors would like to thank Daren Brown and Mike Pollard for insightful discussions on zearalenone biosynthesis. We are grateful to Benjamin Munn performing the ELISA analyses.

CONCLUSIONS

Analysis of a whole genome sequence has proved to be an effective method to identify the suite of putative polyketide synthase (PKS) in a genome. The genome sequence of the filamentous fungus *Gibberella zeae* released in 2003 was analyzed to predict the PKS genes coded by this organism. Functional analysis of the fifteen identified genes enabled the identification of numerous conditions under which these genes were expressed. Two of the PKS genes were not expressed under any of the conditions assayed. Some of the genes were expressed under very specific conditions while a single PKS genes appeared to be expressed constitutively under the numerous conditions that were tested. Disruption of the genes enabled the identification of five PKS genes that synthesized previously identified compounds. None of the PKS disrupted mutants were affected in sexual reproduction or showed reduction in gross symptoms during plant infection. However, one of the disrupted mutants showed stunted growth even in rich media even though we did not detect the expression of this gene under any of the conditions surveyed. Since the conditions under which all eight of these genes are expressed are known, the disrupted mutants can be cultured under these conditions to identify the compounds produced by the PKSs. There have been no previously reported instances where the entire complement of PKS genes encoded by a single fungal genome have been functionally characterized.

Initially, five pairs of degenerate primers were used in an attempt to identify the PKS gene for zearalenone production. Although several unique PKS gene fragments were

cloned, none of them proved to be from a PKS producing zearalenone. The availability of the whole genome sequence and the ability to identify and examine all the PKS genes in the genome facilitated the identification of two PKS genes responsible for zearalenone biosynthesis. If the genome sequence had not become available, the identification of these PKS genes would have been tedious as the other options available were to screen a bank of mutants and thereby identify a mutant compromised in zearalenone biosynthesis and subsequently identify the mutated gene. The other option would have been to modify the degenerate PCR primers to yield a larger number unique PKS amplicons. Two PKSs were shown to be required for zearalenone biosynthesis. Although two PKS genes have been shown to be involved in the production of a single compound such as lovastatin, one of the enzymes produces a PK chain that is a used to modify the PK backbone that is produced by the second enzyme. Therefore the PK backbone is produced by a single PKS. In aflatoxin biosynthesis, the PK backbone is produced by a PKS and a fatty acid synthase. This is the first reported instance where two PKS genes contribute to the synthesis of a single polyketide backbone. Identification these two PKS genes and analysis of the protein sequence to determine the domain composition of each individual gene enabled us to propose a mechanism for the biosynthesis of zearalenone by these two PKSs.

APPENDICES

APPENDIX A

TABLES

Table 1. Structures of the predicted polyketide synthase genes in *Gibberella zeae*

Gene designation[1]	Gene designation[2]	Kroken designation	Disruption fragment	Reducing or Non-reducing	No. Amino Acids	Domains[3] (other domains: OD)	Product
PLSP1	FG04488	PKS15	103263-103805 (193)	Non-reducing	2172	KS-AT-ACP (choline/carnitine O-acyltransferase)	Unknown
PKS6	FG12109*	PKS6	88677-89734 (329)	Reducing	2554	KS- AT- DH- ME-ER-KR-ACP	Unknown
GzFUS1	FG12100*	PKS10	71008-72251 (320)	Reducing	3920	KS-AT-DH-ME-ER-KR-ACP (nonribosomyl peptide synthase)	Fusarin C
AUR1	FG12040*	PKS 12	134173-134960 (116)	Non-reducing	2072	KS-AT-ACP-TE	Aurofusarin
GRS1	FG03964	PKS14, 16	228126-229359 (168)	Non-reducing	2029	KS-AT-ACP-TE	Unknown
PGL1	FG12125*	PKS3	48922-50045 (371)	Non-reducing	2287	KS-AT-ACP-ACP (fatty acyl-CoA reductase; AR)	Perithecium pigment
ZEA2	FG12055*	PKS13	6149-7355 (119)	Reducing	2345	KS-AT-DH-ER-KR-ACP	Zearalenone (Gaffoor et al.)

Table 1. (cont'd).

ZEA1	FG02395	PKS4	2628-3760 (118)	Non-reducing		KS-AT-ACP	Zearalenone (Gaffoor et al.)
PKS1	FG10548	PKS1, 8	180638-181700 (441)	Reducing	2463	KS-AT-DH-ER-KR-ACP	Unknown
PKS9	FG12121*	PKS9	4984-6117 (436)	Reducing	2642	KS-AT- DH- ME-KR-ACP	Unknown
PKS11	FG01790	PKS11	52197-53594 (93)	Reducing	2465	KS-AT-DH-ME-ER-KR-ACP	Unknown
PKS7	FG08795	PKS7	76385-77657 (355)	Reducing	2350	KS-AT-DH-ER-KR-ACP	Unknown
PKS17	FG03340	--	31914-32951 (152)	Reducing	2529	KS-AT- DH- ME-ER-KR-ACP	Unknown
PKS5	FG05794	PKS5	303919-311398 (233)	Reducing	3177	KS-AT-DH-ME-ER-KR-ACP-(unknown conserved domain)	Unknown
PKS2	FG04694	PKS2	14355-16061(196)	Reducing	2563	KS-AT-DH-ME–ER-KR-ACP	Unknown
KSA1	FG07226	--	117170-118209 (303)		427	KS	Unknown

1. Based on the Broad Institute assigned gene designation (www.broad.mit.edu/cgi-bin/annotation/fusarium) and sequence design.
2. Asterisk (*) indicates name revision based on MIPS annotation (mips.gsf.de/genre/proj/fusarium).
3. Domains not usually associated with PKS genes are indicated in parentheses and domains that may be inactive due to disruption of the sequence are italicized.

Table 2. Primers used to generate disruption fragments of polyketide synthase genes

Gene designation	Forward Primer (5'-3')	Reverse Primer (5'-3')
Disruption		
AUR1	GGATTCACCGTGCCCGACAT	TTCAACGCAGAGCTCCATTACGAC
GzFUS1	CTTGGGCCACGGCTGAGATTC	ATTGGCACTTCCTGTCGCTTCC
PGL1	TCCTAGGCGCGTATACGAACCATT	GAGGCCCAGAGCTTGCTTAGTGTG
PKS1	ATCGCTATCGCTATCTGGGCTGTA	AGGTCTTGATTGGCGTGATGTGTT
PKS2	GATGAACGGGCCAACGGGTATGC	ATGGCGCCTGGAGATGATGC
PKS5	TTTGCGCCGAGACGAATCCA	TGCGCCCACCATCCAGACAG
PKS6	GTCCCAGTGCCGGTGCTTGTGA	GTGGAGAACGTTGGAGGCGATGAG
PKS7	CTGCGCAAAGTCTCCGAACAAAAG	TAGCGCGGAAAACCTCAAAACACA
PKS9	AAGTTCGGTGGTTGGGTCTAA	GTGTCTTTGGATACTCGCTTTTG
PKS11	CCCCTGGAATGACTGTGGCAATGA	AGGCGATGACAACACCCGACTGAA
GRS1	ATCAGAAGCGCCCAAGTCAACCA	TGCAACGAGGCGGAATGTATCAC
PLSP1	CAGTCCGTCATCCTCAGTCACAGA	CGGTAGAGATGGCTTGCGATTTC
PKS17	CTGGCGAGTGTGACGGTGCTGTTA	TTGTCGGCGTTGTTCTCCTCGTG
ZEA1	GCAATGCGTCCAGCTCCAAAAG	TCGGTTCACCTCGGTCAAATCCAG
ZEA2	GGAGGATATGGGCGTGGTGAAGGA	GGCTGGCTGATCTCGGGCAAAGT
Expression		
PLSP1	CTGGCGTATGCTGGACTCGGAATG	AGTGTTAGCGCTTGGCCCTGTTGA
PKS6	GGCAAGCCTGGAAGAACGAGTA	GAGCCGATGGGAAGTGGTGAGTCT
ZEA1	GAAGAGGCCCCGGTAGCGATAAC	TGAAGCCACTCCAGCAGCAGATT
PKS9	TTACAAACGGAACGAACGGACTC	GGGCAGCCAGGGAAATACG
PKS7	CGCTGCCTTTGACGCTTCTT	TGATTGCCCTTTAGTCCACGAG
PKS5	GAGGCACATGGAACTGGAACACAA	GGCCCAACCTCGTGAAAACACTC
KSA1	TGAGCAAAGGCGAATGTCCAAGTT	GCCGAAGCCTGCAAATGTCAAG
PKS1	GTCGCGGCTGGCACAACACTGA	ACAAAAAGCTCGCGCCCCATCC

Table 3. Predicted domain architecture of *ZEA1* and *ZEA2* proteins.

Gene	Protein Domain	Sequence1
ZEA1	β-Ketoacyl Synthase	RIAFQFKWEGPTYSLDSACASTASSIH
ZEA1	Acyl Transferase	GIQPSVVIGHSLGEYAALHVSGVLS
ZEA1	Acyl Carrier Protein	DTLIADLGVDSIMAIEIASQV
ZEA2	β-Ketoacyl Synthase	NRISHFFDIHGPSATVHTACSSSLVAIH
ZEA2	Acyl Transferase	GVAPVSVVGHSSGEIAAAYCIEALSHKD
ZEA2	Dehydratase	DDEPWIRGHTVGTTVLFPGAGMVSIV
ZEA2	Enoyl Reductase	LQRGQSVLIHAAAGGVGQAA
ZEA2	β-Ketoacyl Reductase	TYLFVGGLGGLGRSLAKEFVSCGAKNIAFISR
ZEA2	Acyl Carrier Protein	VTSLSS////YGVDSLVALEVRNWI

Table 4. Characteristics of the wheat head disease phenotype at day 20 conferred by the parental isolate PH-1 and nine insertional mutants[a]

Treatment	Disease phenotype			
	Bleaching[b]		Choking[d]	Rachis response[e]
	No. of spikelets	SD		
None	0	0	0	0
SNA only	0	0	0	0
PH-1	15.33	1.21	1	1
Daf mutant				
10	1.17	0.26	0	0.5
11	3.17	0.98	0	0.6
14	5	1.67	0.33	0.67
15	2.44	0.82	0.33	0.5
26	1.75	0.42	0	0.83
36	2.17	0.41	0.67	1
37	3.75	2.60	0.5	1
38	1.83	0.41	0	0
43	4.17	3.96	0	0.83

[a] Point inoculation of wheat heads at anthesis with agar plugs containing mycelium of a single isolate.

[b] Glume, lemma and palea tissues turns from green to white / pale brown, in head regions B and C (Figure8, Appendix B) (n=6)

[c] Mean number of spikelets +/- SD (n=6)

[d] All the spikelets above the point of inoculation (head region A, Figure 8, Appendix B exhibit the bleached phenotype assessed on a 0 to 1 scale where 1 is completely bleached.

[e] Brown streaking of rachis segments in head regions B and C assessed on a 0 to 1 scale

Table 5. Impact *F. graminearum* infection on grain weight, number and quality in the entire head and the three different sub-regions A, B and C[1]

Treatment	ENTIRE HEAD			PER SPIKELET			
				B-REGION		C-REGION	
	Grain weight (mg)	Grain number	Visible disease Spikelet No.	Grain weight (mg)	Number	Grain weight (mg)	Number
None	2255 c	41.3 b	0	80 c	2.1 c	144 c	2.69 c
SNA only	1718 bc	37.5 b	0	67.5 bc	1.79 bc	109.38 bc	2.45 c
PH-1	219 a	0.5 a	15.33	0 a	0 a	109.5 bc	1.3 b
Daf mutant							
10	1561 bc	33.5 b	2.17	6.45 a	0.46 ab	92.36 b	2.32 c
11	838 ab	26 ab	3.17	0 a	0.25 a	64.36 b	1.79 bc
14	1463 b	21.5 ab	5.00	27 ab	1.3 abc	123 bc	2.13 bc
15	1596 b	15.7 ab	2.33	5.15 a	0.47 ab	112 bc	1.74 ba
26	1465 b	22.5 ab	1.75	2.86 a	0.28 a	96.08 bc	1.84 bc
36	936 ab	17.3 ab	2.17	0a	0.32 ab	71.55 b	2.31 c
37	873 ab	23 ab	3.75	11.57 ab	0.85 ab	69.51 b	2.4 c
38	1277 ab	30.2 b	1.83	2.19 a	0.44 ab	86.26 b	2.41 c
43	1506 b	34.5 b	4.17	24.7ab	1.39 abc	95.44 bc	2.75 c
S^2 at 5%	1196	27.53		60	1.48	51.46	0.94

Table 5. (cont'd).

Treatment	REGION A- above the point of inoculation			REGION B-with visible symptoms			REGION C- with symptomless/no infection		
	Grain weight mean[3] (mg)	Grain number mean[3]	Grain Quality[4] L; M; S	Grain weight mean (mg)	Grain number mean	Grain Quality L; M; S	Grain weight mean (mg	Grain number mean	Grain Quality L; M; S
None	243 b	5.8 abc	86; 14; 0	160 a	4.2	100; 0; 0	1872 b	31.3	98; 01; 01
SNA only	161 b	4.5 abc	89; 04; 07	135 a	3.5	90; 0; 10	1422 b	29.5	98; 0; 02
PH-1	0 a	0.4 a	0 ; 0; 100	0 a	0	no seed	219 a	2.6	0; 0; 100

Table 5. (cont'd).

daf mutant									
10	362 b	10.8 bc	88; 03; 09	14 a	1	0; 0; 100	1185 ab	30.6	81; 09; 10
11	78 a	5.4 abc	74; 22; 04	0 a	0.8	0; 25; 75	760 ab	21.8	92; 04; 04
14	98 a	5.3 abc	53; 19; 28	135 a	6.5	05; 18; 77	1230 ab	22	53; 43; 04
15	165 ab	3.5 ab	62; 38; 00	0 a	1.1	0; 33; 66	1419 b	22.6	52; 36; 12
26	187ab	5.5 abc	82; 09; 09	5 a	0.5	0; 0; 100	1273 ab	25	66; 24; 10
36	18 a	4.5 abc	59; 26; 15	0 a	0.7	0; 0 ; 100	918 ab	30.5	42; 18; 40
37	48 a	4.3 abc	62; 08; 30	43 a	3.2	0; 0; 100	782 ab	27.9	55; 13; 32
38	137 ab	4.7 bc	50; 36; 14	4 a	0.8	0; 0; 100	1136 ab	32.6	75; 09; 16
43	274 b	7.3 bc	75; 02; 23	103 a	5.8	0; 23; 77	1129 ab	30.6	70; 09; 21
Region size		constant			variable			variable	
None	243 b	5.8 abc	86; 14; 0	160 a	4.2	100; 0; 0	1872 b	31.3	98; 01; 01

[1] head region A - above the point of plug inoculation, head region B with visible disease symptoms and head region C with no macroscopically visible disease symptoms

[2] Values in each column which differ by greater than the number indicated are statistically significant from each other at the 5% level.

[3] Means indicate per region per head. Value with different letters are statistically significant from each other at the 5% level.

[4] Grain Quality - L- large, M - medium and S - small grain, expressed as a percent of each category.

Table 6. The effect PH-1 and the various *daf* mutants of *F. graminearum*

Treatment	% seed germination[b]		Aerial Biomass (g) / Germinated Seedlings[c]	
	Exp. 1	Exp. 2	Exp. 1	Exp. 2
None	100	95	0.24	0.33
SNA[a]	95	100	0.20	0.23
PH-1	24	14	0.10	0.20
daf mutant				
10	90	57**	0.15	0.17
11	76	66	0.21	0.23
14	62	76	0.18	0.22
15	80	38**	0.21	0.30
26	90	76	0.26	0.28
36	80	67	0.19	0.19
37	67	52	0.22	0.31
38	90	86	0.30	0.25
43	90	33**	0.21	0.35
Standard dev	21	28.5	0.04	0.08
None	100	95	0.24	0.33

[a] Control inoculated with only plugs of SNA

[b] Percent seed emergence: assessment 14 days after inoculation, where 100% = 21 seeds

[c] mean above ground biomass of a germinated seedling assessed 21 days after inoculation

*in Exp 2 the overall affect of the disease was higher

**significantly lower seed germination in Exp 2

Table 7. DON levels produced in vitro by various *F. graminearum* isolates

	µg DON[1]	
	Rep 1	Rep 2
PH-1	284	71
daf mutant		
10	2.7	4.1
11	4.1	3.9
14	2.9	2.6
15	428	400
26	368	123
36	817	244
37	nd[2]	nd[2]
38	179	166
43	203	351

[1] Calculated as per g (dry weight) of mycelia

[2] n.d. Not determined

Table 8. Correlation coefficients between the various phenotypes quantified in wheat heads following *F. graminearum* infection

Head region	A	B+C	A+B+C	A	A	B	B	C	C	A+B+C	A+B+C
Phenotype	Choking	Rachis response	DON	Grain number	Large grain	Grain number	Large grain	Grain number	Large grain	Total Grain number	Total Grain weight
Bleaching on spikelets	**0.719**[a]	0.417	0.48	-0.612	**-0.863**	-0.061	0.072	-0.311	**-0.798**	-0.477	**-0.758**
Choking		0.599	0.652	**-0.733**	**-0.805**	-0.162	0.047	-0.2	**-0.934**	-0.491	**-0.725**
Rachis response			0.697	-0.276	-0.188	0.134	-0.026	-0.212	-0.541	-0.201	-0.67
DON				-0.338	-0.455	0.541	0.319	0.067	-0.603	0.104	-0.527
Grain number - Region A					**0.738**	0.239	0.004	0.396	0.618	**0.725**	0.536
Large grain - Region A						0.268	0.421	0.32	**0.878**	0.588	**0.759**
Grain number - Region B							0.344	0.084	0.271	0.508	0.477
Large grain - Region B								0.324	0.567	0.348	0.62
Grain number - Region C									0.355	**0.831**	0.353
Large grain - Region C										0.567	**0.718**
Total head grain number											0.605

[a] correlation coefficients > 0.700 are in bold, those < 0.200 are highlighted in grey

APPENDIX B

FIGURES

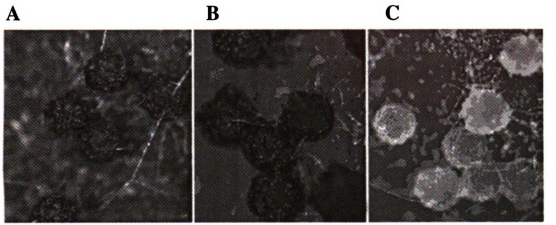

Figure 1. PKS mutations affecting perithecium pigmentation. A. *AUR1* mutant showing black perithecia and black stroma. B. Wild type strain showing heavily pigmented, blue-black perithecia on red stroma. C. Mutant strain with *PGL1* disrupted showing albino perithecia on red stroma.

Figure 2. Expression of putative PKS genes by wild type *G. zeae* under varying conditions. A representative RT-PCR result is presented. Expression is indicated by the appropriately sized band on an agarose gel (+). Absence of expression is indicated by the lack of an appropriately sized band (-). Culture conditions are indicated as follows: 1) Czapek-Dox, liquid 10 d; 2) potato dextrose broth, 48 h: 3) potato dextrose broth, 60 h; 4) yeast extract sucrose, liquid, 60 h; 6-8) carrot agar, 4, 5, and 6 d after treatment to induce perithecial development; 9-11) 48.72 and 96 h post inoculation of wheat head; 12) carbon starvation conditions; 12) nitrogen starvation conditions; 14) rice agar, 9 d; 15016) corn meal, 48 h and 96 h; 17) carboxymethyl cellulose media, 4d; 18) DON inducing media.

Figure 2.

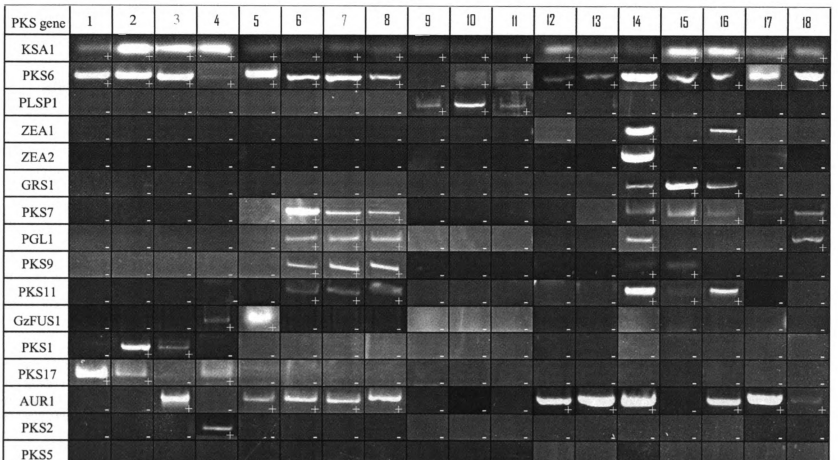
Conditions
PKS gene
1
2
3
4
5
6
7
8
9
10
11
12
13
14
15
16
17
18
KSA1
PKS6
PLSP1
ZEA1
ZEA2
GRS1
PKS7
PGL1
PKS9
PKS11
GzFUS1
PKS1
PKS17
AUR1
PKS2
PKS5

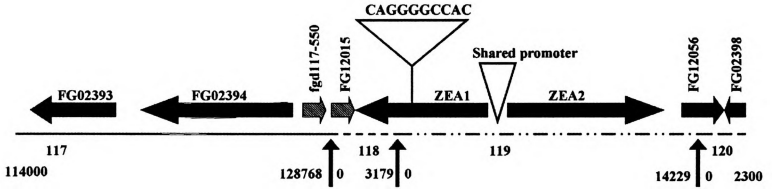

	FG02393	FG02394	fgd117-550	FG12015	ZEA1	ZEA2	FG12056	FG02398
I	+	-	+	-	+	+	+	+
N	-	-	+	-	-	-	-	+

Figure 3. Schematic representation of the zen gene cluster. The predicted genes are organized on several contigs represented by the horizontal line. Direction of transcription is indicated by arrows. Two partial genes, fg12015 and fg117-550, are indicated by crosshatching. The novel sequence connecting contigs 118 and 119 is shown in bold. The contig number and coordinates of the contig are indicated below the line. Expression of the genes under zen inducing (I) and noninducing (N) conditions are shown.

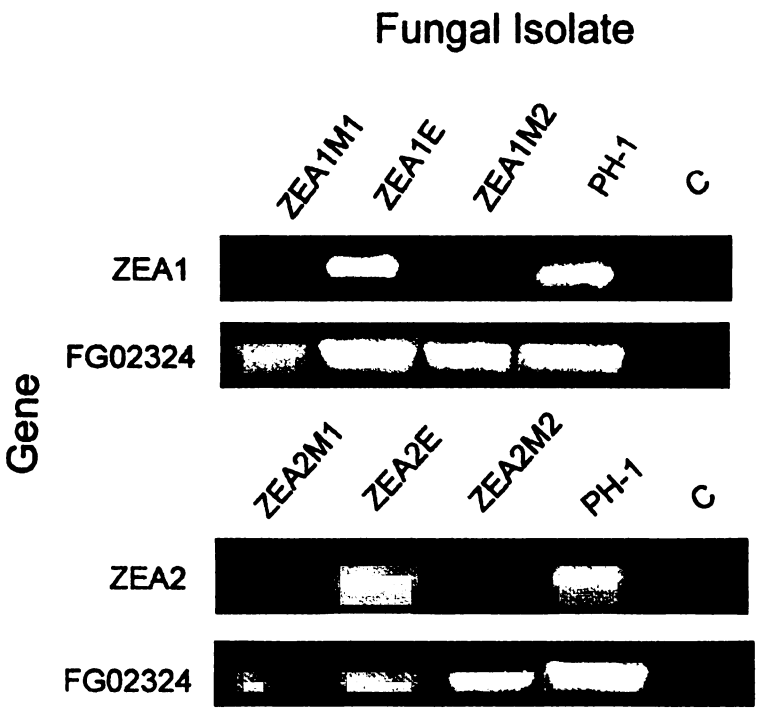

Figure 4. Expression analysis of *ZEA1* and *ZEA2* in disrupted mutants.
PCR analysis of expression of genes *ZEA1*, *ZEA2*, and FG02324 in *zea1* and *zea2* mutants and in PH-1 under zen-inducing conditions. C = no cDNA added; E = ectopic insertion.

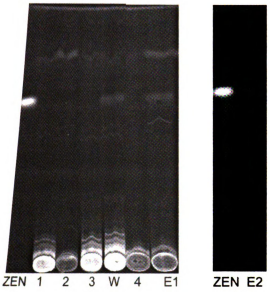

Figure 5. TLC analysis of ZEA1 and ZEA2 disruption mutants: ZEN = zen control; 1 = *zea1m1*; 2 = zea2m1; W = PH-1; 4 = zea2m2; E1 = zea1 ectopic control; E2 = zea2 ectopic control.

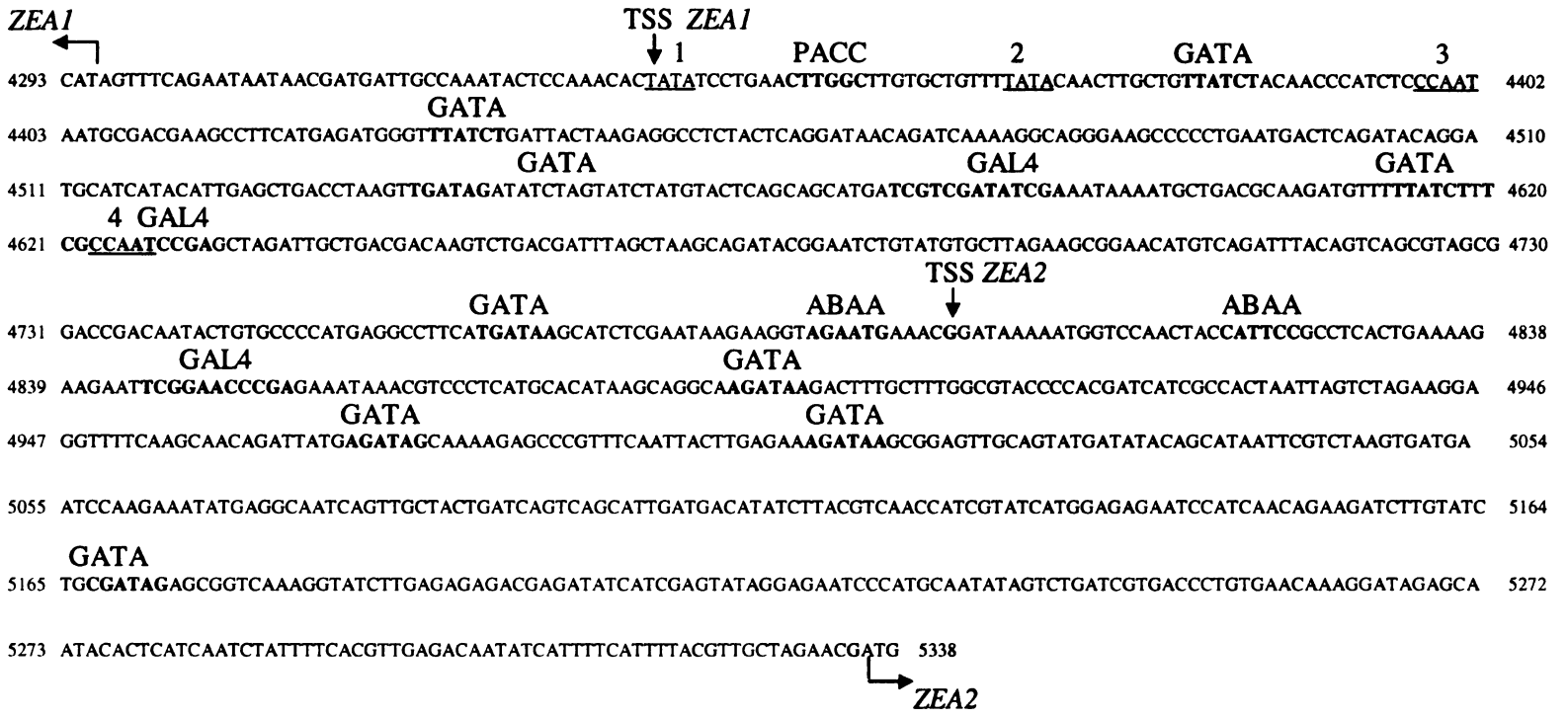

Figure 6. Analysis of the putative shared promoter region between the start codons of ZEA1 and ZEA2 spanning 1040 bp on contig 119. Consensus sequences of fungal transcription factor binding sites are indicated in bold script. The putative TSS (Transcription Start Site) for each gene is indicated by a vertical arrow. The TATA (1 and 2) and CCAAT (3 and 4) boxes are underlined

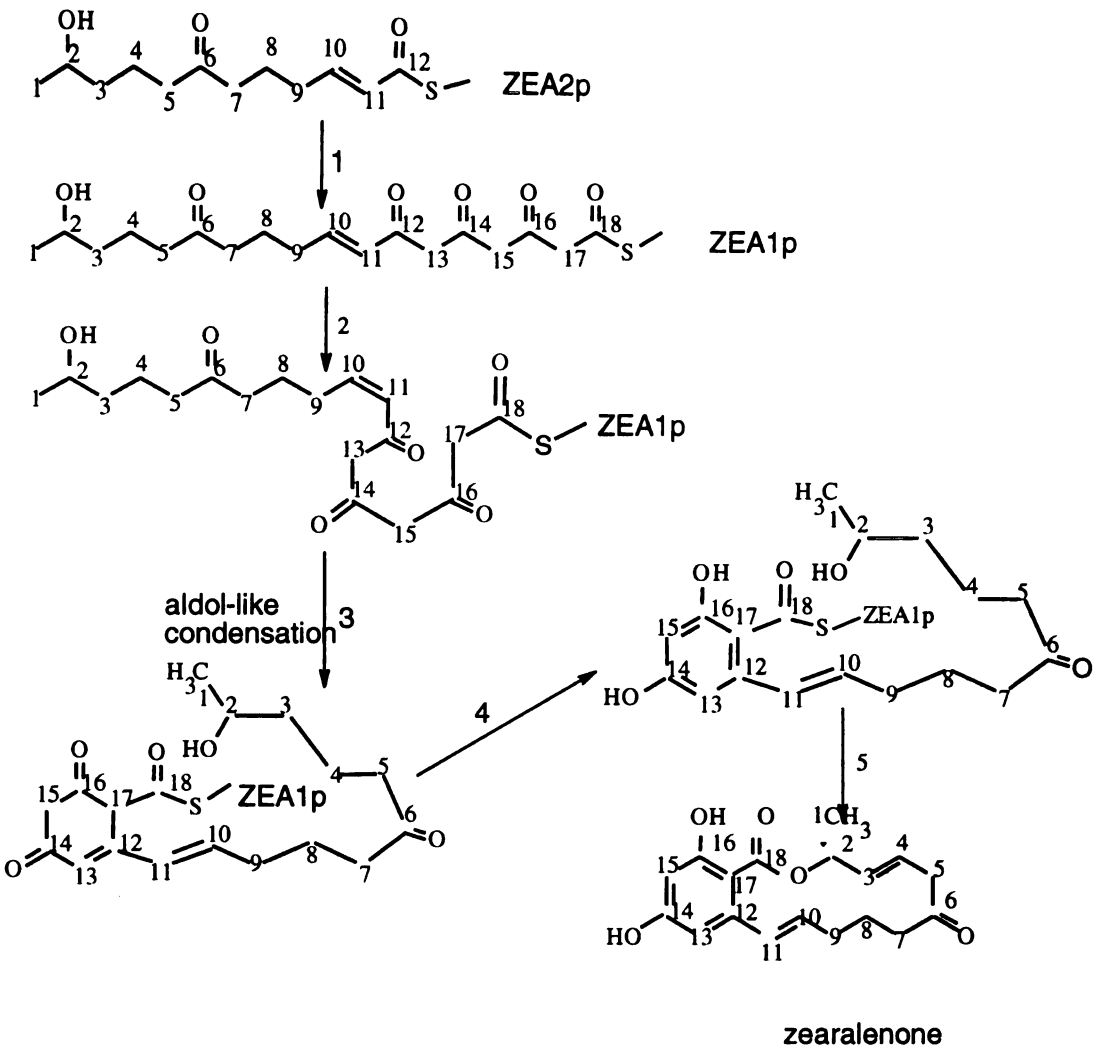

Figure 7. Proposed mechanism for zen biosynthesis by ZEA1p and ZEA2p.

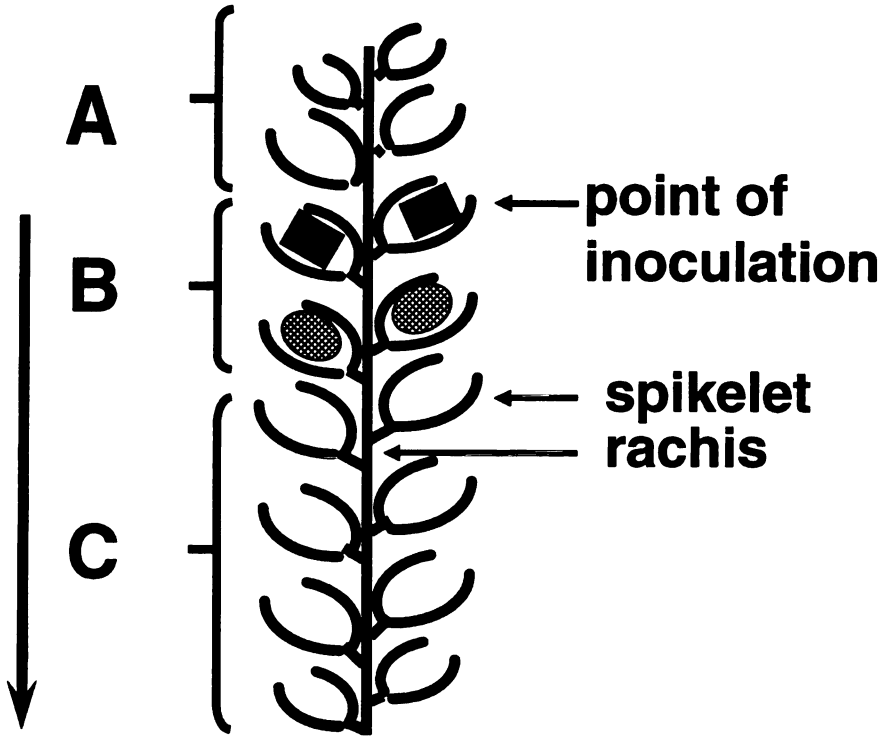

Figure 8. Diagrammatic representation of a *Triticum aestvum* wheat head comprising alternate parallel rows of spikelets separated by rachis segments. Agar plugs containing *F. graminearum* mycelium were inserted into the florets contained within the spikelets indicated by solid black squares. The 3 head regions used for the quantitative assessment of visible disease symptoms, grain number and grain quality are indicated: Region A, above the point of inoculation; Region B, inoculated spikelets and below those with bleached symptoms on glumes, lemma and palea (filled ovoid); Region C, below the point of inoculation and with no disease symptoms.

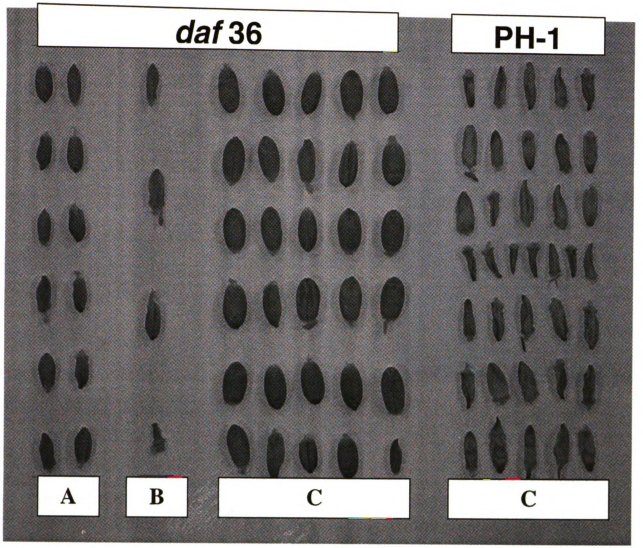

Figure 9. Macroscopic appearance of mature grain harvested from a single head infected with *daf* 36 and PH-1. For *daf* 36, seeds developing above (A) the point of inculation, (B) at the point of inoculation, and (C) below the point of inoculation are clustered. For PH-1, no grain was recovered from head regions

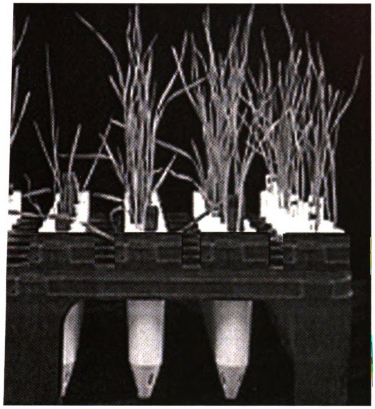

PH-1 ***daf*14** ***daf*15** **SNA**

Figure 10. A wheat seedling container test used to explore root infection by *F. graminearum*. Three wheat seed were planted in each container at the same time as the mycelium/conidia inoculum. The photograph was taken at 21days after inoculation with the parental strain PH-1 (left), the mutants *daf* 14 and *daf* 15 (middle) or with SNA only, as the control (right).

APPENDIX C

SOUTHERN ANALYSIS OF PKS DISRUPTED MUTANTS

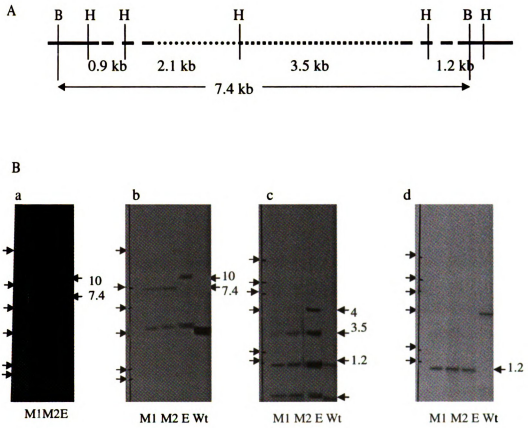

Figure 11. Disruption of *PKS11* by single-crossover homologous recombination.
A. Schematic of disruption vector (pPKS11) integrated in the chromosome at *PKS11*. The numbers represent the size of the predicted fragments. B, BstBI restriction sites; H, HindIII restriction sites; ——, genomic DNA; - - - - -, insert sequence used to generate pPKS11 disruption vector; ·····, pHYG4 vector used to generate pPKS11. M1 and M2, two independent disrupted mutants; E, ectopic mutant; Wt, wild type.
B. Southern analysis of genomic DNA from M1, M2, E and Wt digested with BstBI (**a** and **b**) and HindIII (**c** and **d**). Probes were generated with the insert sequence to pPKS11 (**a** and **c**) and an internal fragment of *hph1* (b and d). The arrows to the left of the Southern blots represent the molecular size markers in kb; 23.1, 9.4, 6.6, 4.4, 2.3 and 2.0 from top to bottom and sizes at the right indicate the hybridization signals for each isolate in kb.

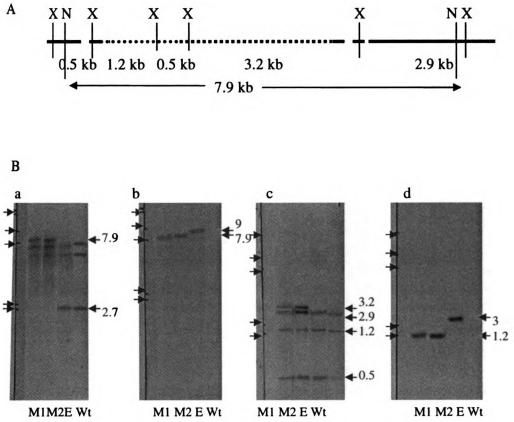

Figure 12. Disruption of *AUR1* by single-crossover homologous recombination.
A. Schematic of disruption vector (pAUR1) integrated in the chromosome at *AUR1*. The numbers represent the size of the predicted fragments. N, NruI restriction sites; X, XhoI restriction sites; ——, genomic DNA; - - - - -, insert sequence used to generate pAUR1 disruption vector; ·····, pHYG4 vector used to generate pAUR1. M1 and M2, two independent disrupted mutants; E, ectopic mutant; Wt, wild type.
B. Southern analysis of genomic DNA from M1, M2, E and Wt digested with NruI (**a** and **b**) and XhoI (**c** and **d**). Probes were generated with the insert sequence to pAUR1 (**a** and **c**) and an internal fragment of *hph1* (b and d). The arrows to the left of the Southern blots represent the molecular size markers in kb; 23.1, 9.4, 6.6, 2.3 and 2.0 from top to bottom and sizes at the right indicate the hybridization signals for each isolate in kb.

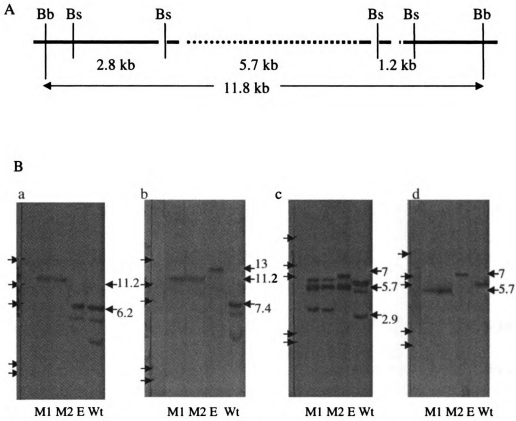

Figure 13. Disruption of *ZEA1* by single-crossover homologous recombination.
A. Schematic of disruption vector (pZEA1) integrated in the chromosome at *ZEA1*. The numbers represent the size of the predicted fragments. Bb, BbsI restriction sites; Bs, BseRI restriction sites; ——, genomic DNA; - - - -, insert sequence used to generate pZEA1 disruption vector; ——, pHYG4 vector used to generate pZEA1. M1 and M2, two independent disrupted mutants; E, ectopic mutant; Wt, wild type.
B. Southern analysis of genomic DNA from M1, M2, E and Wt digested with BbsI (**a** and **b**) and BseRI (**c** and **d**). Probes were generated with the insert sequence to pZEA1 (**a** and **c**) and an internal fragment of *hph1* (b and d). The arrows to the left of the Southern blots represent the molecular size markers in kb; 23.1, 9.4, 6.6, 2.3 and 2.0 from top to bottom and sizes at the right indicate the hybridization signals for each isolate in kb.

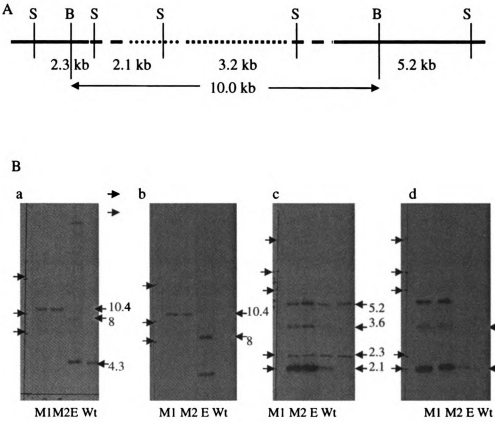

Figure 14. Disruption of *ZEA2* by single-crossover homologous recombination.
A. Schematic of disruption vector (pZEA2) integrated in the chromosome at *ZEA2*. The numbers represent the size of the predicted fragments. **B,** BsaBI restriction sites; **S,** SphI restriction sites; ——— , genomic DNA; - - - - -, insert sequence used to generate pZEA2 disruption vector; ..... , pHYG4 vector used to generate pZEA2. M1 and M2, two independent disrupted mutants; E, ectopic mutant; Wt, wild type.
B. Southern analysis of genomic DNA from M1, M2, E and Wt digested with BsaBI (**a** and **b**) and SphI (**c** and **d**). Probes were generated with the insert sequence to pZEA2 (**a** and **c**) and an internal fragment of *hph1* (b and d). The arrows to the left of the Southern blots represent the molecular size markers in kb; 23.1, 9.4, 6.6, 2.3 and 2.0 from top to bottom and sizes at the right indicate the hybridization signals for each isolate in kb.

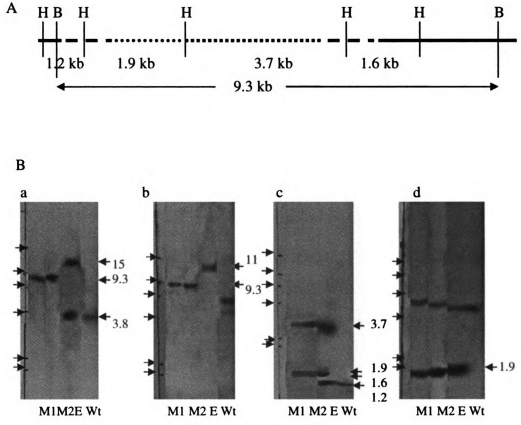

Figure 15. Disruption of *PKS17* by single-crossover homologous recombination.
A. Schematic of disruption vector (pPKS17) integrated in the chromosome at *PKS17*. The numbers represent the size of the predicted fragments. **B,** BsaBI restriction sites; **H,** HindIII restriction sites; ——, genomic DNA; - - - -, insert sequence used to generate pPKS17 disruption vector; ·····, pHYG4 vector used to generate pPKS17. M1 and M2, two independent disrupted mutants; E, ectopic mutant; Wt, wild type.
B. Southern analysis of genomic DNA from M1, M2, E and Wt digested with BsaBI (**a** and **b**) and HindIII (**c** and **d**). Probes were generated with the insert sequence to pPKS17 (**a** and **c**) and an internal fragment of *hph1* (b and d). The arrows to the left of the Southern blots represent the molecular size markers in kb; 23.1, 9.4, 6.6, 4.4, 2.3 and 2.0 from top to bottom and sizes at the right indicate the hybridization signals for each isolate in kb.

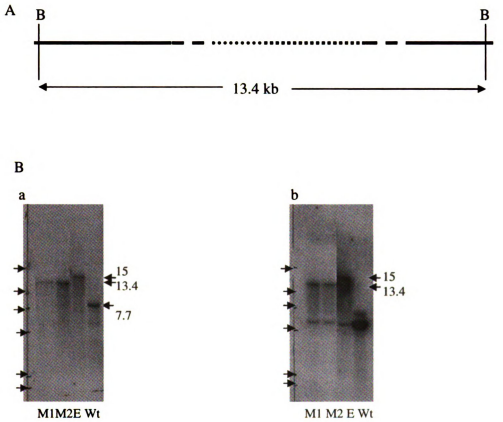

Figure 16. Disruption of *GRS1* by single-crossover homologous recombination.
A. Schematic of disruption vector (pGRS1) integrated in the chromosome at *GRS1*. The numbers represent the size of the predicted fragments. B, BstBI restriction sites; ——, genomic DNA; - - - - -, insert sequence used to generate pGRS1 disruption vector; ·····, pHYG4 vector used to generate pGRS1. M1 and M2, two independent disrupted mutants; E, ectopic mutant; Wt, wild type.
B. Southern analysis of genomic DNA from M1, M2, E and Wt digested with BstBI (**a** and **b**). Probes were generated with the insert sequence to pGRS1 (a) and an internal fragment of *hph1* (b). The arrows to the left of the Southern blots represent the molecular size markers in kb; 23.1, 9.4, 6.6, 4.4, 2.3 and 2.0 from top to bottom and sizes at the right indicate the hybridization signals for each isolate in kb.

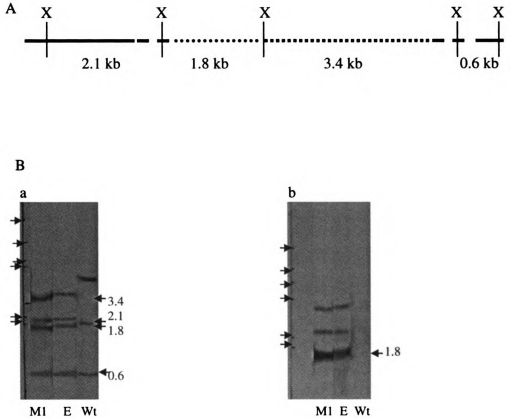

Figure 17. Disruption of *PLSP1* by single-crossover homologous recombination.
A. Schematic of disruption vector (pPLSP1) integrated in the chromosome at *PLSP1*. The numbers represent the size of the predicted fragments. **A**, AccI restriction sites; ——, genomic DNA; - - - - -, insert sequence used to generate pPLSP1 disruption vector; ·····, pHYG4 vector used to generate pPLSP1. M1, disrupted mutant; E, ectopic mutant; Wt, wild type.
B. Southern analysis of genomic DNA from M1, E and Wt digested with AccI (**a** and **b**). Probes were generated with the insert sequence to pPLSP1 (**a**) and an internal fragment of *hph1* (b). The arrows to the left of the Southern blots represent the molecular size markers in kb; 23.1, 9.4, 6.6, 4.4, 2.3 and 2.0 from top to bottom and sizes at the right indicate the hybridization signals for each isolate in kb.

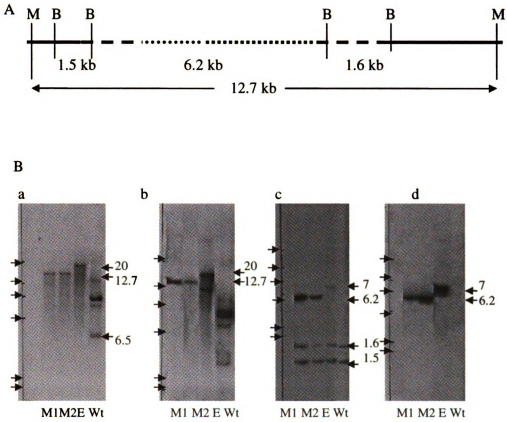

Figure 18. Disruption of *PKS2* by single-crossover homologous recombination.
A. Schematic of disruption vector (pPKS2) integrated in the chromosome at *PKS2*. The numbers represent the size of the predicted fragments. M, MluI restriction sites; **B,** BbsI restriction sites; ——, genomic DNA; - - - - -, insert sequence used to generate **pPKS2** disruption vector; ·····, pHYG4 vector used to generate pPKS2. M1 and M2, two independent disrupted mutants; E, ectopic mutant; Wt, wild type.
B. Southern analysis of genomic DNA from M1, M2, E and Wt digested with **MluI (a** and **b)** and BbsI (**c** and **d**). Probes were generated with the insert sequence to pPKS2 (**a** and **c**) and an internal fragment of *hph1* (b and d). The arrows to the left of the Southern blots represent the molecular size markers in kb; 23.1, 9.4, 6.6, 4.4, 2.3 and 2.0 from top to bottom and sizes at the right indicate the hybridization signals for each isolate in kb.

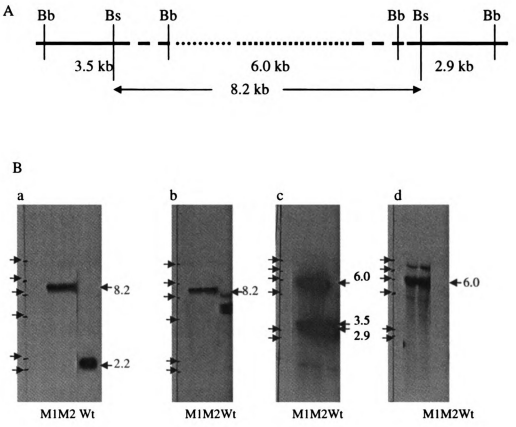

Figure 19. Disruption of *PKS5* by single-crossover homologous recombination.
A. Schematic of disruption vector (pPKS5) integrated in the chromosome at *PKS5*. The numbers represent the size of the predicted fragments. Bs, BstBI restriction sites; Bb, BbsI restriction sites; ____, genomic DNA; - - - - -, insert sequence used to generate pPKS2 disruption vector; ·····, pHYG4 vector used to generate pPKS5. M1 and M2, two independent disrupted mutants; Wt, wild type.
B. Southern analysis of genomic DNA from M1, M2, and Wt digested with BstBI (**a** and **b**) and BbsI (**c** and **d**). Probes were generated with the insert sequence to pPKS5 (**a** and **c**) and an internal fragment of *hph1* (b and d). The arrows to the left of the Southern blots represent the molecular size markers in kb; 23.1, 9.4, 6.6, 4.4, 2.3 and 2.0 from top to bottom and sizes at the right indicate the hybridization signals for each isolate in kb.

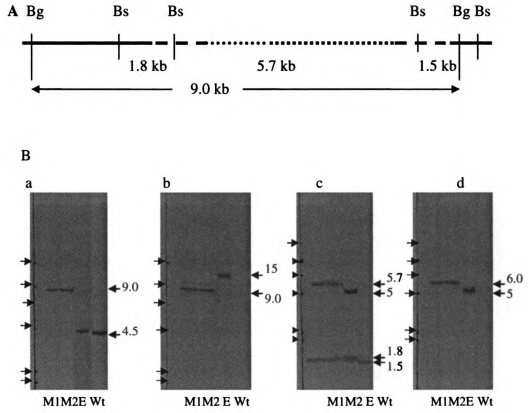

Figure 20. Disruption of *GzFUS1* by single-crossover homologous recombination.
A. Schematic of disruption vector (pGzFUS1) integrated in the chromosome at *GzFUS1*. The numbers represent the size of the predicted fragments. Bg, BglII restriction sites; Bs, BsaBI restriction sites; ——, genomic DNA; - - - - -, insert sequence used to generate pGzFUS1 disruption vector; ·····, pHYG4 vector used to generate pGzFUS1. M1 and M2, two independent disrupted mutants; E, ectopic mutant; Wt, wild type.
B. Southern analysis of genomic DNA from M1, M2, E and Wt digested with BglII (**a** and **b**) and BsaBI (**c** and **d**). Probes were generated with the insert sequence to pGzFUS (**a** and **c**) and an internal fragment of *hph1* (b and d). The arrows to the left of the Southern blots represent the molecular size markers in kb; 23.1, 9.4, 6.6, 4.4, 2.3 and 2.0 from top to bottom and sizes at the right indicate the hybridization signals for each isolate in kb.

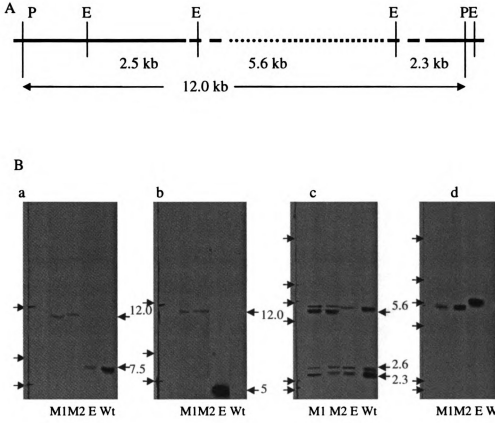

Figure 21. Disruption of *PKS6* by single-crossover homologous recombination.
A. Schematic of disruption vector (pPKS6) integrated in the chromosome at *PKS6*. The numbers represent the size of the predicted fragments. **P,** PpuMI restriction sites; **E,** EcoNI restriction sites; ——, genomic DNA; - - - - -, insert sequence used to generate pPKS6 disruption vector; ……, pHYG4 vector used to generate pPKS6. M1 and M2, two independent disrupted mutants; E, ectopic mutant; Wt, wild type.
B. Southern analysis of genomic DNA from M1, M2, E and Wt digested with PpuMI (**a** and **b**) and EcoNI (**c** and **d**). Probes were generated with the insert sequence to pPKS6 (**a** and **c**) and an internal fragment of *hph1* (b and d). The arrows to the left of the Southern blots represent the molecular size markers in kb; 23.1, 9.4, 6.6, 4.4, 2.3 and 2.0 from top to bottom and sizes at the right indicate the hybridization signals for each isolate in kb.

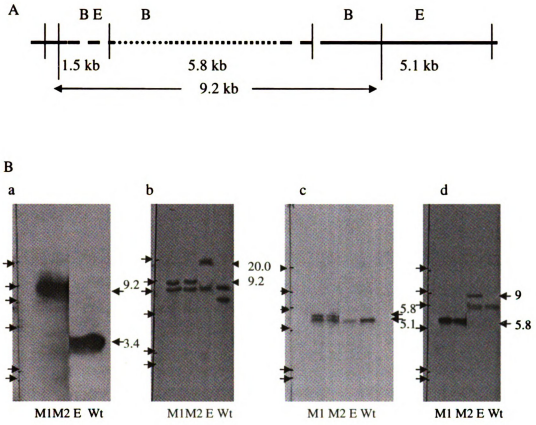

Figure 22. Disruption of *PKS7* by single-crossover homologous recombination.
A. Schematic of disruption vector (pPKS7) integrated in the chromosome at *PKS7*. The numbers represent the size of the predicted fragments. E, EcoNI restriction sites; **B,** BstBI restriction sites; ——, genomic DNA; - - - - -, insert sequence used to generate pPKS7 disruption vector; ……, pHYG4 vector used to generate pPKS7. M1 and M2, two independent disrupted mutants; E, ectopic mutant; Wt, wild type.
B. Southern analysis of genomic DNA from M1, M2, E and Wt digested with EcoNI (**a** and **b**) and BstBI (**c** and **d**). Probes were generated with the insert sequence to pPKS7 (**a** and **c**) and an internal fragment of *hph1* (b and d). The arrows to the left of the Southern blots represent the molecular size markers in kb; 23.1, 9.4, 6.6, 4.4, 2.3 and 2.0 from top to bottom and sizes at the right indicate the hybridization signals for each isolate in kb.

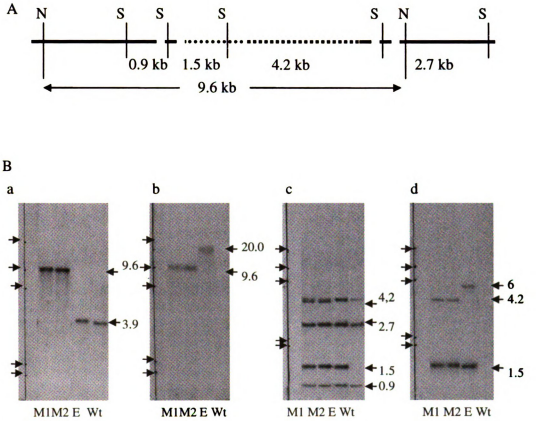

Figure 23. Disruption of *PLG1* by single-crossover homologous recombination.
A. Schematic of disruption vector (pPGL1) integrated in the chromosome at *PGL1*. The numbers represent the size of the predicted fragments. N, NruI restriction sites; S, SphI restriction sites; ____, genomic DNA; - - - - -, insert sequence used to generate pPGL1 disruption vector; ..... , pHYG4 vector used to generate pPGL1. M1 and M2, two independent disrupted mutants; E, ectopic mutant; Wt, wild type.
B. Southern analysis of genomic DNA from M1, M2, E and Wt digested with NruI (**a** and **b**) and SphI (**c** and **d**). Probes were generated with the insert sequence to pPGL1 (**a** and **c**) and an internal fragment of *hph1* (b and d). The arrows to the left of the Southern blots represent the molecular size markers in kb; 23.1, 9.4, 6.6, 2.3 and 2.0 from top to bottom and sizes at the right indicate the hybridization signals for each isolate in kb.

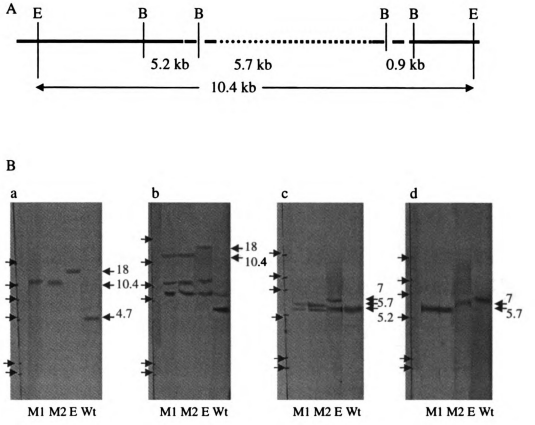

Figure 24. Disruption of *PKS9* by single-crossover homologous recombination.
A. Schematic of disruption vector (pPKS9) integrated in the chromosome at *PKS9*. The numbers represent the size of the predicted fragments. **E,** EcoNI restriction sites; **B,** BseRI restriction sites; ——, genomic DNA; - - - - -, insert sequence used to generate pPKS9 disruption vector; ·····, pHYG4 vector used to generate pPKS9. M1 and M2, two independent disrupted mutants; E, ectopic mutant; Wt, wild type.
B. Southern analysis of genomic DNA from M1, M2, E and Wt digested with EcoNI (**a** and **b**) and BseRI (**c** and **d**). Probes were generated with the insert sequence to pPKS9 (**a** and **c**) and an internal fragment of *hph1* (b and d). The arrows to the left of the Southern blots represent the molecular size markers in kb; 23.1, 9.4, 6.6, 4.4, 2.3 and 2.0 from top to bottom and sizes at the right indicate the hybridization signals for each isolate in kb.

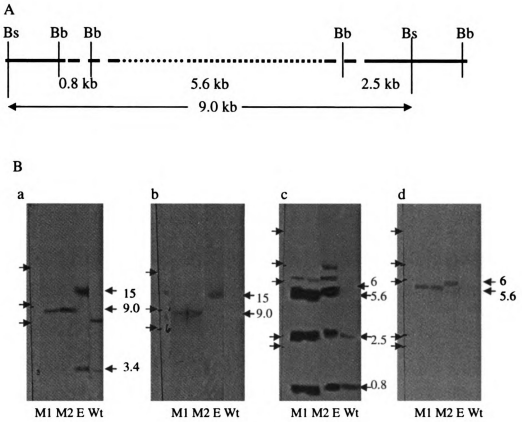

Figure 25. Disruption of *PKS1* by single-crossover homologous recombination.
A. Schematic of disruption vector (pPKS1) integrated in the chromosome at *PKS1*. The numbers represent the size of the predicted fragments. Bs, BsaBI restriction sites; Bb, BbsI restriction sites; ____ , genomic DNA; -----, insert sequence used to generate pPKS1 disruption vector; —— , pHYG4 vector used to generate pPKS1. M1 and M2, two independent disrupted mutants; E, ectopic mutant; Wt, wild type.
B. Southern analysis of genomic DNA from M1, M2, E and Wt digested with BsaBI (**a** and **b**) and BbsI (**c** and **d**). Probes were generated with the insert sequence to pPKS1 (**a** and **c**) and an internal fragment of *hph1* (b and d). The arrows to the left of the Southern blots represent the molecular size markers in kb; 23.1, 9.4, 6.6, 2.3 and 2.0 from top to bottom and sizes at the right indicate the hybridization signals for each isolate in kb.

APPENDIX D

EJECTION MECHANICS AND TRAJECTORY OF THE ASCOSPORES OF *Gibberella zeae* (ANAMORPH *Fusarium graminearum*)

Trail, F., I. Gaffoor, and S. Vogel. 2005. Ejection mechanics and trajectory of the ascospores of *Gibberella zeae* (anamorph *Fuarium graminearum*). Fungal Genetics and Biology **42:**528-533.

Sexual reproduction in *G. zeae* results in the formation of meiotic ascospores within asci which are saclike structures. Numerous asci are enclosed within a perithecium which is an enclosed fruiting body. At maturity the ascospores are forcibly ejected from the asci. Since the boundary layer of air surrounding the perithecia are relatively still, the spores need to achieve sufficient acceleration to escape this boundary layer so that the spores reach the air currents above so that the spores can be dispersed widely.

This study describes the analysis of ascus function and the source of turgor pressure. My contribution to this study consisted of determining the average volume of asci.

Available online at www.sciencedirect.com
SCIENCE DIRECT®
Fungal Genetics and Biology 42 (2005) 528–533
FUNGAL GENETICS AND BIOLOGY
www.elsevier.com/locate/yfgbi

Ejection mechanics and trajectory of the ascospores of *Gibberella zeae* (anamorph *Fuarium graminearum*)

Frances Trail [a,*], Iffa Gaffoor [a], Steven Vogel [b]

[a] *Departments of Plant Biology and Plant Pathology, Michigan State University, East Lansing, MI 48824, USA*
[b] *Department of Biology, Duke University, Durham, NC 27708, USA*

Received 2 September 2004; accepted 15 March 2005

Abstract

Since wind speed drops to zero at a surface, forced ejection should facilitate spore dispersal. But for tiny spores, with low mass relative to surface area, high ejection speed yields only a short range trajectory, so pernicious is their drag. Thus, achieving high speeds requires prodigious accelerations. In the ascomycete *Gibberella zeae*, we determined the launch speed and kinetic energy of ascospores shot from perithecia, and the source and magnitude of the pressure driving the launch. We asked whether the pressure inside the ascus suffices to account for launch speed and energy. Launch speed was 34.5 m s^{-1}, requiring a pressure of 1.54 MPa and an acceleration of 870,000 g—the highest acceleration reported in a biological system. This analysis allows us to discount the major sugar component of the epiplasmic fluid, mannitol, as having a key role in driving discharge, and supports the role of potassium ion flux in the mechanism.

Keywords: Ascospore discharge; Perithecia; Turgor pressure; Mannitol; Reynolds number; Stokes' Law

1. Introduction

Forcible discharge of ascospores forms the basis of spore dispersal in the Ascomycota, the largest group of fungi. Yet despite the importance of this phenomenon, little is known of its mechanism. Nearly 100 years ago, Buller (1909) studied the forcible ejection of ascospores in *Ascobolus immersus*. He observed fluid accompanying the ejection and predicted the behavior of the spores once launched from the ascus. Ingold (1966, 1971) studied spore discharge in many groups of fungi and speculated that glucose and ions were required to generate the turgor force for discharging ascospores in *Sordaria fimicola*. Our goal is to understand the physiological and genetic basis of the mechanism of forcible ascospore discharge in the Pyrenomycete *Gibberella zeae* (Schw.) Petch (anamorph *Fusarium graminearum* Schwabe). Towards this end, we recently characterized the contents of the epiplasmic fluid accompanying the discharged spores and hypothesized that both mannitol and potassium ions were involved in forcible discharge based on analysis of epiplasmic sap by gas chromatography/mass spectrometry and on pharmacological studies (Trail et al., 2002). By contrast, Fischer et al. (2004) used these GC/MS techniques to identify glycerol as the major sugar component of epiplasmic fluid in the apothecium-forming fungus *A. immersus*.

In *G. zeae*, a wheat pathogen which relies on forcible ejection to initiate the transfer of ascospores from the field debris to wheat flowers, asci are contained in a flask-shaped perithecium (Fig. 1; Booth, 1971; Shaner, 2003). Within the perithecium, asci extend singly and in succession to the ostiole to discharge their contents of spores and fluid into the air (Trail and Common,

* Corresponding author. Fax: +1 517 353 1926.
E-mail address: trail@msu.edu (F. Trail).

1087-1845/$ - see front matter © 2005 Elsevier Inc. All rights reserved.
doi:10.1016/j.fgb.2005.03.008

2000; Trail et al., 2002). Although light is important for stimulating perithecium development (Tschanz et al., 1975), ascospore discharge is only mildly increased in the presence of light (Trail et al., 2002). Unlike fruiting bodies of some other ascomycetes [the perithecial necks of *S. fimicola*, (Ingold and Hadland, 1959), for example], those of *G. zeae* do not orient to light to eject their spores.

Here, we continue our analysis of ascus function in *G. zeae*, asking about the source of turgor pressure in these asci. From determinations of shooting range, we estimated the launch speed and kinetic energy of the ascospores. We also determined the source and magnitude of the pressure generated by the osmolytes within the ascus. We then asked whether that pressure suffices to account for launch speed and energy. Our findings show that mannitol is not sufficient to generate the pressure for discharge of the eight ascospores, but the potassium and chloride ions in the fluid would generate the required turgor pressure.

2. Methods

2.1. Ascus measurements, shooting distance, and spore mass

Mature perithecia of *G. zeae* strain PH-1 (FGSC 9075, NRRL 31084), prepared as previously described (Trail and Common, 2000), were placed in water, gently crushed between a slide and cover slip, stained with Calcofluor White, and observed with a Laser Scanning Confocal microscope (Zeiss LSM 210, Germany). The length and the width at 7–8 points of 10 mature asci (Fig. 1C) were measured using image analysis software (LSM version 2.1, Opton Feintechnik GmbH). Standard calculus was applied to calculate the volume. Measurements of the central perithecium cavity from base of asci to ostiole were taken from sections (6 μm thick) through mature perithecia cryofixed in isopentane at approximately −60 °C, affixed to slides and mounted in Gel/Mount (Biomedia, Foster City, CA). Measurements of sections through the center of six perithecia were used to generate the average length of an extended ascus reaching the ostiole. The volume of the extended ascus (Figs. 1A and B) was estimated assuming the ascus maintained an average diameter when extending to the ostiole.

To measure horizontal distance of spore discharge, a glass chamber was constructed as previously described (Aylor and Anagnostakis, 1991) to minimize free convection. A block of agar containing mature perithecia was mounted in the chamber so that spores were ejected horizontally down the length of the chamber onto a removable glass coverslip. Range of spores was then measured microscopically.

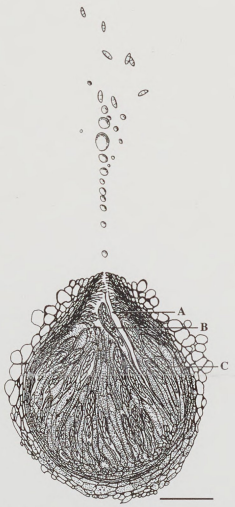

Fig. 1. Longitudinal section through a mature perithecium of *G. zeae*. An ascus retracting following ejection of spores and fluid (A); a mature ascus, extending upward to the end of the ostiolar canal to discharge (B); and a mature, unextended ascus (C). Bar = 50 μm. Rendering based on previous investigations (Trail and Common, 2000).

Spore mass was estimated to be 2.02×10^{-13} kg, calculated from volume and density as follows. We estimated mass of the ascospores from volume and density. *G. zeae* has an average spore length of 21 μm and diameter of 3.5 μm (Booth, 1971). We adopted a cylindrical shape for volume calculation and assumed the density of water, 1000 kg m^{-3}, as an estimate of spore density. A cylindrical shape overestimates volume, since the spores taper at their ends, while using water's density most likely underestimates density since spores normally sink in water. Buller (1909) found densities of basidiospores to vary from slightly higher than water to as much as 20% higher. The lighter spores contained visible oil droplets, as do the ascospores of *G. zeae*. Direct measurement of spores as they are discharged from the ascus was not possible due to the rapid evaporation of fluid as spores are released.

2.2. Concentrations of mannitol, K^+, and Cl^-

Epiplasmic fluid was collected and sugar components identified as previously described (Trail et al., 2002). Mannitol concentration was determined by GC/mass spectrometry in comparison to known standards (Trail et al., 2002). The potassium ion (^{39}K) concentration in epiplasmic fluid was determined by Inductively Coupled Plasma Mass Spectrometry (Micromass Platform; ICP-MS) using a Meinhard concentric nebulizer as the sample introduction system. Before data acquisition, the ICP-MS was optimized while running a standard solution containing 10 μg/L of Be, Co, In, Ce, Bi, and U using indium as the internal standard. The concentration was calculated based on linear regression of standard solutions.

2.3. Effective radii of spores

The following formulas (Cox, 1970) were used to approximate the drag of cylinders or long ellipsoids with their long axes normal and parallel to flow, respectively.

$$D = \frac{4\pi\mu v l}{\ln(l/a) + 0.193} \quad \text{and}$$

$$D = \frac{2\pi\mu v l}{\ln(l/a) + 0.807},$$

where l and a are length and radius, respectively, of cylinder or ellipsoid.

2.4. Computing trajectories

A diameter of 9.27 μm, a density of 1000 kg m^{-3}, an iterative interval of 20 μs, a launch pitch angle of 0°, a landing height (which mattered little) of 10 mm below launch height, and a range of launch speeds were used as inputs for the computer program (Vogel, 1988) used to determine trajectories.

3. Results

3.1. Minimal pressure for ejection of ascospores

The minimal pressure required for ejection of ascospores was estimated by equating pressure–volume change ($p\Delta V$) of launch with the kinetic energy ($mv^2/2$; m: mass, v: speed) of the spores launched. Acceleration within the ascus was estimated from ascus dimensions and launch speed ($v^2/2l$; l: length), assuming constant acceleration.

The average length of a mature ascus was 0.076 mm (standard deviation 0.0030). From that length and from measurements of diameter, the average ascus volume at maturity (Fig. 1C) was calculated to be 3.72×10^{-15} m^3 (standard deviation 7.8×10^{-16}). Asci stretched to approximately 0.159 mm to release spores into the air (Figs. 1A and B), resulting in 8.12×10^{-15} m^3 as the estimated volume of the extended ascus (Fig. 1B). Spore volume encompassed 1.61×10^{-15} m^3, leaving 2.10×10^{-15} m^3 for the epiplasmic fluid in the mature ascus, and 6.52×10^{-15} m^3 in the extended ascus. Spores clustered in the upper portion of the mature ascus, with an acceleration distance of 0.070 mm (standard deviation 0.003 mm).

Launch speed was determined from the range of the projectiles (Fig. 2). Direct photographic determination of launch speed was not possible due to the initial speeds of over a million body lengths per second (determined by dividing launch speed by spore length), the small size of the spores, and the unpredictability of spore release. Accounting for drag requires knowledge of both shape and drag coefficient; with the extreme changes of speed, the latter varies over the course of the trajectory. A spore was assumed to tumble in flight. With no obvious stabilizing structures, this seemed a conservative assumption and it is supported by the photographic observations of the late Robert M. Page (1964 and personal communication) that *Pilobolus* sporangia tumble after release. A tumbling spore would incur a drag about equal to the average of a cylinder travelling cross-wise to flow and one travelling parallel to its long axis (see Section 2). The average of these was set equal to the drag of a sphere as given by Stokes' law, $D = 6\pi\mu av$ (μ: room temperature air viscosity, about 18×10^{-6} Pa s; a: radius), permitting estimation of the diameter of an equivalent sphere from the dimensions of a spore. The Reynolds number, a parameter that indicates the general character of such flows, $Re = \rho dv/\mu$, was determined using that diameter and, ρ, the density of air at room temperature (1.2 kg m^{-3}). That, in turn, was used in a semi-empirical equation for the drag coefficient of

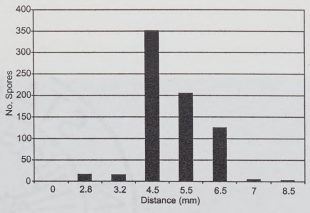

Fig. 2. Number of ascospores discharged to various distances in still air. Total number of spores accumulating within a band extending 0.6 mm on either side of distance shown. Combined results from a total of 720 spores assessed from seven independent trials.

spheres based on maximal cross-sectional area, S (White, 1974),

$$C_d = \frac{24}{Re} + \frac{6}{1 + Re^{1/2}} + 0.4,$$

where $D = C_d \rho S v^2/2$. Note that the term, $24/Re$, corresponds to Stokes' law.

Using these formulas, though, requires knowing speed—which is what we wanted to find. Moreover, drag will cause speed to decrease rapidly after launch. Thus, we used an iterative approach together with successive approximations to work back from mean distance travelled to launch speed. A version of an earlier computer program (Vogel, 1988), using the formula above, gave a trajectory based on 3000 successive points equally spaced in time. At each point, drag coefficient and drag were calculated and used to get new values of speed and direction. Launch speed for a horizontal range of 4.6 mm turned out to be 34.5 m s^{-1}. While some spores travelled further, possible assistance by air currents suggested using this more conservative figure.

From that launch speed and the distance of 0.07 mm, the average acceleration of a spore prior to launch is 8.5×10^6 m s^{-2} or 870,000g. From that launch speed and spore mass, the energy imparted to an individual spore comes to 1.2×10^{-10} J. Assuming the ascus empties in launch and assuming the volume given above, the launch energy requires a pressure of 185 kPa. To launch eight spores would take a pressure of 1.48 MPa. To launch eight spores plus the epiplasm requires slightly more—1.54 MPa. These pressures, of course, represent minimal estimates, assuming such idealizations as no pressure drop during the course of launch, perfectly unidirectional shooting, and no other losses. Calculations based on an estimate of spore cross sections and force gave essentially the same results.

3.2. Identification and quantification of the osmolytes in the epiplasmic fluid

When spores are discharged from asci of *G. zeae*, droplets of epiplasmic fluid accompany the projectiles (Fig. 1; Trail et al., 2002). Analysis of this fluid revealed the presence of three major osmolytes: mannitol, K^+, and Cl^-. The concentration of mannitol in the discharged epiplasmic fluid was determined to be 4.7×10^{-12} g per ascus (standard deviation 2.2×10^{-12}). The concentration of mannitol in the epiplasmic fluid would be approximately 0.012 M in the mature ascus before it begins to extend (Fig. 1C). This concentration will generate 0.029 MPa (Davis et al., 2000), insufficient pressure for discharging the spores and fluid.

Using ICP-MS analysis, we found the concentration of K^+ ions in the epiplasmic fluid to be 4.72×10^{-11} µg per ascus, or 0.57 M in the mature ascus (Fig. 1C) and 0.18 M in the fully extended ascus (Figs. 1A and B). The corresponding pressure is 1.4 MPa in the former and 0.45 in the latter. Associated with potassium ions is the Cl^- counterion. Measurements of the counterion by a chloride electrode indicated a final concentration of 0.192 M in the unextended ascus, corresponding to a pressure of 0.46 MPa. These pressures, while a little lower than that calculated as necessary, are reasonably close, given the assumptions involved (see Section 4).

4. Discussion

From the measurements of osmolyte concentrations and the calculations of minimal pressures to propel eight spores, we can infer that mannitol may be used as a source of energy, or as a "pump-priming" mechanism to initiate ascus enlargement, but we can eliminate it as *the* osmolyte sufficient to generate the turgor pressure necessary for discharge. Potassium, the main osmolyte in the epiplasmic fluid, is likely to provide the osmoticum for spore discharge in *G. zeae* along with chloride. Parasitic organisms and saprophytes growing on plant debris are in potassium-rich environments, as potassium has been sequestered in the host tissues (Benito et al., 2002). Therefore, the environment where perithecia are formed is likely to be potassium rich, not potassium limited.

The predicted spore trajectory appears in Fig. 3. It divides into two almost entirely distinct portions. Drag overwhelmingly dominates the first, causing rapid deceleration (initially at about 3×10^5 m s^{-2}, or about 30,000 times that of gravity). Distance depends minimally on launch angle, with maximum horizontal range occurring with near-horizontal launches. In the second phase, the spore falls vertically at constant speed as the forces of drag and gravity quickly come into balance. Terminal velocity and impact speed, 2.58 mm s^{-1}, is over 10,000 times lower than launch speed. In the field, the spore

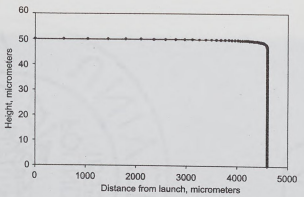

Fig. 3. Spore trajectory. 20 µs intervals between points, 34.5 m s^{-1} initial speed, 2.58 mm s^{-1} impact speed.

would ordinarily reach air moving well above this latter speed by the end of the first portion.

The average pre-launch acceleration of 8,500,000 m s^{-2} (or almost 870,000 times that of gravity) far exceeds the highest value of acceleration reported in a biological system, the nematocyst discharge in the coelenterate, *Hydra* (Holstein and Tardent, 1984), 400,000 m s^{-2} (propelled by a pressure of 15 MPa; Tardent, 1995). It exceeds by almost a 100-fold that of the sporangium of the best-known ballistic fungus, *Pilobolus* (Vogel, 1988). Still, one should perhaps restrain one's awe at such high values of acceleration. By Newton's second law, acceleration is force divided by mass. Force, whether one considers achievable pressures or the tension a muscle can exert, should scale very roughly with the square of the length of the system. Mass, reflecting volume, should scale with the cube of length. Thus acceleration will vary inversely with length, and small systems should yield very high values. In compensation, as it were, they accelerate over shorter distances and therefore achieve final velocities comparable to those of larger ones.

Not only is the predicted acceleration higher than any previous biological datum, but so also is the launch speed relative to the length of the moving object, 1.7 million. A few living systems do achieve higher absolute speeds. Especially fast birds, such as diving falcons (Tucker et al., 1998), and the explosively discharged seeds of a euphorb, *Hura crepitans* (Swaine and Beer, 1977), reach or perhaps exceed 50 m s^{-1}, but they are far larger than *Gibberella* spores. The 40-μm spore clusters of the perithecium-forming fungus *Sordaria*, from our calculations based on data of Ingold and Hadland (1959) come closest, with launch speeds around 30 m s^{-1} and thus a speed-to-length ratio of 750,000 s^{-1}.

Stokes' law has long been regarded as unreliable above a Reynolds number of one, and various formulas can be found in the literature of fluid mechanics that extend its predictions of drag as a function of Reynolds number above that value, with results that correspond closely with direct measurements. In *G. zeae*, with an initial Reynolds number of about 20, based on the diameter of an equivalent sphere, using Stokes' law results in a 2.6-fold underestimate of drag. Thus, the launch speed needed to achieve the observed range would be nearly 2.6-fold lower with the use of Stokes' law. The present iterative approach, however awkward, thus seems preferable to any explicit single calculation based on Stokes' law. It predicts, for instance, a launch speed several times greater for the eight-ascospore projectile of *A. immersus*, for which the Reynolds number is about 300, than that estimated by Fischer et al. (2004).

A pressure probe and a microprobe device were used to measure pressure at the wall of the ascus in *A. immersus* and glycerol was identified as the major sugar derivative in the epiplasmic sap (the presence of ions was not explored; Fischer et al., 2004). This approach is not possible in perithecia-forming fungi, as the asci will not reliably discharge following the destruction of the perithecium (essential to using the probe), so access to discharging asci is not possible. Furthermore, the small size of the asci in *G. zeae* prohibits the use of this technology.

In well-studied systems, ascospores are discharged most prominently in association with high humidity (MacHardy, 1996; McOnie, 1964; Pinkerton et al., 1998; Shaner, 2003). A mechanism that relies on free water for discharge of spores would be beneficial to the fungus, as it ensures that spores are dispersed during optimal conditions for germination. A feature of many of the perithecial fungi is the formation of cirrhi, spores exuded *en masse* from the ostiole. In the present system, this occurs under drier conditions, when active discharge is not optimal (Trail et al., 2002). We hypothesize that mannitol serves two functions: it is generated and accumulates as the ascus matures and, in the presence of sufficient moisture, initiates membrane stretching, which activates the ion channels that trigger rapid discharge. If conditions for forcible discharge are not optimal (low relative humidity), the mannitol accumulates sufficiently to force the extrusion of the spores from the perithecium as a cirrhus. Experiments are underway to generate genetic mutants of genes important to ion transport and to mannitol biosynthesis to test our model of discharge.

Acknowledgments

We thank Ken Nadler and C.C. Trail for insightful discussions, Chil Kwon for determining launch distance, Lina Patina for assisting with the ICP-MS analysis, and Marlene Cameron for rendering Fig. 1. Funding for this work was provided by grants from the USDA Wheat and Barley Scab Initiative and USDA-NRICGP (2001-35319-10898) and by the Michigan Agricultural Experiment Station to F.T.

References

Aylor, D.E., Anagnostakis, S.L., 1991. Active discharge distance of ascospores of *Venturia inaequalis*. Phytopathology 81, 548–551.

Benito, B., Garciadeblas, B., Rodriguez-Navarro, A., 2002. Potassium- or sodium-efflux ATPase, a key enzyme in the evolution of fungi. Microbiology 148, 933–941.

Booth, C., 1971. The Genus *Fusarium*. CMI, London.

Buller, A.H.R., 1909. Researches on Fungi, vol. 1. Longman's Green and Co., New York.

Cox, R.G., 1970. The motion of long, slender bodies in a viscous fluid. Part I. General theory. J. Fluid Mech. 44, 791–810.

Davis, D.J., Burlak, C., Money, N.P., 2000. Osmotic pressure of fungal compatible osmolytes. Mycol. Res. 104, 800–804.

Fischer, M., Cox, J., Davis, D.J., Wagner, A., Taylor, R., Huerta, A.J., Money, N.P., 2004. New information on the mechanism of forcible

ascospore discharge from *Ascobolus immersus*. Fung. Genet. Biol. 41, 698–707.
Holstein, T., Tardent, P., 1984. An ultrahigh-speed analysis of exocytosis: nematocyst discharge. Science 223, 830–832.
Ingold, C.T., 1966. Aspects of spore liberation: violent discharge. In: Madelin, M.F. (Ed.), The Fungus Spore, Proceedings of the Eighteenth Symposium of the Colston Research Society, Bristol, England. Buttersworths, London, pp. 113–132.
Ingold, C.T., 1971. Fungal Spores: Their Liberation and Dispersal. Clarendon Press, Oxford.
Ingold, C.T., Hadland, S.A., 1959. The ballistics of *Sordaria*. New Phytol. 58, 46–57.
MacHardy, W.E., 1996. Apple Scab: Biology, Epidemiology and Management. APS Press, St. Paul, 545 pp.
McOnie, K.C., 1964. Orchard development and discharge of ascospores of *Guignardia citricarpa* and the onset of infection in relation to the control of citrus black spot. Phytopathology 54, 1448–1453.
Page, R.M., 1964. Sporangium discharge in *Pilobolus*: a photographic study. Science 146, 925–927.
Pinkerton, J.N., Johnson, K.B., Stone, J.K., Ivors, K.L., 1998. Factors affecting the release of ascospores of *Anisogramma anomala*. Phytopathology 88, 122–128.
Shaner, S., 2003. Epidemiology of Fusarium head blight of small grain cereals in North America. In: Leonard, K.J., Bushnell, W.R. (Eds.), Fusarium Head Blight of Wheat and Barley. APS Press, St. Paul, pp. 84–119.
Swaine, M.D., Beer, T., 1977. Explosive seed dispersal in *Hura crepitans*, L. (Euphorbiaceae). New Phytol. 78, 695–708.
Tardent, P., 1995. The cnidarian cnidocyte, a high-tech cellular weaponry. BioEssays 17, 351–362.
Trail, F., Xu, H., Loranger, R., Gadoury, D., 2002. Physiological and environmental aspects of ascospore discharge in *Gibberella zeae* (anamorph *Fusarium graminearum*). Mycologia 94, 181–189.
Trail, F., Common, R., 2000. Perithecium development in *Gibberella zeae*: a light microscopy study. Mycologia 92, 130–138.
Tschanz, A.T., Horst, R.K., Nelson, P.E., 1975. Ecological aspects of ascospore discharge in *Gibberella zeae*. Phytopathology 65, 597–599.
Tucker, V.A., Cade, T.J, Tucker, A.E., 1998. Diving speeds and angles of a gyrfalcon (*Falco rusticolus*). J. Exp. Biol. 201, 2061–2070.
Vogel, S., 1988. Life's Devices. The Physical World of Animals and Plants. Princeton University Press, Princeton.
White, F.M., 1974. Viscous Fluid Flow. McGraw Hill, New York.

APPENDIX E

ISOLATION OF *Fusarium graminearum* INSERTIONAL MUTANTS COMPROMISED FOR MYXOTOXIN PRODUCTION AND PATHOGENESIS ON WHEAT

Trail, F., E. Mott, C. Andries, T. Farley, I. Gaffoor, M. Urban, W. Phillips, J. Pitkin, and K. Hammond-Kosack. Isolation of Fusarium graminearum insertional mutants compromised for mycotoxin production and pathogenesis on wheat. Molecular Plant-Microbe Interactions.

G. zeae causes the disease Fusarium Head Blight when it infects cereal crops such as wheat, oats and barley and corn. In wheat, the airborne spores initiate an infection by colonizing extruded anthers during anthesis. As the wheat plant matures, the fungus ramifies throughout the wheat head colonizing the developing grain and eventually spreads to the vegetative tissue. This process has been studied intensively in an effort to identify pathogenicity/virulence factors. This study was initiated to identify factors contributing to pathogenicity/virulence. For this purpose a bank of mutants generated by Random Insertional Mutagenesis was screened of loss of pathogenicity/virulence. My contribution to this study was to screen 1 000 mutants whereby I was able to identify 81 mutants that showed symptoms of reduced virulence in a preliminary screen.

Title: Isolation of *Fusarium graminearum* insertional mutants compromised for mycotoxin production and pathogenesis on wheat.

Frances Trail[1], Ellie Mott[2], Corrie Andries [1], Tom Farley[2], Iffa Gaffoor [1], Martin Urban[3], Wendy Phillips[4], John Pitkin[5], Kim Hammond-Kosack[3*].

Addresses

1 Departments of Plant Biology and Plant Pathology, Michigan State University, East Lansing MI 48824, USA

2 Department of Plant Sciences, University of Cambridge, Downing Street, Cambridge, CB2 3EA, UK

3 Plant-Pathogen Interaction Division, Rothamsted Research, Harpenden, Herts, AL5 2JQ, UK

4 Biovation Limited, Babraham Hall, Babraham, Cambridge, CB2 4AT, UK

5 Plant Protection, Monsanto Company, Main stop GG4C, 700 Chesterfield Parkway North, Chesterfield, Missouri 63198, USA

*To whom all correspondence should be addressed.

Kim.Hammond-Kosack@bbsrc.ac.uk;

Tel +44-(0)1582 763133, Ext 2240

Fax +44-(0)1582 715009

Abstract

A mutational analysis of pathogenicity of the head blight fungus, *Fusarium graminearum* (*Gibberella zeae*) was undertaken. Mutants were generated by random integration of a plasmid, and were screened for their ability to infect wheat heads. From a total of 1170 transformants screened, 9 were confirmed to be highly reduced in their ability to produce visible disease symptoms. We have called these disease attenuated *F. graminearum* mutants, *daf* mutants. Compared to the parental strain, a higher grain yield and/or improved grain quality was recovered from the heads inoculated with 6 of the *daf* mutants. However, when 3 head regions (above the point of inoculation, within the visibly diseased region, and below the diseased region) were examined in detail, each *daf* mutant caused a distinct phenotype on grain set, size and yield in the head regions. Two *daf* mutants caused an increase in grain set above the point of inoculation. The data also suggests that grain fill throughout the head is affected by these localized infections. Levels of the mycotoxins, deoxynivalenol, in the threshed grain appeared to be negligible for one mutant and absent in another mutant. Molecular genetic analysis of each *daf* mutant will yield important information regarding this host-pathogen system.

Keywords:

Deoxynivalenol

Fusarium ear blight

Rachis

Wheat grain safety

INTRODUCTION

Worldwide, *Fusarium* head blight infections of cereal crops cause considerable losses to grain quality and safety (Parry et. al., 1995; Windels, 2000, http://www.scabusa.org). *Fusarium* infections in wheat, barley, rye and maize crops have been steadily increasing since the early 1990s due to changes to the crop rotation, the introduction of maize into previously solely wheat growing regions and the use of low/minimal tillage practices (McMullen et al., 1997). The two main causative agents of *Fusarium* head blight disease on wheat are the homothallic *F. graminearum* Schw. [sexual stage *Gibberella zeae* (Schw.)] and the asexual *F. culmorum* (Smith) Saccardo. In Europe, the disease is more commonly called *Fusarium* ear blight. The disease is primarily monocyclic with head infections occurring when moist conditions prevail at anthesis and inoculum is available (Parry et al., 1995). The air-borne fungal spores gain entry into the plant either via colonizing the extruded anther and then the anther filament, or by penetrating directly the exposed ovary as each floret opens (Pugh, 1933; Kang and Buchenauer, 2000a). No specialized fungal penetration structures have been reported. Subsequent floral tissue colonization involves a mixture of intercellular and intracellular growth, and also saprophytic aerial growth (Pugh, 1933; Kang and Buchenauer, 2000a, M. Urban, unpublished). Infected wheat and barley heads prematurely bleach and masses of pink conidia form on infected spikelets under moist conditions. Grain threshed from infected heads is often shriveled, has a "tombstone" appearance (Parry et al., 1995) and can also be internally infected with fungal hyphae. Post-harvest, ascospores form within perithecia that develop on crop debris remaining on the soil surface (Pugh, 1933; Parry et

al., 1995). The detailed biology of perithecia formation has recently been explored (Trail and Common, 2000).

In wheat, two main types of natural resistance mechanisms to *Fusarium* head blight are known to exist and other resistance types have been suggested (Mesterhazy, 1995; reviewed by Bushnell et al. 2003, Mesterhazy, 2002). Type I resistance prevents initial infection. Type II resistance reduces the rate of disease spread within an infected ear. Exotic wheat germplasm with Type I resistance exists but is rare, whilst the polygenic based resistance to spread within an infected ear is currently in commercial use or under selection in breeding programs (Ban and Suenaga, 2000; Del Blanco et al., 2003).

Many isolates of *F. graminearum* and *F. culmorum* produce mycotoxins during colonization and post-harvest during storage. The estrogenic polyketide, zearalenone is associated with stored grain, whereas the trichothecene mycotoxins, primarily deoxynivalenol (DON), 3-acetyl DON, 15-acetyl DON and nivalenol (NIV) are produced during plant colonization. Isolates representing the 7 genetic lineages of *F. graminearum* can produce most chemotypes of trichothecene mycotoxins (O'Donnell et al., 2000; Ward et al., 2002). Legislation now limits DON concentrations in finished grain products for human consumption to 1 ppm in the USA and 0.75 ppm in Denmark, Austria and The Netherlands (Scholten et al., 2001). Quantities in grain samples from the Red River Valley in the upper Midwestern USA routinely exceed these quantities (McMullen et al., 1997). The target site for DON in plant, microbial and animal eukaryotic cells is the peptidyl transferase protein in the ribosome, and this binding results in the inhibition of protein synthesis (Cundliffe et al., 1974). Genes involved in trichothecene production

have been cloned (Hohn and Desjardins, 1992; Brown et al., 2001; Lee et al., 2002). The role of trichothecene mycotoxins in fungal penetration is unclear (McCormick *et al.*, 1998; Kang and Buchenauer, 1999, 2000b). However, DON production has been shown to enhance virulence of *F. graminearum* towards wheat, but is not an essential pathogenicity factor (Proctor et al., 1995).

The repertoire of *F. graminearum* genes required to infect and colonize cereal host plant species and those required to complete the life cycles are poorly understood. Besides the trichothecene biosynthetic genes (Proctor et al., 1995, 2002), targeted gene knock-out studies have shown that two different mitogen activated protein (MAP) kinase signaling cascades are essential for *F. graminearum* pathogenicity and sexual perithecia formation and contribute to DON trichothecene production (Hou et al., 2002; Jenczmionka et al., 2003; Urban et al., 2003).

Numerous experimental approaches are used to identify fungal genes required for plant pathogenicity. These include gene expression pattern studies (reviewed by Skinner et al, 2001), targeted deletion of genes encoding a known function (for recent examples involving *Fusarium* species see: Desjardins et al, 1996; Hou et al, 2002) or the isolation of insertional pathogenicity mutants, (reviewed by Gold et al., 2001). Insertional mutagenesis has the advantage of not only generating mutants but affords a method to clone the corresponding genes. Fungal insertional mutagenesis approaches include (1) the insertion of plasmids containing a selectable marker gene (insertional mutagenesis), (2) restriction enzyme mediated DNA integration (REMI) which uses a restriction enzyme in conjunction with a selectable plasmid during transformation, (3) transposon-based insertional mutagenesis and (4) the random mutagenesis of cosmids by *in vitro*

activated transposons prior to fungal transformation. All 4 approaches have been applied successfully to multiple filamentous fungal species, as reviewed by Sweigard and Ebbole (2001).

In this study, we describe the use of insertional mutagenesis to generate a library of hygromycin resistant transformants of *F. graminearum*. Over 1000 transformants were screened for reduced ability to produce visible disease symptoms. Nine pathogenicity mutants have been identified and the pathogenic effects on wheat head development and mycotoxin production have been characterized.

RESULTS

Molecular assessment of insertional mutagenesis

A random insertional mutagenesis approach was used to recover non-pathogenic mutants of *Fusarium graminearum*. To optimize the recovery of random insertional mutants, 4 different hygromycin-based plasmids were transformed into *F. graminearum*. The full details of each plasmid are given in the materials and methods section. Substantially more hygromycin-resistant colonies were obtained following transformation with pHA1.3 and pUCH2-8; therefore, these two plasmids were chosen to generate a large pool of transformants. Transformation of protoplasts of *F. graminearum* was conducted by incubation of protoplasts with linearized plasmid DNA, in the presence and absence of single restriction enzymes. Rates of transformation were higher without REMI (0.2 - 2.37 transformants (Tx)/μg plasmid DNA using linearized pHA1.3 only and 0.08 Tx/μg plasmid DNA from pHA1.3 using REMI). The transformation rate of protoplasts incubated with linearized pUCH2-8 was 0.2 - 1.2 Tx/μg plasmid DNA. No

transformants were recovered from control transformations without vector DNA. Of 5022 mutants generated, 3537 were generated by transformation with pHA1.3, and 1485 were generated by transformation with pUCH2-8. Thirteen (0.26%) of the 5022 insertional mutants contained mutations that prevented them from completing the sexual life cycle as homothallic isolates. Nine of the life cycle mutants were generated by transformation with pHA1.3, 4 were generated by transformation with pUCH2-8. All other insertional mutants appeared phenotypically normal in culture and produced functional perithecia by selfing.

To ascertain the average number of plasmid copies inserted into the *F. graminearum* genome, DNA was prepared from 10 Hyg^R transformants generated with each plasmid. DNA gel blot analyses revealed that 7 of the 10 transformants generated with plasmid pUCH2.8 had single copy insertions, and 9 of the 10 transformants generated with plasmid pHA1.3 had single copy insertion events (data not shown). Meiotic stability tests were performed on 3 life cycle mutants (2 pHA1.3 mutants and 1 pUCH2-8) to test stability. In each case, the mutant phenotype co-segregated with the HygR phenotype, indicating the mutation is likely to be tagged (data not shown). Twelve transformants (six transformed with each vector) were subjected to a mitotic stability test by transferring three cycles on V8 juice medium (VM) successively amended with or lacking HygB. No sectoring was observed and DNA gel blot analysis indicated the integrated plasmid remained stable throughout these transfers in all transformants (data not shown).

Identification of reduced pathogenicity mutants

A preliminary screen was performed in the greenhouse in which 2 wheat heads near anthesis were inoculated with each of 1170 Hyg^R randomly selected transformants. This population was comprised of 847 transformants harboring plasmid pHA1.3 and 323 transformants harbouring plasmid pUCH2.8. Infections by the parental isolate PH-1 caused the entire wheat head to bleach and impeded grain development. Eighty-one transformants caused significantly lower disease symptoms on both inoculated heads.

Each of the 81 putative reduced pathogenicity mutants was re-tested initially on 2 additional wheat heads using the secondary screen. For this screen each wheat head used had either two or three spikelets with visibly extruded anthers. Nine of the putative reduced pathogenicity mutants were confirmed to be highly reduced in their ability to cause disease symptoms on wheat heads. We have called these disease attenuated *F. graminearum* mutants, *daf* mutants. The *daf* mutants 10, 11, 14, 15, 26, 37, 38 were generated by pHA1.3, and *daf* 26 and *daf* 43 were generated by pUCH2.8. The full infection phenotype of each *daf* mutant was then explored in detail by inoculating a further 6 flowering wheat heads by placing a plug of inoculum in the 1st full sized spikelet at the top of the wheat head (Table 4, Appendix A). In these infection tests, hyphae of PH-1 colonized the entire wheat head within 20 days and caused every spikelet to bleach and the awns to assume a horizontal posture.

Five of the 9 pathogenicity mutants (*daf* 10, 15, 26, 36 and 38) caused externally visible disease symptoms only on the two originally inoculated spikelets. The other 4 pathogenicity mutants (*daf* 11, 14, 37, 43) caused disease symptoms to spread down the

head below the point of inoculation. However, none of the 9 mutants caused visible symptoms on more than seven spikelets at and below the point of inoculation by day 20 post inoculation. After this time no further visible disease progression occurred [Table 4, (Appendix A) and Figure 8(Appendix B)].

F. graminearum head infection is associated with impairment of both grain set and grain fill within the bleached spikelets (Parry et al., 1995; Bushnell et al., 2003, Mesterhazy et al., 2002). These disease phenotypes are hypothesized to be caused by hyphae blocking the main vascular tissue of the rachis and impairing water movement to the developing grain or by DON-mediated inhibition of protein translation in the developing grain (Cundliffe et al., 1974). We have termed the disease symptom, which specifically develops above the point of infection (region A, Figure 8, Appendix B) as *choking*, because it is unclear whether symptoms are related to mycelial colonization. Five or six immature spikelets were present above the inoculated spikelet at the start of the infection time-course. Choking was visible in all the wheat heads inoculated with PH-1 (Table 4, Appendix A). Interestingly, the 9 *daf* mutants caused either reduced choking or no choking (Table 4, Appendix A). Overall, there was a positive correlation between the extent of visible disease symptoms at and below the point of inoculation and the extent of choking in the upper head ($r= 0.719$). However, pathogenicity of *daf* 11 and *daf* 43 exhibit no choking, but disease symptoms were visible on 3-4 spikelets.

A further feature of *Fusarium* head infections is the brown streaking of rachis tissue interconnecting the wheat spikelets. This brown streaking most probably signifies plant cell necrosis occurring behind the advancing hyphal front. In heads inoculated with PH-1, brown streaking occurred 2-3 rachis segments in advance of visible bleaching

symptoms (Table 4, Appendix A). For each of the insertional mutants, except *daf* 38, streaking of the rachis occurred less frequently, but never on fewer than 50 % of the inoculated heads. Head infection by *daf* 38 never caused visible disease symptoms to develop on the rachis.

The impact of disease on grain set, grain quality and grain yield

Both grain quality and yield can be directly affected when *Fusarium* infects wheat floral tissue. In contrast, fungal pathogens that attack leaves, stems and root tissues of wheat, only indirectly affect harvestable grain, through reducing the total photosynthetic leaf area. It is also known that some natural *F. graminearum* isolates are able to cause symptomless head infections in the field (Gang et al., 1998) and (B. Hollins and K. Hammond-Kosack, unpublished). Therefore, we decided to examine the impact of the infection caused by each of the 9 *daf* mutants on both grain set and grain quality. To investigate these parameters in detail, not only was the total grain yield per head examined but also each head was sub-divided into 3 separate sampling regions and then the individual grains were removed from each region with a pair of forceps and assessed for both size and appearance. The 3 head regions were designated Region A- above the point of inoculation, Region B – point of inoculation and below with visible disease symptoms, and C – the rest of the head below the last visibly diseased spikelet (Figure 8, Appendix B).

The differences in the overall impact of infection on reducing head yield and grain quality was striking amongst the different treatments (Table 5, Appendix A). Inoculations with PH-1 caused an 87% reduction in the mature grain yield from a single

head (Table 5, Appendix A), when compared to the SNA inoculated heads. In contrast, heads inoculated with *daf* 10, 14, 15, 26 and 43 caused grain yield reduction of only 15% or less. This group of *daf* mutants produced two different visible symptom types, both types showed minimal choking. *daf* 14 and 43 showed the highest visible disease symptoms on spikelets; whilst *daf* 10, 15 and 26 caused minimal bleaching of spikelets. For total grain number per head only a single pattern emerged. The *daf* mutants 10, 38 and 43 caused a grain set that was statistically equivalent to the SNA inoculated heads. None of these three mutants caused the choking phenotype above the point of inoculation.

The grain recovered from the three regions of the head, defined above, was each explored separately. Point inoculations with PH-1 completely eliminated grain development in the 2 initially inoculated spikelets and all the other spikelets exhibiting the bleaching symptoms [Regions A and B, Figure 9 (Appendix B) and Table 5 (Appendix A)]. In contrast, the mock inoculation of SNA agar plugs permitted > 3 full-sized (large) grains to form within each inoculated spikelet [Region B, Figure 9 (Appendix B); Table 5(Appendix A)]. For each of the 9 *daf* mutants with reduced disease causing ability, some grain was recovered from the visibly diseased region. However, this grain was typically small and shrunken (Figure 9, Appendix B). On a per spikelet basis, the grain yield and number recovered from the visibly diseased region B was best in the heads inoculated with either *daf* 14, 37 or 43. The *daf* mutants 14 and 43 also had some of the highest visible symptom scores (Table 4, Appendix A), which suggests that the head infections may have been somewhat restricted to the peripheral tissue layers. The *daf* 11 and 26 which only produced very restricted macroscopic disease

symptoms, still caused an equivalent effect to grain set as the PH-1 isolate in the visibly infected region.

Region A, above the point of inoculation, is of constant size. Spikelets in this region typically entered anthesis 3-7 days later than the inoculated spikelets. There was considerable grain set and development in both the untreated and SNA inoculated heads, ie. > 4 large grains per head per region A. Infections by PH-1 caused < 1 small shrunken grain to form. In each of the mutant infected heads a mixture of large, medium and small grains formed. For example, *daf* 26 mutant permitted a comparable grain number and type to that found in control heads. In contrast, *daf* 10 and *daf* 43 appeared to permit a significantly higher set of large grains in each head than in the untreated and SNA inoculated heads. However, this different was not statistically significant at the 5% level (Table 5, Appendix A).

In the symptomless region C at the bottom of the head (Figure 9, Appendix B), grain quality and number were highly reduced by PH-1 (Table 5, Appendix A). However, when assessed on a per spikelet basis, grain weight was not affected by the PH-1 infections. Infections by each *daf* mutant also impacted grain development to varying degrees in the visibly non-diseased Region C. All infections, except those involving *daf* 11 reduced the number of large seed recovered. Only *daf* mutants 10, 36, 37, 38 and 43 did not cause a statistically significant reduction in total grain number in region C. Most of the medium and small seed isolated from region C was recovered from the 2-3 spikelets immediately adjacent to the visible diseased spikelets of each insertional mutant (data not shown).

These detailed analyses of the grain within the 3 sub-head regions for each *daf* mutant, have revealed a complexity to this host-pathogen interaction that was previously not known. Each *daf* mutant caused a unique effect on grain set, grain quality and grain yield that also varied between the three different head regions examined. These data also indicate that it is not possible to predict the impact of the infection on grain number, size and weight just by assessing the macroscopic disease symptoms.

Ability of *Fusarium* mutants to invade root and stem tissues

A seed germination assay in the presence or absence of *F. graminearum* hyphae was established (Urban et al., 2003), to examine the ability of each *daf* mutant to parasitize the root and stem base tissue of young seedlings. In the field, this type of infection, often arising from *Fusarium* infected crop residues or infected seed, causes a seedling blight disease that lowers the initial crop density (Parry et al., 1995).

PH-1 severely impaired both seedling emergence to between 14 and 24% of that recovered from the uninoculated controls (Table 6, Appendix A). In the 1st experimental replica, aerial seedling biomass was also significantly reduced following PH-1 infection. The 9 *daf* mutants, with a reduced ability to invade wheat heads at flowering, permitted both good seedling emergence and seedling growth in both experimental replicas [Table 6 (Appendix A), Figure 10 (Appendix B)]. For reasons unknown, 3 *daf* mutants caused a significantly greater impact on seedling emergence, in experiment 2, but this effect was still considerably less than PH-1.

When the wheat roots were washed free of vermiculite, clear differences between the root systems were visible. Infections by PH-1 caused extreme stunting of the roots

system with only 2-3 short main roots, no lateral roots or root hairs and roots were a light brown color (data not shown). In contrast, the roots recovered from the mutant-inoculated plants were all large, with many primary, secondary and tertiary roots and appeared very similar to those of the uninoculated plants. Microscopic examination of trypan blue stained roots, revealed that hyphae of PH-1 had infected the roots and colonized both intercellularly and intracellularly the various tissue layers. In contrast, microscopic observations of roots inoculated with each *daf* mutant failed to identify the presence of fungal mycelium inside root tissue (data not shown). It is possible that small peripheral root infections formed by a mutant were removed when the vermiculite was washed away from the roots and thereby lost from the subsequent analyses.

In vitro growth and sexual and asexual spore production of the *daf* mutants

The *in vitro* hyphal growth rates for the *daf* mutants were compared on SNA and VM media for 5 days. No statistically significant differences to the PH-1 strain were evident in the daily rate of hyphal extension on either growth media (data not shown). For each *daf* mutant the onset of asexual conidiation and the overall abundance of conidia formed on both SNA and VM plates were comparable to that observed for PH-1 (data not shown).

Perithecial formation was assessed by growing each *daf* mutant on carrot agar. Eight of the 9 *daf* mutants produced normal sized perithecia containing abundant ascospores in an identical manner to PH-1. For *daf* 38 perithecia, developed after an additional 5 days in culture compared to other mutants and the wild type.

DON mycotoxin production

In vivo, DON production was measured in the grain harvested from the 3 head regions, where sufficient material remained for the assay, by competitive ELISA. PH-1 produced DON in all grain samples examined within the range 200-405 µg/ g dry weight seed (n = 9). The *daf* 10 and *daf* 11 mutants produced no detectable DON levels in any of the grain samples that were assayed. The *daf* 15, *daf* 26, and *daf* 38 mutants produced low levels of DON in grain ranging between 5 and 30 µg/ g dry weight seed, and *daf* 14, *daf* 36, *daf* 37 and *daf* 43 produced wild type levels. DON production *in vitro* (Table 7, Appendix A) did not correlate well with DON production in the wheat head. Only *daf* 36 and *daf* 43 produced wild type levels of DON *in vitro* as well as in wheat grain. The *daf* 10, *daf* 11, and *daf* 14 mutants produced low DON levels *in vitro* and the DON detected in cultures of the *daf* 15, *daf* 26, *daf* 36, *daf* 38, and *daf* 43 mutants were in the range of PH-1.

DISCUSSION

Screening of a Fusarium graminearum population of 1170 isolates, mutagenized through plasmid insertion, identified 9 mutants with a reduced ability to invade and cause disease on wheat heads. In vitro each mutant exhibited a growth rate and phenotype equivalent to the parental PH-1 isolate. This result represents a pathogenicity mutant recovery rate of 0.8 %. This frequency of reduced and non-pathogenic mutant recovery is similar to what has been observed in several other plasmid insertion studies of ascomycetous fungi that are pathogenic towards plants (for example: Sweigard et al. 1998; Thon et al. 2000). The attenuated disease phenotype of the nine F. graminearum

mutants could be caused by (1) an inability of the mutants to produce the correct pathogenicity factors, (2) the production of pathogenicity factor(s) in an incorrect spatial and temporal order, or (3) the ill-timed synthesis of compounds that activate plant defense responses. We have called these disease attenuated F. graminearum mutants, daf mutants.

The nine F. graminearum daf mutants with reduced pathogenicity towards wheat floral tissue, also exhibited a non-pathogenicity phenotype towards the roots of wheat seedlings. Therefore a common mechanism must exist that permits F. graminearum hyphae to infect and colonize physiologically distinct plant tissue types. In contrast to our results, an exploration of the ability of several leaf pathogenicity mutants of the rice blast fungus (*Magnaporthe grisea*) for their ability to invade barley leaf and root tissue (Dufresne and Osbourn, 2001), identified 3 distinct sub-groups of pathogenicity mutants. Some *M. grisea* pathogenicity genes were required to cause disease on either leaf or root, whilst a third sub-group of the pathogenicity genes were required for general plant infection. For leaf penetration, but not root tissue penetration, *M. grisea* requires the formation of highly melanized appressoria, whereas, *F. graminearum* does not form any specialized infection structure to complete plant tissue infection. The molecular mechanisms of pathogenicity of wide host range, generalized fungal pathogens, such as *F. graminearum*, have not been well studied. These mutants should provide many clues into this type of interaction. The isolation of additional pathogenicity mutants from the remaining insertional mutants generated in this study is underway.

Comparison of each daf *mutant's various disease phenotype*

Quantitative assessment of 3 distinct macroscopic disease symptoms on wheat heads was used in this study to differentiate between the various mutant infection phenotypes. The symptoms evaluated were, (1) the number of spikelets exhibiting bleaching on glumes, lemma and palea tissue at and below the point of inoculation (ear regions B and C), (2) brown streaking on the rachis segments in advance of spikelet bleaching (ear regions B and C) and (3) the total bleaching of all spikelets above the point of inoculation (ear region A), termed choking [Table 4 (Appendix A) and Figure 8 (, Appendix B)]. The data indicate that *daf* 38 caused the least severe disease symptoms, when measured by any of the 3 criteria examined. However, the other eight *daf* mutants are difficult to rank precisely, because although there is a good relationship between the total number of bleached spikelets and the formation of the choking phenotype ($r = 0.719$), there was only a modest relationship between choking and brown streaking on the rachis ($r = 0.599$) and the relationship between spikelet bleaching and brown streaking on the rachis was poor ($r = 0.417$) (Table 8, Appendix A). A tentative ranking of the *daf* mutant's order according to increasing disease symptom severity is 38< 26, 10 < (15, 36) <11, 37, 43 <14. The recovery of only a modest to low correlation in the severity of 2 of the 3 symptom phenotypes indicates that greater than 50 % of the variation observed between the mutants can be attributed to additional independent biological causes. The underlying cause of the choking phenomena has not been explored for each *daf* mutant. Choking may be caused by direct hyphal colonisation, constriction of the vascular tissue with hyphae solely at the point of inoculation, caused by fungal hyphae or plant defense

responses or a mixture of these scenarios. It is also plausible that the underlying cause may differ between *daf* mutants.

Of considerable economic importance is the impact of *F. graminearum* head infection on total grain yield, quality and safety. Therefore it was considered very important to evaluate these parameters when assessing disease severity. In addition, natural *F. graminearum* isolates are also capable of causing symptomless head infections, i.e. without bleaching symptoms on glumes, lemma and palea tissue. By separately hand threshing the A, B and C head region separately (Table 4, Appendix A), our analyses distinguished between the impacts of both macroscopically visible disease and symptomless infections on grain set and grain fill for each mutant. Region A above the point of inoculation was considered separately, because an effect on grain number and grain fill in this region is likely to be influenced by the progress of the infection in the lower region of the head and may not have arisen through direct colonization. Grain set and grain fill in the upper regions of the head could be particularly influenced by interaction components transported through the xylem vessels from the lower infected head regions. PH-1 severely reduced grain recovery and quality in both the visible disease and non-diseased regions of the ear. A tentative ranking of the *daf* mutant's order according to increasing severity on grain number and grain quality is 10 < (43,38) < (26,36,37) < (14,11) < 15, whilst the ranking based on total grain yield recovered per wheat head increases in the order (11, 36, 37) < 38 < (10, 14, 15, 26, 43). For increasing DON production in harvested grain the ranking is (10, 11) < (15, 26,38) < (14, 36, 37, 43). The comparison of these rankings is particularly informative and indicates the existence of 3 very distinct *daf* mutants. The large infections of *daf* 43 are mainly

restricted to peripheral tissue and cause minimal impact on grain yield and quality, but produce normal DON levels in the grain. Whereas *daf* 15 produces modest visible infections (< 3 spikelets with visible disease symptoms) that have a large impact on grain number and grain quality throughout the ear and is only a modest producer of DON *in vivo*. Although the *daf* 10 mutant causes some visible symptoms, it results in minimal effects on grain yield and quality and is a DON non-producer *in vivo*.

Inter-relationships between the various head phenotypes examined

Table 8 (Appendix A) shows the correlation coefficients for the comparisons among the 3 macroscopic disease symptoms, grain number and quality recovered from the 3 head regions A, B, and C (Figure 9, Appendix B), and the total grain yield and grain number per head. R values of > 0.70 and < 0.25 are considered to indicate respectively, high and low correlations. Seven of the 66 comparisons gave high R values and seven gave low R values. Of greatest significance, were the seven highest negative relationships between the extent of spikelet bleaching (region B) and choking (region A) and the total grain number, total grain weight and the large grains recovered from both head regions A and C. Some of these negative relationships could have been anticipated because the larger the visibly diseased head region B, the smaller head region C becomes. Similarly in head region A, a high negative correlation between the extent of choking and total grain number was expected. This R value ties in well with field observations where grain numbers above the diseased area tend to be very low. However, these findings also indicate that at least for the wheat cultivar Bobwhite, increased grain fill outside of the visibly diseased area does not compensate for the loss of grain fill within the diseased

area, even through presumably the total available photosynthates arriving into the head has remained relatively constant. Indeed, the strong negative relationship between choking at the top of the inoculated head and the lack of large grain recovered from the symptomless head region C is particular informative. This result suggests that grain fill throughout the head is affected even when the visible Fusarium infection is highly localised. However, it is known that the infection front in the *F. graminearum*-wheat interaction may be up to 2 cm ahead of symptom development (Strausbaugh and Maloy, 1986; Trail and Guenther, unpub.).

Three of the 7 high positive correlations identified in Table 8 (Appendix A) were between the number of large grains recovered in head regions A and C, between grain number and large grain in head region A, and between the spikelet bleaching and the choking phenotype. The correlation between total grain number and regional grain number was best for head regions A and C, whilst total grain weight correlated best with the number of large grains in regions A and C. Overall the data presented in Table 8 (Appendix A) reinforces the notion that a series of highly complex host-pathogen inter-relationships are activated when *F. graminearum* infects a developing wheat head. Some of these relationships may be caused directly by factors released from the fungal hyphae. Others correlations may reflect the consequences of the activation of plant defense responses, which frequently occurs later in compatible plant-pathogen interactions (Hammond-Kosack and Jones, 1996).

Enhanced grain numbers in head region A

Infections of wheat heads by *daf* 10 and *daf* 43 appeared to cause in each head inoculated an increased recovery of grain from the non-choked head region A, compared to the same region in the control heads (Table 5, Appendix A). Although this increase was not statistically significant at $P<0.05$, this consistent trend in two independent *daf* mutants and merits further comment. Flowering and grain fill in head region A would have taken place after the *F. graminearum* inoculation. Many fungi are known to synthesize phytohormones, especially *Fusarium* species. For example *Gibberella fujikuroi* is known to produce gibberellins (Yabuta and Hayshi, 1939). Artemenko et al. (1999) also noted that *F. graminearum* conidia contain the gibberellins GA_3, GA_7 and their conjugates GA_4, Ga_{13} and *iso*-GA_7. During conidia germination *in vitro* gibberellins were secreted into the culture medium, and the authors suggest that gibberellins function as compatibility factors during plant invasion. However, this hypothesis was not tested experimentally. Thus is it possible that the contained fungal hyphae are modifying the hormonal balance in the plants, thereby enhancing fertilization and/or reducing aborting of immature grain. Recently, a nonpathogenic mutant of the cucurbit pathogen *Colletotrichum magna* was shown to interact with the host as a mutualistic endophyte, increasing fruit yields and protecting from disease in field trials (Redman et al, 2002). Certainly, the availability of such a mutant for biological control of wheat scab would be desirable.

DON production

PH-1 produces large amounts of DON both in wheat grain and *in vitro* (Table 7, Appendix A). For 7 of the 9 *daf* mutants *in planta* DON levels of > 5 μg per g dried grain were recovered from multiple independent samples, indicating that these mutants are still DON producers. Only *daf* 10 and 11 did not produce detectable DON *in planta*. In culture, all of the mutants produced some level of DON, although for *daf* 10, *daf* 11 and *daf* 14, the levels were extremely low. *Daf* 14 produced wildtype levels of DON *in planta* and extremely low levels in culture. This discrepancy could indicate differences in regulation of DON production in culture versus *in planta*. The mutant *daf* 11 produced no detectable mycotoxin production *in planta*, but has the ability to cause bleaching of at least 3 spikelets, and to lower grain number and quality in both the visibly diseased and non-visibly diseased head regions. This result indicates that DON production in *F. graminearum* hyphae is not required to cause disease on wheat heads. In culture, however, both *daf* 10 and *daf* 11 produced low, but detectable levels of DON, indicating the cultures are capable of producing this mycotoxin. It will be interesting to identify the mutated genes in these isolates, as they may be involved in regulation of DON production. In addition, it is possible *daf*10 and *daf*11 now produce a different repertoire of trichothecene mycotoxins, for example nivalenol, to compensate for the loss of DON mycotoxin production. It will be interesting to determine the exact mycotoxin chemotype of each *daf* mutant when growing under both *in planta* and *in vitro* conditions. Some isolates belonging to genetic lineage group 7 are known to produce other types of mycotoxins (O' Donnell et al., 2000; Ward et al., 2002). The isolate PH-1 is known to produce 3- acetyl DON, DON , 15-acetyl DON (Hou et al., 2002) and zearalenone (Trail

unpublished) but does not produce nivalenol (C. Kistler, pers comm.). In Table 8 (Appendix A), it is also worthy to note that there is a positive correlation of > 0.65 between both the choking and rachis browning symptoms and the levels of *in planta* DON production. These significance of these observations will be explored in greater detail.

Comparison of the *daf* mutant phenotypes to other known *F. graminearum* gene disruptants

Prior to this study, relatively few *F. graminearum* genes had been identified that contribute to pathogenicity towards wheat heads. These genes are either involved in biosynthesis of the trichothecene mycotoxins, or are MAP kinase genes, intimately involved in fungal development. *Tri5* encoding trichodiene synthase (Proctor et al., 1995), and *Tri8*, a C-3 esterase involved in trichothecene biosynthesis (McCormick and Alexander, 2002) have both been disrupted in *F. graminearum* and eliminate DON mycotoxin production. *Tri10*, a regulatory gene for the DON pathway, and *Tri101*, required for biosynthesis of the trichothecene T-2 toxin, have been disrupted in *F. sporotrichioides*, a closely related DON-producing species (Tag et al., 2001 ; McCormick et al, 1999). However, the *F. graminearum* mutants harboring a disrupted *Tri5* gene are still able to infect wheat heads and cause some disease symptoms (Proctor et al., 1995; Hui et al., 1997). Two homologues of the mitogen activated protein (MAP) kinases, *gPMK1/ MAP1* (Jenczmionka et al., 2003; Urban et al., 2003) and *MGV1* (Hou et al., 2002), have been disrupted in *F. graminearum*. Both gene knockouts separately reduce disease symptom production on wheat heads. It is worth noting that the MAP kinase

studies each used a different parental *F. graminearum* strain from that used to generate the 9 *daf* mutants reported in this study. However, 2 striking differences are worthy of comment. First, the *MAP1* disruption (Urban et al., 2003) caused the most dramatic reduction to pathogenicity. On wheat heads, *map1* hyphal colonization was restricted to anther tissue. Secondly, *daf* 10 and *daf* 11 identified in this study, eliminate DON mycotoxin production, almost as effectively as the *Tri5* mutation. The *Mgv1* and *Map1* mutations only confer a quantitative reduction in mycotoxin production *in vitro* and *in vivo*.

Efficiency of plasmid insertion and REMI techniques

We observed a decrease (2.5 to 30 times fewer transformants) in the frequency of transformation associated with inclusion of a restriction enzyme in the transformation mixture. However, we did not extensively test the use of REMI in this system as others have done (Redman and Rodriguez, 1994; Thon et al., 2000). REMI mutagenesis has also been associated with enhancing single-vector insertion and a higher percentage of transformants with random single integrations (Mullins and Kang, 2001). We had a relatively high frequency of single copy integrations (90%) using pHA 1.3 without the REMI procedure. Of the 4 hygromycin conferring plasmids tested for *F. graminearum* transformation, the plasmid pHA1.3 gave the highest and most consistent transformation efficiency. This pUC based plasmid, contains the *hph* coding region linked to the *Aspergillus parasiticus* TrpC promoter and TrpC 3' non-coding region, instead of the corresponding *A. nidulans* regulatory sequences. Also downstream of the *hph* gene, is a telomeric region from *Fusarium oxysporum*. Studies in *F. oxysporum* with this telomeric

sequence showed that it enhances chromosomal rearrangement when inserted into a transformation vector (Powell and Kistler, 1990). In other fungal species, the latter sequence has been shown to enhance stability and increase integration frequency (Redman and Rodriguez 1994; Powell and Kistler, 1990). In the present study, transformation of *F. graminearium* with pHA1.3 appears to enhance the frequency of integration as compared to other plasmids tested. Furthermore, these integrations appear to be stable as indicated by the segregation analysis and the mitotic stability tests. The plasmid pHA1.3 has recently been used successfully to generate 176 REMI mutants reduced in pathogencity of the curcurbit pathogen *Colletotrichum magna* with a recovery efficiency of 0.012% (Redman et al., 1999).

Future prospects

The nine *daf* mutants identified in this study cause highly reduced disease symptoms on both wheat heads and roots. The pathogenicity screen was slow and expensive because inoculations were performed on the flowering heads of intact wheat plants. The perfect correlation between the head and root pathogenic ability of the nine independent *daf* mutants, suggests it would be feasible to undertake the primary screening using initially only the seedling root test and then to re-test all the non-root invading mutants obtained for their ability to invade head tissue. By adopting this indirect screening strategy, a considerable savings of time and space would be obtained. However, this type of screen would miss the very interesting class of *F. graminearum* mutants solely compromised in head infection ability.

The nine *daf* mutants, with various infection phenotypes will be an extremely useful resource when trying to correlate specific changes in global plant and fungal gene expression with certain aspects of the infection biology. Wheat transcriptome analyses of infection involving PH-1 and mutants 10 and 11 will be able identify the plant genes specifically induced and repressed by mycotoxin production. An exploration of head region A, involving uninoculated heads and those infected with mutants 10 and 43 should identify the patterns of gene expression associated with the enhanced grain phenotype. Furthermore, the availability of over 8000 ESTs from various growth conditions on dbEST (Trail et al., 2003; http://cogeme.ex.ac.uk/index.html) and the genomic sequence of *Fusarium graminearum* PH-1, (http://www-genome.wi.mit.edu/annotation/fungi/fusarium/) will permit parallel investigation of the global changes in fungal gene expression hyphae accompanying the different interaction types.

MATERIALS AND METHODS

Strains and growth conditions

F. graminearum strain PH-1 (NRRL 31084; Trail and Common, 2000) was isolated from infected wheat in Michigan. The PH-1 strain belongs to genetic lineage group 7 (O'Donnell et al., 2000). Nitrate-non-utilizing mutants 4232 and 4233 (Bowden and Leslie, 1999) were provided by R. Bowden (Kansas State University). All strains were maintained as soil stocks at -20 C and were induced to produce perithecia on carrot agar as described by (Klittich and Leslie, 1988). Cultures were routinely cultured on SNA plates (synthetic nutrient-poor agar) containing 0.1% KH_2PO_4 ,0.1% KNO_3 , 0.1% $MgSO_4$ x 7 H_2O, 0.05% KCl, 0.02% Glucose, 0.02% Saccharose, 2% Bacto Agar [Difco] supplemented with 200ppm Biotin and 200ppm Thiamine) at 22 C under continuous white and blue fluorescent lights. In addition, strains were grown on V8 juice agar (36% V8 juice, 0.5% $CaCO_3$, 1.4% Bacto-agar), and Oatmeal agar [Crawford, 1986 #233].

Vectors for transformation of *F. graminearum*

Four plasmids were originally tested for transformation frequency, and all harbor the coding region on *E. coli* for the hygromycin B phosphotransferase gene (*hph*). Plasmids pUCATPH (Lu et al, 1994) and pCB1004 (Sweigard et al., 1998) have the *hph* coding region linked to the *Aspergillus parasiticus trpC* promoter and terminator sequences, but are constructed with different backbone plasmids and other small

sequence modifications. Plasmid pHA1.3 is constructed similarly to pUCATPH, but has a telomeric region from *Fusarium oxysporum* inserted downstream of the trpC terminator (Redman and Rodriguez, 1994). Plasmid pUCH2-8 has the *hph* coding region fused to promoter 1 from *Cochliobolus heterostrophus* (Turgeon *et al.*, 1987).

Fungal transformation

Transformations were performed on germinated conidia using a previously published protocol (Proctor et al., 1995) with the following modifications. Approximately 0.3 g soil stock was used to inoculate carboxymethylcellulose (CMC) medium and incubated for 72 hr at 25 ^{o}C at 250 rpm (Cappellini and Peterson, 1965). Conidia were harvested by centrifugation and germinated in YEPD (0.3% yeast extract, 1% bactopeptone, and 2% D-glucose) broth for 12 - 14 hours at room temperature (RT) at 175 rpm. Isolation of protoplasts occurred in 25 mg/ml driselase, 0.05 mg/ml chitinase (Sigma Chemical Co., St. Louis), and either 0.5 mg/ml mureinase (USB-Amersham Pharmacia Biotech Inc., Piscataway, NJ) or 5 mg/ml lysing enzyme (Sigma Chemical Co., St. Louis) in a 1.2 M KCl buffer. Protoplasts were collected by filtration through a 30 µm Nitex nylon membrane (Tetko Inc., Kansas City, MO) and washed three times in STC buffer (1.2 M sorbitol; 10 mM Tris-HCl, 50 mM $CaCl_2$, pH 8.0). Transformation took place in the presence of 30% polyethylene glycol solution (10 mM Tris-HCl, 50 mM $CaCl_2$, pH 8.0), STC buffer and linearized plasmid. Restriction enzyme mediated integration (REMI) transformations included an additional 10, 50, or 100 units of *NdeI* or *HindIII*.

Protoplasts recovered on Regeneration Medium (RM: 0.1% yeast extract, 0.1% casein enzyme hydrosylate, 0.8 M sucrose , 1% agarose) for 15 hr and then were overlaid with 10 ml of RM amended with 150 μg/ml hygromycin B (HygB) (Calbiochem-Novabiochem Corp., San Diego, CA). Putative transformants were selected within 4 - 7 days and retested for hygromycin resistance on V8 juice medium amended with 450 μg/ml HygB. Hygromycin resistant (Hyg^R) colonies were transferred to a 2% water agar (WA) medium and hyphal-tipped to obtain genetically pure isolates.

Mitotic and meiotic stability tests

Twelve transformants that were Hyg^R (six containing pHA1.3 and six containing pUCH2-8) were placed on VM amended with HygB, and incubated at 25 ^{o}C for 7 days. Mycelia were transferred to VM without HygB and incubated under the same conditions. This procedure was repeated three times, DNA was collected from mycelia at each transfer and DNA gel blot analysis was performed to determine mitotic stability of the inserts. To test meiotic stability and to test for co-segregation of the HygR marker and the mutant phenotype, transformants were mated with nitrate-non-utilizing (*nit*), hygromycin sensitive mutants 4232 and 4233. Ascospores were selected from eight recombinant perithecia and germinated on MMTS medium (Bowden and Leslie, 1999) which distinguishes *nit* mutants from wild type. Colonies were then placed on VM amended with HygB. Inheritance of mutations was compared to expected Mendelian ratios.

DNA isolation and gel blot analyses

For DNA isolation, isolates were grown in YES broth (2% yeast extract, 6% sucrose) for 4 - 6 days. Mycelium was collected by filtration and ground to a fine powder in liquid nitrogen. DNA was isolated according to the manufacturer's instructions using DNeasy Plant Maxi Kit (Qiagen Inc., Valencia, CA). DNA gel blot analyses were performed as previously described (Trail and Koeller, 1993).

Infection assays on wheat plants

Preliminary screening of mutants was carried out on greenhouse grown wheat, cultivar Norm. Seeds (4 per 6" pot) were sown in high porosity professional planting mix (Michigan Peat Company, Houston, TX). Plants were fertilized weekly, starting two weeks after germination until they reached the boot stage. Plants at early anthesis were selected for inoculation. Mutant strains of *G. zeae* were induced to produce perithecia on carrot agar. Ascospores were harvested using sterile distilled water and filtered through Miracloth (Calbiochem, La Jolla CA) Miracloth. Each spore suspension was streaked onto a plate of V8 agar to ensure viability and purity of spores. Spore suspensions that were inviable or showed contaminants after culture for 4 days were eliminated from the trial. Plants were inoculated by placing 10 µl of the spore suspension within the floral chamber of a floret midway along the head. Each mutant was inoculated in duplicate and ascospores harvested from PH-1 were inoculated on other heads as controls. The plants were placed in a misting chamber (misting frequency 10 s every 6 min) for 72 h and returned to standard greenhouse conditions. Wheat heads were assessed 8 to 13 days post

inoculation for development of symptoms relative to that of PH-1. Symptoms observed were the extent of bleaching on the heads (two or more spikelets from the point of inoculation), deformation of the awn and extent of seed set. If one of the two heads showed these symptoms, the strain was considered pathogenic.

For the secondary screen, wheat seeds of spring cultivar Bobwhite were sown in Levingtons C2 coarse potting compost. Seedlings were transplanted singly into 10 cm pots and grown for an additional 2 months in a controlled environment growth room at 18 ^{o}C during the 16-hr day and 16 ^{o}C during the 8-h night, at 50% relative humidity. Light was supplied by a mixture of metal hyalide and incandescent lamps to produce a fluence level of 207 microM at 86.2 W/msq at the plant surface. Once the plants entered anthesis, individual attached heads were selected that bore 2 to 5 spikelets with extruded anthers. A small agar plug (2mm diameter) cut from the hyphal edge of each *Fusarium* insertional mutant growing on SNA media was then inserted into the first full sized single floret down from the head apex (Figure 8, Appendix B). A second hyphal agar plug was inserted into an adjacent spikelet. The glumes of the two inoculated spikelets were marked with a waterproof pen. After inoculation the entire plant was placed into a high humidity chamber (> 95% relative humidity) for the next 3-4 days. Light was also excluded from the plants for 16 hours post–inoculation. The plants were then returned to the standard growth room conditions. All 81 putative mutants were screened initially in this fashion and wheat heads were assessed at day 20 post-inoculation for disease symptoms. In this manner, the 9 *daf* mutants were identified. These were then inoculated onto a minimum of 6 heads per mutant for a detailed study. Wheat heads were assessed at days 4, 8, 12, 16 and 20 days post inoculation for disease. Disease symptoms were

quantified by (a) counting the total number of spikelets at and below the point of inoculation exhibiting bleaching symptoms, (b) noting the extent of brown streaking on the rachis segments below the point of inoculation and (c) examining the head region above the point of inoculation for bleaching.

The ability of certain insertional mutants to invade young wheat seedlings was explored by germinating Bobwhite wheat seeds in a mixture of vermiculite and *Fusarium* hyphae. A 50 ml plastic container tube with drainage holes at the base (Steuwe and Sons, Inc, Oregon, USA) was two-thirds filled with moist sterile vermiculite. Into the top surface was incorporated $1/8^{th}$ of an entire 7 day old SNA plate (diam 10cm) of *Fusarium* that had been chopped into small pieces (5 mm^3). Three Bobwhite wheat seeds, from a stock known to give 100% germination, were placed onto the surface of the vermiculite/ hyphal agar surface, and then a further 15 ml of moist sterile vermiculite was added to completely cover completely the seeds. Seven identical containers were set up for each insertional *Fusarium* isolate tested. The finished containers were placed vertically in racks. Control containers were established with SNA agar only. To each container was added 10 ml of water ever 2^{nd} day for the 7 days and then daily thereafter.

At 14 days after sowing each container was scored non-destructively for seedling emergence. At 21 days after sowing, each container was disassembled, the vermiculite gentle washed from the root system and the roots then scored for browning discoloration and physical appearance. In addition, the aerial parts of the emerged seedlings above the

1st leaf sheath were excised and the fresh weight determined. The experiment was repeated on 2 separate occasions.

Trypan blue staining and microscopy

Root tissue samples was taken at 21 days after inoculation from each insertional *Fusarium* isolate interaction. Conventional histochemical staining of fungal hyphae was performed using lactophenol-trypan blue and destaining with chloral hydrate (Keogh et al., 1980). Microscopic observations were made on a Carl Zeiss " Axioskop 2" instrument under phase contrast.

Grain sampling

After the completion of the inoculation experiment, the heads were allowed to ripen naturally in the controlled growth room environment. Once both the inoculated and non-inoculated heads on a single plant were ripe, each head was harvested separately. The heads were divided into 3 regions. Region A represented all spikelets above the point of inoculation, Region B contained all spikelets which displayed any visible signs of disease and included the originally inoculated pair, whilst Region C consisted of any spikelets below the visible disease symptoms. A pair of forceps was used to remove any grain found in each spikelet in each of the 3 separate regions and the physical appearance of this grain was recorded. The grain was rated as large (L) if the seed was full, rounded and golden, medium (M) if the grain was not full sized, darkened or covered in mycelium/conidia, small (S) if the grain was shrivelled and < 1/4 of the size of

the healthy grain or absent/prematurely aborted (A). In order to ascertain the extent to which visible infections influenced grain development in the non-symptom expressing regions, the spikelets in region C were sampled sequentially in a downwards direction, and the results obtained from each pair of spikelets noted. A numerical scoring system was then used to semi-quantify the total grain yield per head L=3, M=2, S=1 and A =0.1 In addition, the total weight of grain recovered from the 3 regions of the ear was determined. Two different types of control heads were also harvested, these had either been inoculated with agar only plugs (indicated as SNA) or were non-inoculated heads put through the standard inoculation procedure (indicated as None).

Fungal growth rate and spore production

To measure fungal growth rates, mycelium plugs from 1 week old cultures on SNA minimal agar plates were transferred onto fresh agar plates using a 5 mm cork borer. Fungal growth was recorded as colony diameter in daily intervals during 5 days. Experiments were done in at least 3 replicates.

DON measurement

Quantitative combined DON and 3-acetyl DON measurements were made using the commercial competitive ELISA-based Veratox 5/5 kit (Neogen Corp., Lansing, Michigan USA) and deploying a standard curve for DON ranging from 0.25 to 3.00 ppm. OD_{650} values were measured after the addition of the stop solution to the multiwells. To ensure accuracy, each biological sample was quantified twice. The kit does not

distinguish DON and 3-acetyl DON, and does not detect 15-acetyl DON. Throughout the paper, the designation DON will indicate DON and 3-acetyl DON combined.

Statistical analyses

Statistical analyses were conducted according to Snedecor and Cochran (1980) and using either the SAS statistical package or the data analysis tools in MS Excel.

ACKNOWLEDGEMENTS

The experiments were conducted under the UK MAFF import license PHL 39A/3490 (1/2001) and plant inoculations and fungal culture were conducted under the UK MAFF license PHL 39A/3493 (5/2001). The authors thank Benjamin Munn for his technical assistance in performing the DON assays and Chil Kwon, John Guenther and Lukesha Davis for their assistance with the pathogenicity assays. Alan Todd provided guidance on the various the statistical analyses undertaken. This work was supported in part by The Monsanto Company, the USDA Wheat and Barley Scab Iniatitive, and the Michigan State University Agricultural Experiment Station.

REFERENCES

Artemenko, E. N., Devyatkina, G. A., and Sadovskaya, V. L. 1999. Involvement of gibberellins from germinating conidia of *Fusarium graminearum* Schw. in the pathogenesis of Fusarium Wheat Head Blight. Russ. J. Plant Physiol. 46: 252-254.

Ban, T. and Suenaga, K. (2000) Genetic analysis of resistance to Fusarium head blight caused by *Fusarium graminearum* in Chinese wheat cultivar Sumai-3 and the Japanese cultivar Saikai 165. Euphytica 113: 87-99.

Bowden, R.L., and Leslie, J.F. 1999. Sexual recombination in *Gibberella zeae*. Phytopathology 89:182-188.

Brown, D.W., McCormick, S.P., Alexander, N.J., Proctor, R.H., Desjardins, A.E. 2001. A genetic and biochemical approach to study trichothecene diversity in *Fusarium sporotrichioides* and *Fusarium graminearum*. Fungal Genet. Biol. 32: 121-133.

Bushnell, W.R., Hazen, B.E., and Pritsch, C. 2003. Histology and physiology of Fusarium head blight. Pp. 44-83 In: Fusarium Head Blight of Wheat and Barley, K.J. Leonard and W.R. Bushnell, eds. APS Press, St. Paul.

Cappellini, R. A., and Peterson, J. L. 1965. Macroconidium formation in submerged cultures by a non-sporulating strain of *Gibberella zeae*. Mycologia 57:962-966.

Cundliffe, E., Cannon, M. and Davies, J. 1974. Mechanism of inhibition of eukaryotic protein synthesis by trichothecene fungal toxins. Proc. Natl. Acad.Sci USA 71: 30-34.

Del Blanco I.A., Frohberg R.C., Stack R.W., Berzonsky W.A. and Kianian S.F. (2003) Detection of QTL linked to Fusarium head blight resistance in Sumai 3-derived North Dakota bread wheat lines. Theor Appl Genet. 106: 1027-1031.

Desjardins, A.E., Proctor, R.H., Bai, G., McCormick, S.P., Shaner, G., Buechley, and Hohn, T.M. 1996. Reduced virulence of trichothecene-nonproducing mutants of *Gibberella zeae* in wheat field tests. Molecular Plant Microbe Interactions 9: 775-781.

Dufresne, M. and Osbourn, A. E. 2001. Definition of tissue-specific and general requirements for plant infection in a phytopathogenic fungus. Mol. Plant-Microbe Interaction 14: 300-307.

Gang, G., Miedaner, T., Schuhmacher, U., Schollenberger, M. and Geiger, H.H. 1998. Deoxynivalenol and nivalenol production by *Fusarium culmorum* isolates differing in aggressiveness towards winter rye. Phytopathol. 88: 879-884.

Gold, S.E., Garcia-Pedradas, M.D. and Martinez-Espinoza, A. D. (2001) New (and used) approaches to the study of fungal pathogenicity. Annu. Rev. Phtyopathol. 39:337-365.

Hammond-Kosack K.E. and Jones J.D.G 1996. Inducible plant defence mechanisms and resistance gene function. The Plant Cell 8:1773-1791.

Hohn, T.M. and Desjardins, A.E. 1992. Isolation and gene disruption of the *Tox5* gene encoding trichcodiene synthase in *Gibberella pulicaris*. Mol. Plant-Microbe Interact. 5:249-256.

Hou, Z., Xue, C., Peng, Y., Katan, T., Kistler H. C. and Xu J-R 2002. A MAP kinase gene (*MGV1*) in *Fusarium graminearum* is required for female fertility, heterokaryon formation, hyphal growth and plant infection. Mol. Plant-Microbe Interact. 15: 1119-1127.

Hui, Y., Evans, C.K., Kolaczkowski, E.K., Dill-Macky, R. and Mirocha, C.J. 1997. Chemistry, physiology and role of deoxynivalenol in pathogenicity. Bull. Inst. Compr. Agr. Sci. Kinki Uni 5: 1-11.

Jenczmionka N.J., Maier F.J., Losch A.P. and Schafer W. (2003) Mating, conidiation and pathogenicity of *Fusarium graminearum*, the main causal agent of the head-blight disease of wheat, are regulated by the MAP kinase gpmk1. Curr Genet. 43 :87-95.

Kang, Z. and Buchenauer, H. 1999. Immunocytochemical localisation of *Fusarium* toxins in infected wheat spikes by *Fusarium culmorum*. Physiol. Mol. Plant Pathol. 55: 275-288.

Kang, Z. and Buchenauer, H. 2000a. Cytology and ultrastructure of the infection of wheat spokes by *Fusarium culmorum*. Mycol. Res. 104: 1083-1093.

Kang, Z. and Buchenauer, H. 2000b. Ultrastructural and immunocytochemical investigations of pathogen development and host responses in resistant and susceptible wheat spikes infected by *Fusarium culmorum*. Physiol. Mol. Plant Pathol. 57: 255-268.

Keogh, R.C., Deverall, B. J. and Mcleod, S. 1980. Comparison of histological and physiological responses to *Phakopsora pachyrhizi* in resistant and susceptible soybean. Trans. Br. Mycol. Soc. 74: 329-333.

Klittich, C. J. R., and Leslie, J. F., 1988. Nitrate reduction mutants of *Fusarium moniliforme* (*Gibberella fujikuroi*). Genetics 118:417-423.

Lee, T., Han, Y.K., Kim, K.H., Yun, S.H., Lee, Y.W. 2002. *Tri13* and *Tri7* determine deoxynivalenol- and nivalenol-producing chemotypes of *Gibberella zeae*. Appl Environ. Microbiol. 68: 2148-2154.

Lu, S.W., Lyngholm, L., Yang, G., Bronson, C., Yoder, O.C.and Turgeon, B.G. 1994. Tagged mutations at the *Tox1* locus of *Cochliobolus heterostrophus* by restriction enzyme-mediated integration. Proc. Natl. Acad. Sci (USA) 26: 12649-12653.

McCormick S.P and Alexander N.J. 2002. *Fusarium Tri8* encodes a trichothecene C-3 esterase. Appl. Environ. Microbiol. 68: 2959-2964.

McCormick S. P, Alexander N.J., Trapp S.E. and Hohn T.M. 1999. Disruption of *TRI101*, the gene encoding trichothecene 3-O-acetyltransferase, from *Fusarium sporotrichioides*. Appl. Environ. Microbiol. 65: 5252-5256.

McCormick, S.P., Hohn, T.M., Desjardins, A.E., Proctor, R.H. and Alexander, N.J. 1998. Role of toxins in plant microbial interactions. Phytochemical Signals and Plant-Microbe Interact. 32: 17-30.

McMullen, M., Jones, R and Gallenberg, D. 1997. Scab of wheat and barley: a re-emerging disease of devastating impact. Plant Disease 81: 1340-1348.

Mesterhazy, A. 1995. Types and components of resistance to *Fusarium* head blight of wheat. Plant Breeding 114: 377-386.

Mesterhazy, A. 2002. Role of deoxynivalenol in agressiveness of *Fusarium graminearum* and *F. culmorum* and in resistance to *Fusarium* head blight. European Journal of Plant Pathology 108: 675-684.

Mullins, E.D. and Kang S. 2001. Transformation: a tool for studying fungal pathogens of plants. Cell. Mol. Life Sci. 58:2043-2052.

O'Donnell, K., Kistler, H.C., Tacke, B. K. and Casper, H.H. 2000. Gene genealogies reveal global phylogeographic structure and reproductive isolation among lineages of *Fusarium graminearum*, the fungus causing wheat scab. Proc. Natl. Acad. Sci USA 97: 7905-7910.

Parry, D.W., Jenkinson, P and McLeod, L. 1995. *Fusarium* head blight (scab) in small grain cereals-a review. Plant Pathol. 44: 207-238.

Powell W.A. and Kistler, H.C. 1999. In vivo rearrangement of foreign DNA by Fusarium *oxysporum* produces linear self-replicating plasmids. J. Bact. 172: 3163-3171.
Proctor, R.H., Hohn, T.M., and McCormick, S.P. 1995. Reduced virulence of *Gibberella zeae* caused by disruption of a trichothecene toxin biosynthetic gene. Mol. Plant-Microbe Interact. 8: 593-601.

Proctor, R.H., Desjardins, A.E., McCormick, S.P., Plattner, R.D., Alexander, N.J., and Brown, D.W. 2002. Genetic analysis of the role of trichothecene and fumonisin mycotoxins in the virulence of *Fusarium*. European Journal of Plant Pathology 108: 691-698.

Pugh, G.W. 1933. Factors affecting infection of wheat heads by *Gibberella saubinetti*. J. Agr. Res. 46: 771-797.

Redman, R. S., and Rodriguez, R. J., 1994. Factors affecting the efficient transformation of *Colletotrichum* species. Exp. Myc. 18:230-246.

Redman, R.S., Ranson, J. C., and Rodriguez, R.J. 1999. Conversion of the pathogenic fungus *Colletotrichum magna* to a nonpathogenic, endophytic mutualist by gene disruption. Mol. Plant-Microbe Interact. 12: 969-975.

Redman R.S., Roossinck M.J., Maher S., Andrews Q.C., Schneider W.L., and Rodriguez, R.J. 2002. Field performance of cucurbit and tomato plants colonized with a nonpathogenic, mutualistic mutant (path-1) of *Colletotrichum magna* (Teleomorph : *Glomerella magna*; Jenkins & Winstead) Symbiosis 32: 55-70.

Scholten, O.E., Ruckenbauer, P., Visconti, A., van Osenbruggen, W.A., and den Nijs, A.P.M. 2001: Food Safety of Cereals: A chain-wide approach to reduce *Fusarium* Mycotoxins. (Commission of the European Communities).

Snedecor, G.W. and Cochran, W.G. 1980 Statistical Methods. Ames, IA: Iowa State University Press.

Skinner, W., Keon, J. P. R. & Hargeaves, J. A. 2001 Gene information for fungal plant pathogens from expressed sequences. Curr. Opin. Microbiol. 4: 381-386.

Stausbaugh, C.A. and Maloy, O. C. 1986 Fusarium scab of irrigated wheat in central Washington. Plant Disease 70 :1104-1106.

Sweigard, J.A., Carroll, A.M., Farrall, L., Chumley, F. G., and Valent, B. 1998. *Magnaportha grisea* pathogenicity genes obtained through insertional mutagenesis. Mol Plant-Microbe Interact. 11: 404-412.

Sweigard, J. A. and Ebbole, D. J. 2001. Functional analysis of pathogenicity genes in a genomics world. Curr. Opin. Microbiol. 4: 387-392.

Tag A.G., Garifullina G.F., Peplow A.W., Ake C., Phillips T.D., Hohn T.M. and Beremand M.N. 2001. A novel regulatory gene, *Tri10*, controls trichothecene toxin production and gene expression. Appl. Environ. Microbiol. 67: 5294-5302.

Thon, M.R., Nuckles, E.M. and Vaillancourt, L.J. 2000. Restriction enzyme-mediated integration used to produce pathogenicity mutants of *Colletotrichum graminicola.* Mol. Plant-Microbe Interact. 13: 1356-1365.

Trail, F., and Common, R. 2000. Perithecial development of *Gibberella zeae*: A light microscopy study. Mycologia 92:130-138.

Trail, F. and Koller, W. 1993. Diversity of cutinases from plant pathogenic fungi: Purification and characterization of cutinases from *Alternaria brassicicola*.. Physiological and Molecular Plant Pathology 42: 205-220.

Trail, F., Xu, J.-R., San Miguel, P., Halgren, R. G. and Kistler, H. C. 2003. Analysis of Expressed Sequence Tags from *Gibberella zeae* (anamorph *Fusarium graminearum*). Fungal Genetics and Biology 38: 187-197.

Turgeon, B. G., Garber, R. C., and Yoder, O. C. 1987. Development of a fungal transformation system based on selection of sequences with promoter activity. Mol. Cell Bio. 7:3297-3305.

Urban, M., Mott, E, Farley, T, Phillips, W and Hammond-Kosack K.E. 2003. The *Fusarium graminearum MAP1* gene is essential for pathogenicity and perithecia formation Mol. Plant-Pathol. (in press).

Ward, T.J., Bielawski, J.P., Kistler, H.C., Sullivan, E., and O'Donnell, K. 2002. Ancestral polymorphism and adaptive evolution in the trichothecene mycotoxins gene cluster of phytopathogenic *Fusarium*. Proc. Natl. Acad. Sci. USA 99:9278-9283.

Windels, C. E. 2000. Economic and social impacts of *Fusarium* head blight: Changing farms and rural communities in the Northern Great Plains. Phytopathol. 90: 17-21.

Yabuta, T. and Hayshi, T. 1939. Biochemical studies on the 'bakanae' fungus of rice. II. Isolation of 'gibberellin', the active principle which makes the rice seedlings grow slenderly. J. agric. Chem. Soc. Japan. 15: 257-266.

BIBLIOGRAPHY

1. **Abe, Y., T. Suzuki, C. Ono, K. Iwamoto, M. Hosobuchi, and H. Yoshikawa.** 2002. Molecular cloning and characterization of an ML-236B (compactin) biosynthetic gene cluster in Penicillium citrinum. Molecular Genetics and Genomics **267:**636-646.

2. **Agrios, G. N.** 1997. Plant Pathology, 4th ed. Harcourt Brace & Company, San Diego, CA.

3. **Andrianopoulos, A., and W. E. Timberlake.** 1994. The *Aspergillus nidulans* abaA gene encodes a transcriptional activator that acts as a genetic switch to control development. Molecular and Cellular Biology **14:**2503-2515.

4. **Argyris, J., D. Van Sanford, and D. TeKrony.** 2003. *Fusarium graminearum* Infection During Wheat Seed Development and Its Effect on Seed Quality. Crop Science **43:**1782-1788.

5. **Bai, G. H., and G. Shaner.** 1996. Variation in *Fusarium graminearum* and cultivar resistance to wheat scab. Plant Disease **80:**975-979.

6. **Bailey, T. L., and C. Elkan.** 1994. Fitting a mixture model by expectation maximization to discover motifs in biopolymers. Proceedings, International Conference on Intelligent Systems for Molecular Biology **2:**28-36.

7. **Bailey, T. L., and M. Gribskov.** 1998. Combining evidence using p-values: application to sequence homology searches. Bioinformatics **14:**48-54.

8. **Baker, P. M., and J. C. Roberts.** 1966. Studies in mycological chemistry. Part XXI. The structure of aurofusarin, a metabolite of some Fusarium species. Journal of the Chemical Society:2234-2237.

9. **Bastmeyer, M., H. B. Deising, and C. Bechinger.** 2002. Force exertion in fungal infection. Annual Review Of Biophysics And Biomolecular Structure **31:**321-341.

10. **Bender, C. L., F. Alarcón-Chaidez, and D. C. Gross.** 1999. *Pseudomonas syringae* phytotoxins: Mode of Action, Regulation, and Biosynthesis by Peptide and Polyketide Synthetases. Microbiology and Molecular Biology Reviews **63:**266-+.

11. **Bender, C. L., V. Rangaswamy, and J. Loper.** 1999. Polyketide Production by Plant-Associated Pseudomonads. Annual Review of Phytopathology **37:**175-196.

12. **Bennett, J. W.** 1983. Differentiation and secondary metabolism in mycelial fungi, p. 1-32. *In* B. J.W. and A. Ciegler (ed.), Secondary metabolism and differentiation in fungi. Marcel Dekker, New York.

13. **Bennett, J. W.** 1995. From Molecular Genetics and Secondary Metabolism to Molecular Metabolites and Secondary Genetics. Canadian Journal of Botany **73:**S917-S924.

14. **Bentley, R., and J. W. Bennett.** 1999. Constructing polyketides: From collie to combinatorial biosynthesis. Annual Review of Microbiology **53:**411-446.

15. **Bhatnagar, D., K. C. Ehrlich, and T. E. Cleveland.** 2003. Molecular genetic analysis and regulation of aflatoxin biosynthesis. Applied Microbiology and Biotechnology **61:**83-93.

16. **Bingle, L. E. H., T. J. Simpson, and C. M. Lazarus.** 1999. Ketosynthase domain probes identify two subclasses of fungal polyketide synthase genes. Fungal Genetics and Biology **26:**209-223.

17. **Birzele, B., A. Prange, and J. Krämer.** 2000. Deoxynivalenol and ochratoxin A in German wheat and changes of level in relation to storage parameters. Food Additives and Contaminants **17:**1027-1035.

18. **Bode, H. B., B. Bethe, R. Höfs, and A. Zeeck.** 2002. Big Effects from Small Changes: Possible Ways to Explore Nature's Chemical Diversity. Chembiochem **3:**619-627.

19. **Böhnert, H. U., I. Fudal, W. Dioh, D. Tharreau, J. L. Notteghem, and M. H. Lebrun.** 2004. A Putative Polyketide Synthase/Peptide Synthetase from *Magnaporthe grisea* Signals Pathogen Attack to Resistant Rice. Plant Cell **16:**2499-2513.

20. **Borkovich, K. A., L. A. Alex, O. Yarden, M. Freitag, G. E. Turner, N. D. Read, S. Seiler, D. Bell-Pedersen, J. Paietta, N. Plesofsky, M. Plamann, M. Goodrich-Tanrikulu, U. Schulte, G. Mannhaupt, F. E. Nargang, A. Radford, C. Selitrennikoff, J. E. Galagan, J. C. Dunlap, J. J. Loros, D. Catcheside, H. Inoue, R. Aramayo, M. Polymenis, E. U. Selker, M. S. Sachs, G. A. Marzluf, I. Paulsen, R. Davis, D. J. Ebbole, A. Zelter, E. R. Kalkman, R. O'Rourke, F. Bowring, J. Yeadon, C. Ishii, K. Suzuki, W. Sakai, and R. Pratt.** 2004. Lessons from the genome sequence of Neurospora crassa: Tracing the path from genomic blueprint to multicellular organism. Microbiology And Molecular Biology Reviews **68:**1-+.

21. **Brooks, D. M., G. Hernández-Guzmán, A. P. Kloek, F. Alarcón-Chaidez, A. Sreedharan, V. Rangaswamy, A. Peñaloza-Vázquez, C. L. Bender, and B. N. Kunkel.** 2004. Identification and Characterization of a Well-Defined Series of Coronatine Biosynthetic Mutants of *Pseudomonas syringae* pv. *tomato* DC3000. Molecular Plant-Microbe Interactions **17:**162-174.

22. **Brown, D. W., R. B. Dyer, S. P. McCormick, D. F. Kendra, and R. D. Plattner.** 2004. Functional demarcation of the Fusarium core trichothecene gene cluster. Fungal Genetics and Biology **41:**454-462.

23. **Brown, M. P., C. S. Brown-Jenco, and G. A. Payne.** 1999. Genetic and molecular analysis of aflatoxin biosynthesis. Fungal Genetics and Biology **26:**81-98.

24. **Bu'Lock, J. D.** 1961. Intermediary metabolism and antibiotic synthesis. Advances in Applied Microbiology **3:**293-342.

25. **Bu'Lock, J. D.** 1961. Intermediary metabolism and antibiotic synthesis. Advances in Applied Microbiology **3:**293-342.

26. **Burset, M., I. A. Seledtsov, and V. V. Solovyev.** 2001. SpliceDB: database of canonical and non-canonical mammalian splice sites. Nucleic Acids Research **29:**255-259.

27. **Cantalejo, M. J., P. Torondel, L. Amate, J. M. Carrasco, and E. Hernandez.** 1999. Detection of fusarin C and trichothecenes in Fusarium strains from Spain. Journal Of Basic Microbiology **39:**143-153.

28. **Cappellini, R. A., and J. L. Peterson.** 1965. Macroconidium formation in submerged cultures by a non-sporulating strain of Gibberella zeae. Mycologia **57**:962-966.

29. **Carroll, A. N., J. A. Sweigard, and B. Valent.** 1994. Improved vectors for selecting resistance to hygromycin. Fungal Genetics Newsletter **41**:22.

30. **Chakravarti, R., and V. Sahai.** 2004. Compactin - a review. Applied Microbiology and Biotechnology **64**:618-624.

31. **Challis, G. L., and D. A. Hopwood.** 2003. Synergy and contingency as driving forces for the evolution of multiple secondary metabolite production by Streptomyces species. Proceedings Of The National Academy Of Sciences Of The United States Of America **100**:14555-14561.

32. **Chang, P. K., K. C. Ehrlich, J. E. Linz, D. Bhatnagar, T. E. Cleveland, and J. W. Bennett.** 1996. Characterization of the *Aspergillus parasiticus* niaD and niiA gene cluster. Current Genetics **30**:68-75.

33. **Choquer, M., K. L. Dekkers, H. Q. Chen, L. H. Cao, P. P. Ueng, M. E. Daub, and K. R. Chung.** 2005. The CTB1 gene encoding a fungal polyketide synthase is required for cercosporin biosynthesis and fungal virulence of Cercospora nicotianae. Molecular Plant-Microbe Interactions **18**:468-476.

34. **Christensen, C. M., G. H. Nelson, and C. J. Mirocha.** 1965. Effect on the white rat uterus of a toxic substance isolated from *Fusarium*. Applied Microbiology **13**:653.

35. **Conkova, E., A. Laciakova, G. Kovac, and H. Seidel.** 2003. Fusarial toxins and their role in animal diseases. Veterinary Journal **165**:214-220.

36. **Čonková, E., A. Laciaková, G. Kováč, and H. Seidel.** 2003. Fusarial Toxins and their Role in Animal Diseases. Veterinary Journal **165**:214-220.

37. **Cox, R. J., and F. Glod.** 2004. Fungal polyketide synthases in the information age, p. 69-96. *In* J. S. Tkacz and L. Lange (ed.), Advances in Fungal Biotechnology for Industry, Agriculture, and Medicine. Kluwer Academic/Plenum Publishers, New York.

38. **D'Mello, J. P. F., C. M. Placinta, and A. M. C. Macdonald.** 1999. Fusarium mycotoxins: A review of global implications for animal health, welfare and productivity. Animal Feed Science and Technology **80:**183-205.

39. **Desjardins, A. E., D. W. Brown, S. H. Yun, R. H. Proctor, T. Lee, R. D. Plattner, S. W. Lu, and B. G. Turgeon.** 2004. Deletion and Complementation of the Mating Type (*MAT*) Locus of the Wheat Head Blight Pathogen *Gibberella zeae*. Applied and Environmental Microbiology **70:**2437-2444.

40. **Devereux, J., P. Haeberli, and O. Smithies.** 1984. A comprehensive set of sequence analysis programs for the VAX. Nucleic Acids Research **12:**387-395.

41. **Durbin, R., S. Eddy, A. Krogh, and G. Mitchison.** 1998. Biological Sequence Analysis: Probabilistic Models of Proteins and Nucleic Acids. Cambridge University Press., Cambridge.

42. **Dvorska, J. E., P. F. Surai, B. K. Speake, and N. H. C. Sparks.** 2001. Effect of the mycotoxin aurofusarin on the antioxidant composition and fatty acid profile of quail eggs. British Poultry Science **42:**643-649.

43. **Ehrlich, K. C., B. G. Montalbano, J. W. Cary, and P. J. Cotty.** 2002. Promoter elements in the aflatoxin pathway polyketide synthase gene. Biochimica et Biophysica Acta-Gene Structure and Expression **1576:**171-175.

44. **Feng, B., and G. A. Marzluf.** 1998. Interaction between major nitrogen regulatory protein NIT2 and pathway-specific regulatory factor NIT4 is required for their synergistic activation of gene expression in Neurospora crassa. Molecular and Cellular Biology **18:**3983-3990.

45. **Fernandes, M., N. P. Keller, and T. H. Adams.** 1998. Sequence-specific binding by Aspergillus nidulans AflR, a C-6 zinc cluster protein regulating mycotoxin biosynthesis. Molecular Microbiology **28:**1355-1365.

46. **Fernando, W. G. D., T. C. Paulitz, W. L. Seaman, P. Dutilleul, and J. D. Miller.** 1997. Head blight gradients caused by Gibberella zeae from area sources of inoculum in wheat field plots. Phytopathology **87:**414-421.

47. **Firn, R. D., and C. G. Jones.** 2000. The evolution of secondary metabolism — a unifying model. Molecular Microbiology **37:**989-994.

48. **Foster, J. W.** 1949. Chemical Activities of the fungi. Academic Press, New York.

49. **Fujii, I., Y. Mori, A. Watanabe, Y. Kubo, G. Tsuji, and Y. Ebizuka.** 2000. Enzymatic synthesis of 1,3,6,8-tetrahydroxynaphthalene solely from malonyl coenzyme A by a fungal iterative type I polyketide synthase PKS1. Biochemistry **39:**8853-8858.

50. **Fujii, I., A. Watanabe, and Y. Ebizuka.** 2004. More functions for multifunctional polyketide synthases, p. 97-125. *In* J. S. Tkacz and L. Lange (ed.), Advances in Fungal Biotechnology for Industry, Agriculture, Medicine. Kluwer Academic/Plenum Publishers.

51. **Fujii, I., A. Watanabe, U. Sankawa, and Y. Ebizuka.** 2001. Identification of Claisen cyclase domain in fungal polyketide synthase WA, a naphthopyrone synthase of *Aspergillus nidulans*. Chemistry & Biology **8:**189-197.

52. **Gaffoor, I., and F. Trail.** 2005. Characterization of two distinct polyketide synthase genes involved in zearalenone biosynthesis in *Gibberella zeae*. Applied and Environmental Microbiology - Submitted.

53. **Gelderblom, W. C. A., P. G. Thiel, W. F. O. Marasas, and K. J. Vandermerwe.** 1984. Natural Occurrence of Fusarin C, a Mutagen Produced by *Fusarium moniliforme*, in Corn. Journal of Agricultural and Food Chemistry **32:**1064-1067.

54. **Goswami, R. S., and H. C. Kistler.** 2004. Heading for disaster: *Fusarium graminearum* on cereal crops. Molecular Plant Pathology **5:**515-525.

55. **Hawke, M. A., and G. Lazarovits.** 1994. Production and manipulation of individual microsclerotia of *Verticillium dahliae* for use in studies of survival. Phytopathology **84:**883-890.

56. **Hendrickson, L., C. R. Davis, C. Roach, D. K. Nguyen, T. Aldrich, P. C. McAda, and C. D. Reeves.** 1999. Lavastatin biosynthesis in Aspergillus terreus: characterization of blocked mutants, enzyme activities and a multifunctional polyketide synthase gene. Chemistry & Biology **6:**429-439.

57. **Homdork, S., H. Fehrmann, and R. Beck.** 2000. Influence of Different Storage Conditions on the Mycotoxin Production and Quality of *Fusarium*-infected Wheat Grain. Journal of Phytopathology **148:**7-15.

58. **Hutchinson, C. R., J. Kennedy, C. Park, S. Kendrew, K. Auclair, and J. Vederas.** 2000. Aspects of the biosynthesis of non-aromatic fungal polyketides by iterative polyketide synthases. Antonie Van Leeuwenhoek International Journal of General and Molecular Microbiology **78:**287-295.

59. **Ishige, T., A. Tani, K. Takabe, K. Kawasaki, Y. Sakai, and N. Kato.** 2002. Wax Ester Production from *n*-Alkanes by *Acinetobacter* sp. Strain M-1: Ultrastructure of Cellular Inclusions and Role of Acyl Coenzyme A Reductase. Applied and Environmental Microbiology **68:**1192-1195.

60. **Jacobson, E. S., E. Hove, and H. S. Emery.** 1995. Antioxidant Function Of Melanin In Black Fungi. Infection And Immunity **63:**4944-4945.

61. **Jurgenson, J. E., R. L. Bowden, K. A. Zeller, J. F. Leslie, N. J. Alexander, and R. D. Plattner.** 2002. A genetic map of *Gibberella zeae* (*Fusarium graminearum*). Genetics **160:**1451-1460.

62. **Kawamura, C., J. Moriwaki, N. Kimura, Y. Fujita, S. Fuji, T. Hirano, S. Koizumi, and T. Tsuge.** 1997. The Melanin Biosynthesis Genes of *Alternaria alternata* Can Restore Pathogenicity of the Melanin-Deficient mutants of *Magnaporthe grisea*. Molecular Plant-Microbe Interactions **10:**446-453.

63. **Kawamura, C., T. Tsujimoto, and T. Tsuge.** 1999. Targeted Disruption of a Melanin Biosynthesis Gene Affects Conidial Development and UV Tolerance in the Japanese Pear Aathotype of *Alternaria alternata*. Molecular Plant-Microbe Interactions **12:**59-63.

64. **Kay, R. R.** 1998. The Biosynthesis of Differentiation-Inducing Factor, a Chlorinated Signal Molecule Regulating *Dictyostelium* development. Journal of Biological Chemistry **273:**2669-2675.

65. **Keller, N. P., and T. M. Hohn.** 1997. Metabolic pathway gene clusters in filamentous fungi. Fungal Genetics and Biology **21:**17-29.

66. **Kennedy, D. G., S. A. Hewitt, J. D. G. McEvoy, J. W. Currie, A. Cannavan, W. J. Blanchflower, and C. T. Elliot.** 1998. Zeranol is formed from Fusarium spp. toxins in cattle *in vivo*. Food Additives and Contaminants **15:**393-400.

67. **Kerenyi, Z., K. Zeller, L. Hornok, and J. F. Leslie.** 1999. Molecular standardization of mating type terminology in the Gibberella fujikuroi species complex. Applied and Environmental Microbiology **65:**4071-4076.

68. **Kerényi, Z., K. Zeller, L. Hornok, and J. F. Leslie.** 1999. Molecular standardization of mating type terminology in the *Gibberella fujikuroi* species complex. Applied and Environmental Microbiology **65:**4071-4076.

69. **Kiang, D. T., B. J. Kennedy, S. V. Pathre, and C. J. Mirocha.** 1978. Binding Characteristics Of Zearalenone Analogs To Estrogen Receptors. Cancer Research **38:**3611-3615.

70. **Klittich, C. J. R., and J. F. Leslie.** 1988. Nitrate Reduction Mutants of *Fusarium moniliforme* (*Gibberella fujikuroi*). Genetics **118:**417-423.

71. **Kotik, A. N., and V. A. Trufanova.** 1998. Detection of naphtoquinone fusariotoxin aurofusarin in wheat. Mikologiya I Fitopatologiya **32:**58-61.

72. **Kramer, C. Y.** 1956. Extension of Multiple Range Tests to Group Means with Unequal Numbers of Replications. Biometrics **12:**307-310.

73. **Kroken, S., N. L. Glass, J. W. Taylor, O. C. Yoder, and B. G. Turgeon.** 2003. Phylogenomic analysis of type I polyketide synthase genes in pathogenic and saprobic ascomycetes. Proceedings of the National Academy of Sciences of the United States of America **100:**15670-15675.

74. **Kuiper-Goodman, T., P. M. Scott, and H. Watanabe.** 1987. Risk Assessment of the Mycotoxin Zearalenone. Regulatory Toxicology and Pharmacology **7:**253-306.

75. **Kuipergoodman, T., P. M. Scott, and H. Watanabe.** 1987. Risk assessment of the mycotoxin zearalenone. Regulatory Toxicology and Pharmacology **7:**253-306.

76. **Linnemannstons, P., J. Schulte, M. D. Prado, R. H. Proctor, J. Avalos, and B. Tudzynski.** 2002. The polyketide synthase gene *pks4* from *Gibberella fujikuroi*

encodes a key enzyme in the biosynthesis of the red pigment bikaverin. Fungal Genetics and Biology **37:**134-148.

77. **Lohr, D.** 1997. Nucleosome transactions on the promoters of the yeast GAL and PHO genes. Journal of Biological Chemistry **272:**26795-26798.

78. **Long, G. G., M. Diekman, J. F. Tuite, G. M. Shannon, and R. F. Vesonder.** 1982. Effect of Fusarium roseum corn culture containing zearalenone on early pregnancy in swine. Am J Vet Res **43:**1599-603.

79. **Magan, N., R. Hope, A. Colleate, and E. S. Baxter.** 2002. Relationship between growth and mycotoxin production by *Fusarium* species, biocides and environment. European Journal of Plant Pathology **108:**685-690.

80. **Maier, F. J., and W. Schafer.** 1999. Mutagenesis via insertional or restriction enzyme-mediated-integration (REMI) as a tool to tag pathogenicity related genes in plant pathogenic fungi. Biological Chemistry **380:**855-864.

81. **Malz, S., M. N. Grell, C. Thrane, F. J. Maier, P. Rosager, A. Felk, K. S. Albertsen, S. Salomon, L. Bohn, W. Schäfer, and H. Giese.** 2005. Identification of a gene cluster responsible for the biosynthesis of aurofusarin in the *Fusarium graminearum* species complex. Fungal Genetics and Biology **42:**420-433.

82. **Martin, J. F.** 2000. Molecular control of expression of penicillin biosynthesis genes in fungi: Regulatory proteins interact with a bidirectional promoter region. Journal of Bacteriology **182:**2355-2362.

83. **Martin, P. M., K. B. Horwitz, D. S. Ryan, and W. L. McGuire.** 1978. Phyto-Estrogen Interaction With Estrogen Receptors In Human Breast-Cancer Cells. Endocrinology **103:**1860-1867.

84. **Mayorga, M. E., and W. E. Timberlake.** 1992. The Developmentally Regulated *Aspergillus nidulans* wA Gene Encodes a Polypeptide Homologous to Polyketide and Fatty Acid Synthases. Molecular & General Genetics **235:**205-212.

85. **McCormick, S. P., L. J. Harris, N. J. Alexander, T. Ouellet, A. Saparno, S. Allard, and A. E. Desjardins.** 2004. *Tri1* in *Fusarium graminearum* encodes a P450 oxygenase. Applied and Environmental Microbiology **70:**2044-2051.

86. **Miao, V., M. F. Coeffet-LeGal, D. Brown, S. Sinnemann, G. Donaldson, and J. Davies.** 2001. Genetic approaches to harvesting lichen products. Trends In Biotechnology **19:**349-355.

87. **Mirocha, C. J., and S. V. Pathre.** 1979. Mycotoxins – Their biosynthesis In fungi - Zearalenone biosynthesis. Journal Of Food Protection **42:**821-824.

88. **Mirocha, C. J. S. V., C. M. Pathre, and Christensen.** 1977. Zearalenone, p. 345-36. *In* J. V. Rodricks, C. W. Hesseltine, and M. A. Mehlman (ed.), Mycotoxins in human and animal health. Pathotox Pulishers, Inc., Park Forest South, IL.

89. **Munkvold, G. P.** 2003. Epidemiology of *Fusarium* diseases and their mycotoxins in maize ears. European Journal of Plant Pathology **109:**705-713.

90. **Muro-Pastor, M. I., R. Gonzalez, J. Strauss, F. Narendja, and C. Scazzocchio.** 1999. The GATA factor AreA is essential for chromatin remodelling in a eukaryotic bidirectional promoter. Embo Journal **18:**1584-1597.

91. **Nelson, R. R.** 1971. Hormonal Involvement in Sexual Reproduction in the fungi with special reference to F-2, a fungal estrogen., p. 181-200. *In* S. Adai and S. Ouchi (ed.), Morphological and Biochemical Events in Plant-Parasite Interaction. The Phytopathological Society of Japan, Tokyo.

92. **Nicholson, T. P., B. A. M. Rudd, M. Dawson, C. M. Lazarus, T. J. Simpson, and R. J. Cox.** 2001. Design and utility of oligonucleotide gene probes for fungal polyketide synthases. Chemistry & Biology **8:**157-178.

93. **O'Hagan, D.** 1991. The Polyketide Metabolites. Ellis Horwood Limited, West Sussex, England.

94. **Parry, D. W., P. Jenkinson, and L. McLeod.** 1995. Fusarium Ear Blight (Scab) In Small-Grain Cereals - A Review. Plant Pathology **44:**207-238.

95. **Pathre, S. V., P. V. Khadikar, and C. J. Mirocha.** 1989. Biosynthesis of zearalenone – A simple and efficient method to incorporate [C-13]acetate label by using solid cultures. Applied and Environmental Microbiology **55:**1955-1956.

96. **Paulitz, T. C.** 1996. Diurnal release of ascospores by Gibberella zeae in inoculated wheat plots. Plant Disease **80:**674-678.

97. **Philalay, J. S., C. O. Palermo, K. A. Hauge, T. R. Rustad, and G. A. Cangelosi.** 2004. Genes Required for Intrinsic Multidrug Resistance in *Mycobacterium avium*. Antimicrobial Agents and Chemotherapy **48:**3412-3418.

98. **Placinta, C. M., J. P. F. D'Mello, and A. M. C. Macdonald.** 1999. A review of worldwide contamination of cereal grains and animal feed with Fusarium mycotoxins. Animal Feed Science and Technology **78:**21-37.

99. **Pritsch, C., G. J. Muehlbauer, W. R. Bushnell, D. A. Somers, and C. P. Vance.** 2000. Fungal development and induction of defense response genes during early infection of wheat spikes by Fusarium graminearum. Molecular Plant-Microbe Interactions **13:**159-169.

100. **Procopiou, P. A., B. Cox, B. E. Kirk, M. G. Lester, A. D. McCarthy, M. Sareen, P. J. Sharratt, M. A. Snowden, S. J. Spooner, N. S. Watson, and J. Widdowson.** 1996. The Squalestatins: Inhibitors of Squalene Synthase. Enzyme Inhibitory Activities and *in Vivo* Evaluation of C3-Modified Analogues. Journal of Medicinal Chemistry **39:**1413-1422.

101. **Proctor, R. H., D. W. Brown, R. D. Plattner, and A. E. Desjardins.** 2003. Co-expression of 15 contiguous genes delineates a fumonisin biosynthetic gene cluster in Gibberella moniliformis. Fungal Genetics and Biology **38:**237-249.

102. **Proctor, R. H., A. E. Desjardins, R. D. Plattner, and T. M. Hohn.** 1999. A Polyketide Synthase Gene Required for Biosynthesis of Fumonisin Mycotoxins in *Gibberella fujikuroi* Mating Population A. Fungal Genetics and Biology **27:**100-112.

103. **Proctor, R. H., A. E. Desjardins, R. D. Plattner, and T. M. Hohn.** 1999. A polyketide synthase gene required for biosynthesis of fumonisin mycotoxins in Gibberella fujikuroi slating population A. Fungal Genetics and Biology **27:**100-112.

104. **Proctor, R. H., T. M. Hohn, and S. P. McCormick.** 1995. Reduced Virulence of *Gibberella zeae* Caused by Disruption of a Trichothecene Toxin Biosynthetic Gene. Molecular Plant-Microbe Interactions **8:**593-601.

105. **Proctor, R. H., T. M. Hohn, and S. P. McCormick.** 1997. Restoration of wild-type virulence to Tri5 disruption mutants of Gibberella zeae via gene reversion and mutant complementation. Microbiology-Uk **143:**2583-2591.

106. **Punt, P. J., P. A. Greaves, A. Kuyvenhoven, J. C. T. Vandeutekom, J. R. Kinghorn, P. H. Pouwels, and C. Vandenhondel.** 1991. A twin-reporter vector for simultaneous analysis of expression signals of divergently transcribed, contiguous genes in filamentous fungi. Gene **104:**119-122.

107. **Rehnstrom, A. L., and S. J. Free.** 1996. The isolation and characterization of melanin-deficient mutants of *Monilinia fructicola*. Physiological and Molecular Plant Pathology **49:**321-330.

108. **Romero-Martinez, R., M. Wheeler, A. Guerrero-Plata, G. Rico, and H. Torres-Guerrero.** 2000. Biosynthesis and functions of melanin in *Sporothrix schenckii*. Infection and Immunity **68:**3696-3703.

109. **Rose, M. S., S. H. Yun, T. Asvarak, S. W. Lu, O. C. Yoder, and B. G. Turgeon.** 2002. A decarboxylase encoded at the Cochliobolus heterostrophus translocation-associated Tox1B locus is required for polyketide (T-toxin) biosynthesis and high virulence on T-cytoplasm maize. Molecular Plant-Microbe Interactions **15:**883-893.

110. **Rossi, V., S. Giosue, and R. Bugiani.** 2003. Influence of air Temperature on the Release of Ascospores of *Venturia inaequalis*. Journal of Phytopathology-Phytopathologische Zeitschrift **151:**50-58.

111. **Sambrook, J., D. W. Russell, and J. Sambrook.** 2001. Molecular Cloning: A Laboratory Manual, Third ed. Cold Spring Harbor Laboratory Press, Cold Spring Harbor, New York.

112. **Schnitzler, N., H. Peltroche-Llacsahuanga, N. Bestier, J. Zündorf, R. Lütticken, and G. Haase.** 1999. Effect of Melanin and Carotenoids of *Exophiala* (*Wangiella*) *dermatitidis* on Phagocytosis, Oxidative Burst, and Killing by Human Neutrophils. Infection and Immunity **67:**94-101.

113. **Schoental, R.** 1988. Zearalenone, its role in breast and sex-organ tumors. Breast Cancer Research and Treatment **12:**140-140.

114. **Shibata, S., E. Morishita, T. Takeda, and K. Sakata.** 1966. The structure of aurofusarin. Tetrahedron Letters **Volume 7.:**4855-4860.

115. **Song, Z. S., R. J. Cox, C. M. Lazarus, and T. J. Simpson.** 2004. Fusarin C biosynthesis in *Fusarium moniliforme* and *Fusarium venenatum*. Chembiochem **5:**1196-1203.

116. **Steele, J. A., Lieberma.Jr, and C. J. Mirocha.** 1974. Biogenesis of zearalenone (F-2) by *Fusarium roseum* "graminearum". Canadian Journal of Microbiology **20:**531-534.

117. **Steele, J. A., Lieberman.Jr, and C. J. Mirocha.** 1974. Biogenesis of Zearalenone (F-2) by *Fusarium roseum graminearum*. Canadian Journal of Microbiology **20:**531-534.

118. **Stob, M., S. Baldwin, J. F. Tuite, F. N. Andrews, and K. G. Gillette.** 1962. Isolation of an anabolic, uterotrophic compound from corn infected with *Gibberella zeae*. Nature **196:**1318.

119. **Svaren, J., and W. Horz.** 1997. Transcription factors vs nucleosomes: Regulation of the PH05 promoter in yeast. Trends in Biochemical Sciences **22:**93-97.

120. **Swanson, S. P., R. A. Corley, D. G. White, and W. B. Buck.** 1984. Rapid thin-layer chromatographic method for determination of zearalenone and zearalenol in grains and animal feeds. Journal Of The Association Of Official Analytical Chemists **67:**580-582.

121. **Thompson, C. R. L., and R. R. Kay.** 2000. The Role of DIF-1 Signaling in *Dictyostelium* Development. Molecular Cell **6:**1509-1514.

122. **Thompson, J. D., D. G. Higgins, and T. J. Gibson.** 1994. Clustal W: Improving the sensitivity of progressive multiple sequence alignment through sequence weighting, position-specific gap penalties and weight matrix choice. Nucleic Acids Research **22:**4673-4680.

123. **Trail, F., and R. Common.** 2000. Perithecial development by *Gibberella zeae*: a light microscopy study. Mycologia **92:**130-138.

124. **Trail, F., I. Gaffoor, and S. Vogel.** 2005. Ejection mechanics and trajectory of the ascospores of *Gibberella zeae* (anamorph *Fuarium graminearum*). Fungal Genetics and Biology **42:**528-533.

125. **Trail, F., H. X. Xu, R. Loranger, and D. Gadoury.** 2002. Physiological and environmental aspects of ascospore discharge in Gibberella zeae (anamorph Fusarium graminearum). Mycologia **94:**181-189.

126. **Tsai, H. F., Y. C. Chang, R. G. Washburn, M. H. Wheeler, and K. J. Kwon-Chung.** 1998. The Developmentally Regulated *alb1* Gene of *Aspergillus fumigatus*: Its Role in Modulation of Conidial Morphology and Virulence. Journal of Bacteriology **180:**3031-3038.

127. **Tsukamoto, Y., L. M. Cole, and J. E. Casida.** 2000. Avermectin Chemistry and Action: Ester- and Ether-type Candidate Photoaffinity Probes. Bioorganic & Medicinal Chemistry **8:**19-26.

128. **Tuite, J.** 1969. Plant Pathological Methods, Fungi and Bacteria.

129. **Tuite, J., G. Shaner, G. Rambo, J. Foster, and R. W. Caldwell.** 1974. The *Gibberella* ear rot epidemics of corn in Indiana in 1965 and 1972. Cereal Science Today **19:**238-241.

130. **Urry, W. H., H. L. Wehrmeister, E. B. Hodge, and P. H. Hidy.** 1966. The structure of zearalenone. Tetrahedron Letters **7:**3109-3114.

131. **Vahlensieck, H. F., L. Pridzun, H. Reichenbach, and A. Hinnen.** 1994. Identification of the Yeast ACC1 gene-product (Acetyl-Coa Carboxylase) as the target of the polyketide fungicide Soraphen-A. Current Genetics **25:**95-100.

132. **Watanabe, A., I. Fujii, U. Sankawa, M. E. Mayorga, W. E. Timberlake, and Y. Ebizuka.** 1999. Re-identification of *Aspergillus nidulans* wA gene to code for a polyketide synthase of naphthopyrone. Tetrahedron Letters **40:**91-94.

133. **Watanabe, A., Y. Ono, I. Fujii, U. Sankawa, M. E. Mayorga, W. E. Timberlake, and Y. Ebizuka.** 1998. Product identification of polyketide synthase coded by *Aspergillus nidulans* wA gene. Tetrahedron Letters **39:**7733-7736.

134. **Watanabe, C. M. H., D. Wilson, J. E. Linz, and C. A. Townsend.** 1996. Demonstration of the catalytic roles and evidence for the physical association of type I fatty acid synthases and a polyketide synthase in the biosynthesis of aflatoxin B-1. Chemistry & Biology **3:**463-469.

135. **Weinberg, E. D.** 1971. Secondary Metabolism - Raison D'être. Perspectives in Biology and Medicine **14:**565-&.

136. **Wilson, R. A., and H. N. Arst.** 1998. Mutational analysis of AREA, a transcriptional activator mediating nitrogen metabolite repression in Aspergillus nidulans and a member of the "streetwise" GATA family of transcription factors. Microbiology And Molecular Biology Reviews **62:**586-+.

137. **Wolf, J. C., and C. J. Mirocha.** 1973. Regulation of Sexual Reproduction in *Gibberella zeae* (*Fusarium roseum graminearum*) By F-2 (Zearalenone). Canadian Journal of Microbiology **19:**725-734.

138. **Yang, G., M. S. Rose, B. G. Turgeon, and O. C. Yoder.** 1996. A Polyketide Synthase is Required for Fungal Virulence and Production of the Polyketide T-Toxin. Plant Cell **8:**2139-2150.

139. **Yu, J. J., P. K. Chang, J. W. Cary, M. Wright, D. Bhatnagar, T. E. Cleveland, G. A. Payne, and J. E. Linz.** 1995. Comparative Mapping of Aflatoxin Pathway Gene Clusters in *Aspergillus parasiticus* and *Aspergillus flavus*. Applied and Environmental Microbiology **61:**2365-2371.

140. **Yu, J. J., P. K. Chang, K. C. Ehrlich, J. W. Cary, D. Bhatnagar, T. E. Cleveland, G. A. Payne, J. E. Linz, C. P. Woloshuk, and J. W. Bennett.** 2004. Clustered Pathway Genes in Aflatoxin Biosynthesis. Applied and Environmental Microbiology **70:**1253-1262.

141. **Yun, S. H., B. G. Turgeon, and O. C. Yoder.** 1998. REMI-induced mutants of *Mycosphaerella zeae-maydis* lacking the polyketide PM-toxin are deficient in pathogenesis to corn. Physiological and Molecular Plant Pathology **52:**53-66.

142. **Zhou, R., R. Rasooly, and J. E. Linz.** 2000. Isolation and analysis of *fluP*, a gene associated with hyphal growth and sporulation in *Aspergillus parasiticus*. Molecular & General Genetics **264:**514-520.